# THICKNESS REQUIREMENTS FOR SOILS BENEATH LANDING MATS; BARE BASE SUPPORT

Harry H. Ulery, Jr., et al

Army Engineer Waterways Experiment Station
Vicksburg, Mississippi

January 1971


MISCELLANEOUS PAPER S-71-3

# THICKNESS REQUIREMENTS FOR SOILS BENEATH LANDING MATS

## BARE BASE SUPPORT

Project 3782-64

by

H. H. Ulery, Jr., D. P. Wolf



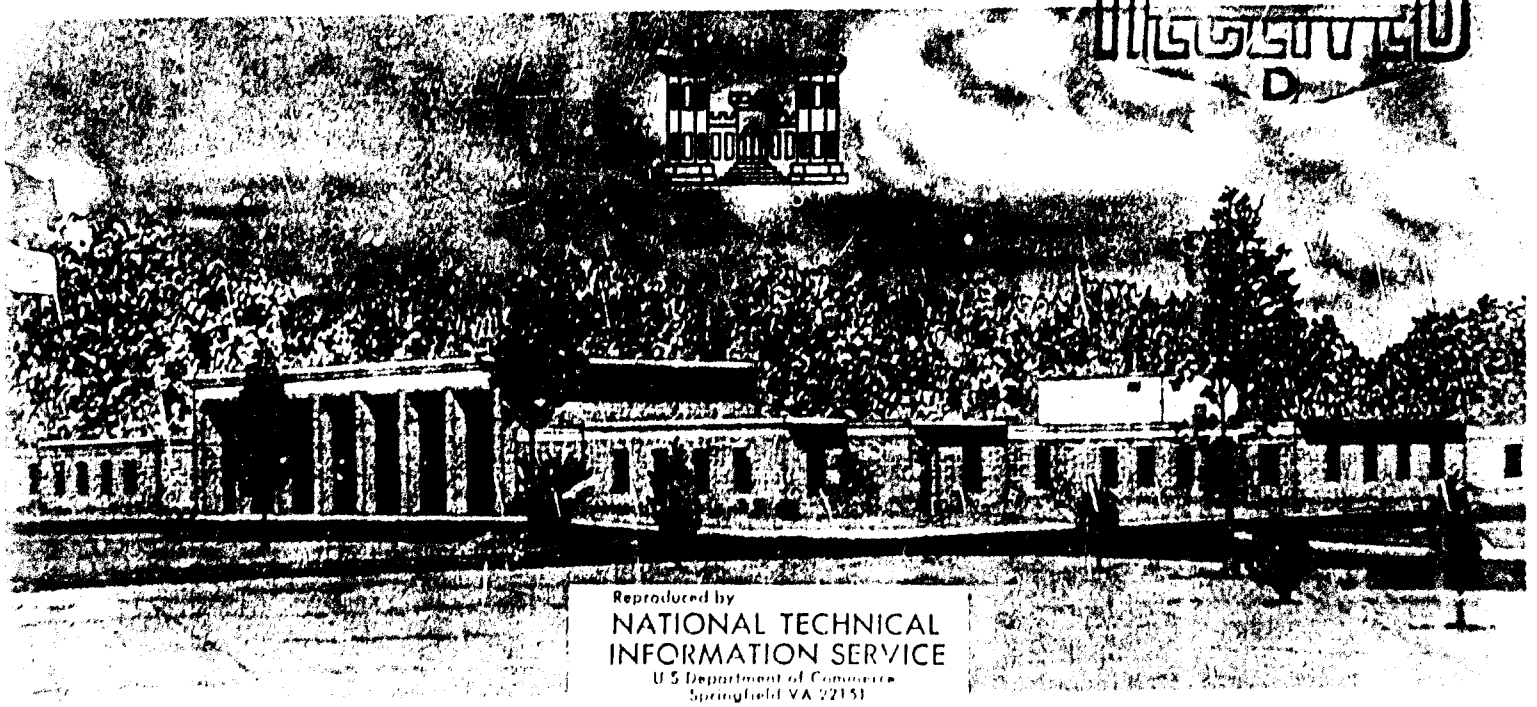



January 1971

Sponsored by Office, Chief of Engineers and U. S. Air Force

Conducted by U. S. Army Engineer Waterways Experiment Station, Vicksburg, Mississippi

129
Q

Unclassified

Security Classification

**DOCUMENT CONTROL DATA - R & D**

*(Security classification of title, body of abstract and indexing annotation must be entered when the overall report is classified)*

| 1. ORIGINATING ACTIVITY (Corporate author) | 2a. REPORT SECURITY CLASSIFICATION |
|---|---|
| U. S. Army Engineer Waterways Experiment Station<br>Vicksburg, Mississippi | Unclassified |
| | 2b. GROUP |

3. REPORT TITLE

THICKNESS REQUIREMENTS FOR SOILS BENEATH LANDING MATS, Bare Base Support

4. DESCRIPTIVE NOTES (Type of report and inclusive dates)

Final report

5. AUTHOR(S) (First name, middle initial, last name)

Harry H. Ulery, Jr.
Denis P. Wolf

| 6. REPORT DATE | 7a. TOTAL NO. OF PAGES | 7b. NO. OF REFS |
|---|---|---|
| January 1971 | 125 | 5 |

| 8a. CONTRACT OR GRANT NO. | 9a. ORIGINATOR'S REPORT NUMBER(S) |
|---|---|
| b. PROJECT NO. 3782-64 | Miscellaneous Paper S-71-3 |
| c. | 9b. OTHER REPORT NO(S) (Any other numbers that may be assigned this report) |
| d. | |

10. DISTRIBUTION STATEMENT

This document has been approved for public release and sale; its distribution is unlimited.

| 11. SUPPLEMENTARY NOTES | 12. SPONSORING MILITARY ACTIVITY |
|---|---|
| | Office, Chief of Engineers<br>U. S. Air Force<br>Washington, D. C. |

13. ABSTRACT—The study reported herein is one phase of the research program being conducted at the U. S. Army Engineer Waterways Experiment Station for the purpose of developing a method for determining thickness requirements for landing-mat-surfaced, membrane-surfaced, and unsurfaced airfields. The phase of the program presented in this report pertains to the development of a method for determining thickness requirements of soil strengthening layers for landing-mat-surfaced airfields. Five landing-mat-surfaced test sections were constructed and tested. The subgrades of the test sections consisted of heavy clay (1.3 to 3.7 CBR) of various thicknesses. The same material placed at a higher strength (3.0 to 8.0 CBR) was used as a strengthening layer between the landing mat and subgrade. Test section I was surfaced with M8A1 landing mat; test sections II, III, and IV were surfaced with XM18 landing mat; and test section V was surfaced with AM2 mat. Aircraft traffic with single-wheel loads of 25,000 to 70,000 lb with tire pressures ranging from 112 to 229 psi and traffic with twin-wheel configurations spaced 32 in. center-to-center with loads ranging from 56,000 to 70,000 lb and tire pressures ranging from 109 to 182 psi were simulated by means of test load carts. Traffic was applied until each test section failed. CBR, water content, and density of the subgrade and overlying higher strength layer were measured before, during, and after the traffic tests, and the condition of the test sections was recorded. Deflections and deformations were determined throughout testing. An equation for determining the required thickness of soil strengthening layers beneath landing mat was developed by correlating the data from this and previous studies with flexible pavement design relations. This equation is proposed for use in establishing design criteria for thicknesses of soil strengthening layers beneath landing mat.

DD FORM 1 NOV 68 1473 REPLACES DD FORM 1473, 1 JAN 64, WHICH IS OBSOLETE FOR ARMY USE.

Unclassified

Security Classification

IA

| 14. KEY WORDS | LINK A | | LINK B | | LINK C | |
|---|---|---|---|---|---|---|
| | ROLE | WT | ROLE | WT | ROLE | WT |
| Airfields | | | | | | |
| Bare base support | | | | | | |
| Landing mats | | | | | | |
| Soil strength | | | | | | |
| Surfaced airfields | | | | | | |
| Unsurfaced airfields | | | | | | |



I b

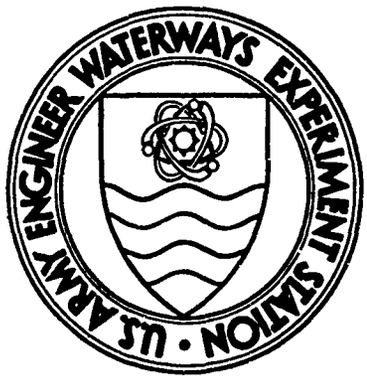


MISCELLANEOUS PAPER S-71-3

# THICKNESS REQUIREMENTS FOR SOILS BENEATH LANDING MATS

## BARE BASE SUPPORT

Project 3782-64

by

H. H. Ulery, Jr., D. P. Wolf

January 1971

Sponsored by Office, Chief of Engineers and U. S. Air Force

Conducted by U. S. Army Engineer Waterways Experiment Station, Vicksburg, Mississippi

## Foreword

The study reported herein was a combined study authorized by the Office, Chief of Engineers, in "Instructions and Outline for Development of Thickness Design Criteria for Landing-Mat- and Membrane-Surfaced and Unsurfaced Airfields, FY 1967," dated May 1966, and by U. S. Air Force (USAF) MIPR No. AS-7-333, dated 3 April 1967, under the general project title Bare Base Support. The study was conducted by personnel of the U. S. Army Engineer Waterways Experiment Station (WES), Vicksburg, Miss., during the period August 1966-March 1969.

General supervision of this study was conducted by Messrs. W. J. Turnbull, A. A. Maxwell, R. G. Ahlvin, D. N. Brown, and C. D. Burns of the Soils Division, WES. Personnel actively engaged in the planning, testing and analyzing phases of this study were Messrs. H. H. Ulery, Jr.; W. N. Brabston; D. M. Ladd; G. M. Hammitt II; J. E. Watkins; and D. P. Wolf. This report was prepared by Messrs. Ulery and Wolf.

Directors of the WES during the conduct of this study and the preparation of this report were COL John R. Oswalt, Jr., CE, COL Levi A. Brown, CE, and COL Ernest D. Peixotto, CE. Technical Directors were Messrs. J. B. Tiffany and F. R. Brown.

## Contents

## Contents

## Conversion Factors, British to Metric Units of Measurement

British units of measurement used in this report can be converted to metric units as follows:

| Multiply | By | To Obtain |
|---|---|---|
| mils | 0.0254 | millimeters |
| inches | 2.54 | centimeters |
| feet | 0.3048 | meters |
| square inches | 6.4516 | square centimeters |
| pounds | 0.45359237 | kilograms |
| kips | 453.59237 | kilograms |
| pounds per square inch | 0.070307 | kilograms per square centimeter |
| pounds per cubic foot | 16.0185 | kilograms per cubic meter |

## Summary

The study reported herein is one phase of the research program being conducted at the U. S. Army Engineer Waterways Experiment Station for the purpose of developing a method for determining thickness requirements for landing-mat-surfaced, membrane-surfaced, and unsurfaced airfields. The phase of the program presented in this report pertains to the development of a method for determining thickness requirements of soil strengthening layers for landing-mat-surfaced airfields.

Five landing-mat-surfaced test sections were constructed and tested. The subgrades of the test sections consisted of heavy clay (1.3 to 3.7 CBR) of various thicknesses. The same material placed at a higher strength (3.0 to 8.0 CBR) was used as a strengthening layer between the landing mat and subgrade. Test section I was surfaced with M8A1 landing mat; test sections II, III, and IV were surfaced with XM18 landing mat; and test section V was surfaced with AM2 mat.

Aircraft traffic with single-wheel loads of 25,000 to 70,000 lb with tire pressures ranging from 112 to 229 psi and traffic with twin-wheel configurations spaced 32 in. center-to-center with loads ranging from 56,000 to 70,000 lb and tire pressures ranging from 109 to 182 psi were simulated by means of test load carts. Traffic was applied until each test section failed. CBR, water content, and density of the subgrade and overlying higher strength layer were measured before, during, and after the traffic tests, and the condition of the test sections was recorded. Deflections and deformations were determined throughout testing.

An equation for determining the required thickness of soil strengthening layers beneath landing mat was developed by correlating the data from this and previous studies with flexible pavement design relations. This equation is proposed for use in establishing design criteria for thicknesses of soil strengthening layers beneath landing mat.

# THICKNESS REQUIREMENTS FOR SOILS BENEATH LANDING MAT

## BARE BASE SUPPORT

## Introduction

### Background

1. In many areas of the world, the in situ soil does not have the strength required to support aircraft operations. This requires the placement of a stronger medium over the weak soil. This, at times, can be accomplished by placing (a) landing mat on the soil, (b) a layer of stronger soil on the weak soil, or (c) a combination of both. This investigation is a study of the latter condition conducted by the U. S. Army Engineer Waterways Experiment Station (WES) for the Office, Chief of Engineers, and the U. S. Air Force.

### Objective

2. The overall objective of this study was to determine the minimum required thickness of soil having a strength at least equivalent to that required for a subgrade directly under landing mat by investigating the effects of load, tire pressure, and soil strength on the performance of landing mat under traffic.

### Scope

3. The objective was accomplished by constructing five test sections and subjecting the sections to accelerated traffic using various single- and twin-wheel loadings and tire pressures. This report presents a description of the materials used, test sections, construction methods, tests conducted and results, and an analysis of the results. Related data obtained from previous studies were also used in the analysis.

## Descriptions of Test Sections and Load Vehicles

### Test sections

4. Five special test sections were constructed under shelter at WES in order that water content and strength of the subgrade could be

controlled. The test sections will be referred to as test sections I through V in this report.

5. The construction of the test sections was accomplished by excavating a specified area for each test section, backfilling the excavation in 6-in.* lifts with a heavy clay (CH),** and compacting each lift with a self-propelled rubber-tired roller. A brief description of each test section is presented as follows:

| Test Section | Type Mat | Item No. | Thickness, in. Subgrade | Thickness, in. Strengthening Layer |
|---|---|---|---|---|
| I | M8A1 | 1 | 30 | 6 |
| | | 2 | 24 | 12 |
| | | 3 | 16 | 20 |
| | | 4 | 12 | 24 |
| II | XM18 | 1 | 28 | 7 |
| | | 2 | 23 | 12 |
| | | 3 | 18 | 17 |
| | | 4 | -- | 35 |
| III | XM18 | 1 | 28 | 6 |
| | | 2 | 22 | 12 |
| | | 3 | 17 | 17 |
| IV | XM18 | -- | 18 | 16 |
| V | AM2 | -- | 30 | 6 |

The subgrades of each of the test items consisted of low-strength clay (1.3 to 3.7 CBR) of various thicknesses. The same material with a higher strength (3.0 to 8.0 CBR) was used as a strengthening layer over the subgrade. In test sections III and IV, 6-mil-thick polyethylene was placed at the interface of the subgrade and the strengthening soil layer to facilitate deformation measurements of the subgrade after completion of traffic tests. Plan and profile views of test sections I through V are shown in plates 1-5, respectively.

Load vehicles

6. Two types of load vehicles were used in trafficking the test

* A table of factors for converting British units of measurement to metric units is presented on page vii.

** Classified according to reference 1.

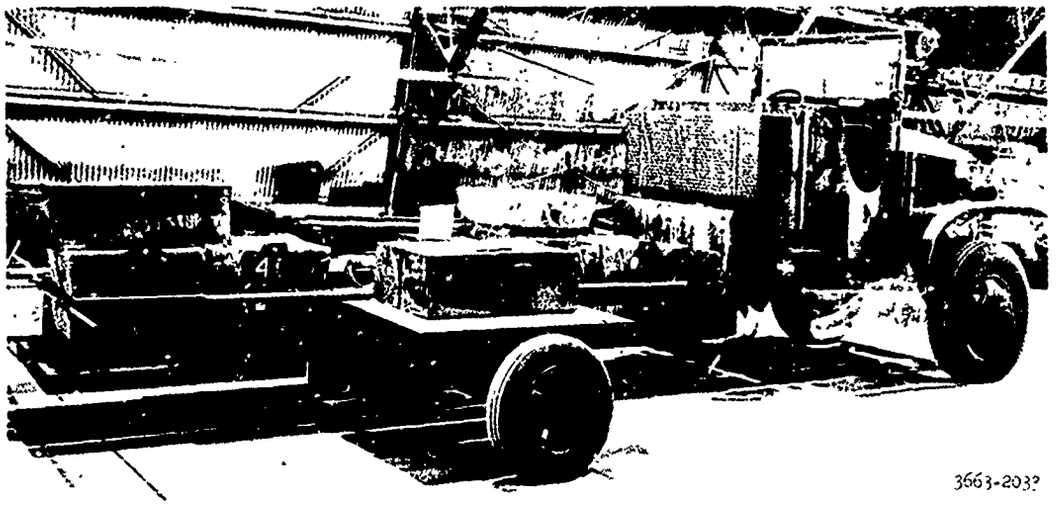


Fig. 1. Test vehicle for 25,000- to 30,000-lb loads

sections. A specially designed single-wheel load cart (fig. 1) was used for tracking with loads varying from 25,000 to 30,000 lb. It was equipped with an outrigger wheel to prevent overturning and was powered by the front half of a four-wheel-drive truck. The load vehicle shown in fig. 2 was

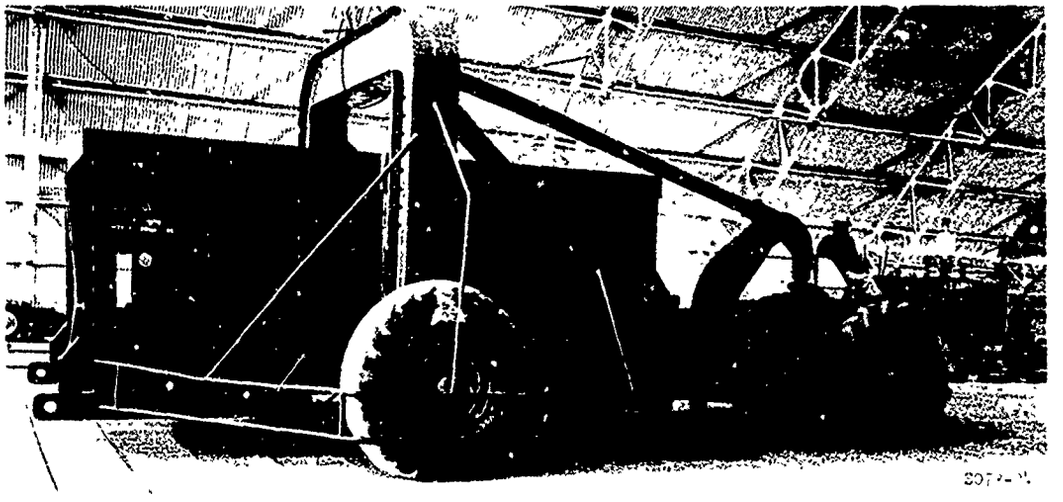

Fig. 2. Test vehicle for 31,000- to 75,000-lb loads

used for tracking with loads varying from 31,000 to 75,000 lb. It consisted of a box-type load compartment and was powered by a two-wheel tractor unit. The tracking wheels within the load compartment were

interchangeable, and single- and twin-wheel assemblies with various tire sizes were used for traffic tests. Pertinent tire data for the various test sections are summarized in table 1.

## Application of Traffic and Failure Criteria

### Application of traffic

7. Traffic was applied to the test sections to simulate the traffic distribution pattern that would be encountered in actual aircraft operation on a taxiway. Each test lane was trafficked by starting at one side of the test lane and driving the load cart forward and then backward in the same path for the length of the traffic lane. The path of the cart was then shifted laterally one tire print width on each successive trip, thus producing two coverages of the entire traffic lane when the load cart had maneuvered from one side of the traffic lane to the other. The number of passes made in each track was varied to provide 100 percent coverage on an area down the center of the traffic lane with less coverage along the edges. All data used for analysis were obtained from 100 percent coverage areas.

### Failure criteria

8. The failure criteria used in these tests were based primarily on the development of roughness and excessive mat breakage due to subgrade deformation. When surface deviations from a 10-ft straightedge approached or equaled 3 in. in any direction within the traffic lane, the test item was considered failed due to roughness.

9. Failure due to mat breakage was based on sufficient breakage to represent a tire hazard during aircraft operations. It was assumed that a certain amount of maintenance would be performed in the field during actual usage and that minor metal or weld breaks could be easily repaired. It is considered feasible to replace up to 10 percent of the mat panels with new mat during the design service life of a runway; however, replacement in excess of 10 percent is considered excessive. Therefore, in these tests, it was assumed that up to 10 percent of the mat panels could be replaced, and when an additional 10 percent of the panels had failed (a total of 20 percent failed), the entire test item was considered failed.

## Data Collection

### Soils data

10. Water content, dry density, and in-place CBR tests were conducted on the strengthening soil layer and subgrade in each test item prior to traffic, at intervals during traffic, and at failure of each test item. These tests were conducted on the surface of the strengthening layer and at intermediate depths up to a depth of approximately 12 in. into the subgrade of each test item. A minimum of three determinations was made at each increment of depth, and, in general, the values reported herein are averages of the values ascertained at each particular depth.

### Traffic data

11. Visual observations of the behavior of the test items under traffic and other pertinent data were recorded throughout the traffic test period. These observations and data were supplemented by photographs. Level readings were taken on the mat prior to traffic and at intervals throughout the traffic test period to record the development of permanent mat deformation and elastic deflection of the mat under the wheel load. Elastic deflections were measured at two locations, i.e., with the tire centered over the center of a panel and with the tire centered over an end joint. Roughness of the test items was determined at various intervals during the traffic test period by measuring the deviation of the mat surface from a 10-ft straightedge placed in longitudinal, transverse, and diagonal positions on the mat surface.

## Traffic Test Results

12. All test items were trafficked to failure. Details of the traffic tests are given in Appendix A; the traffic tests are summarized below and in table 2.

### Test section I

13. A plan and profile of test section I are shown in plate 1. The plan of lane 3 is shown separately in plate 1 for clarity. A 31,000-lb single-wheel load utilizing a 56x16 tire with an inflation pressure of

185 psi was used to traffic lane 1. Lane 2 was trafficked with a 56,000-lb twin-wheel load utilizing 56x16 tires with an inflation pressure of 105 psi. After 612 coverages, the load was increased to 62,000 lb with an inflation pressure of 185 psi. Lane 3 was trafficked with a 62,000-lb twin-wheel load utilizing 56x16 tires with an inflation pressure of 185 psi. Performance under traffic was as follows:

| Test Lane | Item No. | Coverages at Failure | CBR | |
|---|---|---|---|---|
| | | | Subgrade | Strengthening Layer |
| 1 | 1 | 30 | 2.3 | 6 |
| | 2 | 110 | 2.8 | 7 |
| | 3 | 310 | 3.2 | 8 |
| | 4 | 430 | 3.2 | 7 |
| 2 | 1 | 120 | 2.3 | 5 |
| | 2 | 612 | 2.8 | 6 |
| | 3 | 1091 | 2.9 | 6 |
| | 4 | 1324 | 2.8 | 7 |
| 3 | 2 | 120 | 2.3 | 6 |
| | 3 | 408 | 3.0 | 7 |
| | 4 | 750 | 3.0 | 7 |

Test section II

14. A plan and profile of test section II are shown in plate 2. A 30,000-lb single-wheel load utilizing a 30x11.5 tire with an inflation pressure of 250 psi was used to traffic lane 1. Lane 2 was trafficked with a 70,000-lb twin-wheel load utilizing 44x16 tires with an inflation pressure of 185 psi. The performance of the test section is summarized below.

| Test Lane | Item No. | Coverages at Failure | CBR | |
|---|---|---|---|---|
| | | | Subgrade | Strengthening Layer |
| 1 | 1 | 72 | 1.3 | 3.0 |
| | 2 | 170 | 2.3 | 3.1 |
| | 3 | 202 | 1.4 | 3.4 |
| | 4 | 202 | -- | 3.4 |
| 2 | 1 | 32 | 1.4 | 3.3 |
| | 2 | 60 | 1.7 | 3.1 |
| | 3 | 144 | 1.7 | 3.4 |
| | 4 | 300 | -- | 3.7 |

Test section III

15. A plan and profile of test section III are shown in plate 3. A 25,000-lb single-wheel load utilizing a 30x11.5 tire with an inflation pressure of 250 psi was used to traffic lane 1. Lane 2 was trafficked with a 75,000-lb single-wheel load utilizing a 25.00x28 tire with an inflation pressure of 125 psi. Test section performance under traffic was as follows:

| Test Lane | Item No. | Coverages at Failure | CBR | |
|---|---|---|---|---|
| | | | Subgrade | Strengthening Layer |
| 1 | 1 | 528 | 2.1 | 7 |
| | 2 | 884 | 2.0 | 7 |
| 2 | 1 | 56 | 2.1 | 8 |
| | 2 | 72 | 1.8 | 7 |
| | 3 | 92 | 1.9 | 6 |

Test section IV

16. A plan and profile of test section IV are shown in plate 4. The test section consisted of only one test item and was trafficked with a 60,000-lb single-wheel load utilizing a 25.00x28 tire with an inflation pressure of 125 psi. The section failed after 348 coverages. The CBR's of the subgrade and strengthening layer were 1.8 and 7, respectively.

Test section V

17. A plan and profile of test section V are shown in plate 5. The test section consisted of one test item and was surfaced with one-, two-, and three-piece AM2 landing mat and was trafficked with a 25,000-lb single-wheel load utilizing a 30x11.5 tire with an inflation pressure of 250 psi. The section failed after 330 coverages. The CBR's of the subgrade and the strengthening layer were 3.7 and 5, respectively.

## Analysis, Conclusions, and Recommendations

### Analysis

18. The method used to analyze the test data was to relate the load-carrying capabilities of the various types of landing mat to the load-carrying capabilities of a flexible airfield pavement. This was accomplished by expressing mat performance in terms of thickness (top of

subgrade to pavement surface) of conventional flexible airfield pavement effectively replaced by the landing mat (thickness reduction) if both were placed on the same strength subgrade.

19. Since this investigation included strengthening layers of various thicknesses between subgrade and landing mat, the effective thickness of this type of mat-soil system could be defined as the sum of the actual thickness of the strengthening layer and the thickness reduction for the type of mat being tested and analyzed. The reduction in thickness (which varies with load and tire pressure) of subbase, base, and pavement that can be applied to the pertinent flexible pavement thickness in establishing thickness requirements for landing mat can be obtained from reference 2 for M6 and M9 mat and from Part I of reference 3 for M8 mat. Thickness reduction criteria for M8A1, XM18, amd AM2 landing mat used in this analysis were obtained from preliminary relationships developed from other studies and are shown in Appendix B.

20. By using the CBR equation shown below, a required thickness of flexible pavement structure can be calculated that provides the same load-support capability for each loading and subgrade condition found in the actual landing mat tests. This thickness can then be compared with the effective mat-soil thickness. The following equation was used to determine the total required flexible pavement thickness:

$$t = (0.23 \log C + 0.15)\sqrt{\frac{P}{8.1\ CBR} - \frac{A}{\pi}} \qquad (1)*$$

where

t = total thickness of flexible pavement structure (above subgrade), in.

C = number of coverages

P = single- or equivalent single-wheel load, lb

CBR = measure of subgrade strength

A = tire contact area, sq in.

---

* This is a combination of equation 2, page 2, and the equation for slope of curve, plate 6 in reference 4.

In the case of the twin-wheel configurations, a means of relating the twin loading to an equivalent single-wheel load is required, and the procedure outlined in reference 4 was used.

21. Equation 1 was also used to establish an equivalent number of coverages for test items subjected to mixed traffic. Items 3 and 4 of lane 2, test section I, were trafficked with both a 56- and 62-kip twin-wheel loading. In order to establish an equivalent 56-kip twin-wheel loading coverage level, the CBR equation was used to obtain a flexible pavement thickness, based on actual test conditions, for the 62-kip twin loading. This thickness was then used to determine the equivalent coverages of the 56-kip twin-wheel loading. This coverage value plus the actual coverages applied by the 56-kip twin loading represents the total number of coverages applied to the test items by the 56-kip twin-wheel configuration.

22. The basic test data used in this analysis are summarized in table 2. In addition, data used in this analysis but obtained from related investigations are also shown in table 2. These additional data are recorded and discussed in reference 2. Each test was assigned a test number for easy reference. For each test conducted, the following data are shown: test number; test section number and mat type; lane and item number; load per wheel; tire inflation (gage) pressure; tire contact area (measured); tire contact pressure (obtained by dividing the load on a tire by the measured contact area); twin-wheel spacing; tire size and ply rating; coverages; type of failure (either subgrade, strengthening layer, or borderline); rated CBR for subgrade and overlying strengthening layer (a minimum of three determinations were made at each depth increment, and these values were generally averaged for all increments within the subgrade and strengthening layer to obtain a rated CBR value for each); required total flexible pavement thickness (see paragraph 20); actual thickness of strengthening layer; landing mat thickness reduction (see paragraph 19); and effective thickness (thickness reduction plus actual thickness of strengthening layer).

23. From a comparison of results of single- and twin-wheel tests of test section I, twin loads are supported by the mat to a coverage level beyond that anticipated and to the degree that the two loads are supported as

well as (and even somewhat better than) one wheel of the twin configuration acting alone. This can be seen by comparing results of single-wheel tests 2, 3, and 4 with results of twin-wheel tests 9, 10, and 11. Based on past experience, it might be expected that twin wheels spaced at 4.01 radii, as was the case in tests 9, 10, and 11, would act almost the same as one wheel of the twin. (In prior tests conducted at WES,[5] a 50,000-lb twin-wheel load with a center-to-center spacing of 5.4 radii was no more severe than a 25,000-lb single-wheel load). The reason for the twin wheel outperforming the single wheel is not apparent.

24. Plate 6 is a plot of required flexible pavement thickness versus effective thickness. This plot includes all single- and twin-wheel subgrade failure points and borderline failures, as presented in table 2. Borderline failures are landing mat failures, the causes of which cannot be directly attributed to either the subgrade or to the strengthening layer beneath the mat. Only subgrade and borderline failures were used in analysis because the approach to the analysis utilizes the flexible pavement CBR design concept, which is based on a total thickness requirement above a known-strength subgrade. As would be expected, the data grouped according to mat strength (stiffness), which is reflected by the value of the mat thickness reduction. A line of equality (solid line) is shown in plate 6, and this line is a good average for the data. Thus, it can be concluded that the required flexible pavement thickness is equal to the effective thickness of the mat-soil structure. However, for design purposes for thickness requirements for strengthening soils beneath landing mat, it is felt that a conservative line through the data is justified. Thus, a limiting line (dotted line) is shown in plate 6, and this line is proposed for use in the establishment of design criteria for landing-mat-surfaced airfields. The equation of this line is as follows:

$$t_{um} = (0.2875 \log C + 0.1875)\sqrt{\frac{P}{8.1\ CBR} - \frac{A}{\pi}} - TR \qquad (2)$$

where

$t_{um}$ = total thickness of strengthening soil under mat, in.
$C$ = number of coverages

P = single- or equivalent single-wheel load, lb

CBR = measure of subgrade strength

A = tire contact area, sq in.

TR = mat thickness reduction, in.

## Conclusions

25. From the analysis of test results reported herein, it was concluded that thickness criteria for strengthening soils beneath landing mat can be expressed by equation 2. The equation is based on a conservative analysis of the data presented in plate 6. This mathematical expression represents the complete pattern of basic strength requirements for landing-mat-surfaced airfields for single- and multiple-wheel loadings.

## Recommendations

26. Based on the results of this study, the following recommendations are made:

a. Design and evaluation curves based on the design criteria developed herein should be developed for landing-mat-surfaced airfields. Typical curves are shown in Appendix C.

b. From a practical construction standpoint, a minimum strengthening layer thickness of 6 in. should be used wherever required.

c. Although not presently essential to the development of adequate design criteria, additional studies and tests should be made to determine more precisely the relationship between single- and multiple-wheel loads applied to landing-mat-surfaced soils.

## Literature Cited


1. U. S Department of Defense, "Unified Soil Classification System for Roads, Airfields, Embankments, and Foundations," MIL-STD-619B, 12 June 1968, Government Printing Office, Washington, D. C.

2. Thompson, A. B. and Burns, C. D., "Criteria for Designing Runways To Be Surfaced with Landing Mat and Membrane-Type Materials," Technical Report No. 3-539, Apr 1960, U. S. Army Engineer Waterways Experiment Station, CE, Vicksburg, Miss.

3. Ladd, D. M. and Ulery, H. H., Jr., "Aircraft Ground-Flotation Investigation; Part 1, Basic Report," Technical Documentary Report AFFDL-TDR-66-43, Aug 1967, Air Force Flight Dynamics Laboratory, Wright-Patterson

Air Force Base, Ohio; also published as Technical Report No. 3-737, Aug 1967, U. S. Army Engineer Waterways Experiment Station, CE, Vicksburg, Miss.

4. Ahlvin, R. G., "Developing a Set of CBR Design Curves," Instruction Report No. 4, Nov 1959, U. S. Army Engineer Waterways Experiment Station, CE, Vicksburg, Miss.

5. Burns, C. D. and Fenwick, W. B., "Development of CBR Design Curves for Runways To Be Surfaced with M8A1 (Formerly T10) Steel Landing Mat," Miscellaneous Paper No. 4-817, May 1966, U. S. Army Engineer Waterways Experiment Station, CE, Vicksburg, Miss.

Table 1

Summary of Tire Data

| Lane No. | Wheel Assembly | Assembly Load, lb | Tire Size | Ply Rating | Contact Area sq in. | Contact Pressure psi | Inflation Pressure psi |
|---|---|---|---|---|---|---|---|
| | | | Test Section I, M8A1 Mat | | | | |
| 1 | Single | 31,000 | 56x16 | 32 | 208.1 | 149 | 185 |
| 2 | Twin | 56,000 | 56x16 | 24 | 257.7 | 109 | 105 |
| 2,3 | Twin | 62,000 | 56x16 | 32 | 200.5 | 155 | 185 |
| | | | Test Section II, XM18 Mat | | | | |
| 1 | Single | 30,000 | 30x11.5 | 24 | 128.5 | 234 | 250 |
| 2 | Twin | 70,000 | 44x16 | 28 | 192.1 | 182 | 185 |
| | | | Test Section III, XM18 Mat | | | | |
| 1 | Single | 25,000 | 30x11.5 | 24 | 111.0 | 225 | 250 |
| 2 | Single | 75,000 | 25.00x28 | 30 | 648.5 | 116 | 125 |
| | | | Test Section IV, XM18 Mat | | | | |
| 1 | Single | 60,000 | 25.00x28 | 30 | 538.2 | 112 | 125 |
| | | | Test Section V, AM2 Mat | | | | |
| 1 | Single | 25,000 | 30x11.5 | 24 | 111.0 | 225 | 250 |

Table 2

Traffic Test Results

| Test No. | Lane | Load Per Wheel kips | Tire Inflation Pressure psi | Tire Contact Area sq in. | Tire Contact Pressure psi | Twin-wheel Spacing in. | Twin-wheel Spacing radii | Tire Size | Tire Ply Rating | Failures: Coverages | Failures: Type | Rated CBR: Subgrade | Rated CBR: Strengthening Layer | (t) in. | ($t_{um}$) in. | (TK) in. | (TK + $t_{um}$) in. |
|---|---|---|---|---|---|---|---|---|---|---|---|---|---|---|---|---|---|
| **Test Section I, MAI Mat** | | | | | | | | | | | | | | | | | |
| Lane 1 | | | | | | | | | | | | | | | | | |
| 1 | 1 | 31 | 185 | 208 | 149 | -- | -- | 56x16 | 32 | 30 | Subgrade | 2.3 | 6 | 19.6 | 6 | 16.6 | 22.6 |
| 2 | 2 | 31 | 185 | 208 | 149 | -- | -- | 56x16 | 32 | 110 | Borderline | 2.3 | 7 | 22.4 | 12 | 16.6 | 28.6 |
| | 3 | 31 | 185 | 208 | 149 | -- | -- | 56x16 | 32 | 310 | Strengthening layer | 3.2 | 8 | 23.9 | 20 | 16.6 | 36.6 |
| | 4 | 31 | 185 | 208 | 149 | -- | -- | 56x16 | 32 | 530 | -- | 3.2 | 7 | 25.0 | 24 | 16.6 | 40.6 |
| Lane 2 | | | | | | | | | | | | | | | | | |
| 4 | 1 | 28 | 150 | 258 | 109 | 32 | 3.53 | 56x16 | 24 | 120 | Subgrade | 2.3 | 5 | 30.2 | 6 | 20.7 | 26.7 |
| 5 | 2 | 28 | 150 | 258 | 109 | 32 | 3.53 | 56x16 | 24 | 612 | -- | 2.8 | 5 | 36.3 | 12 | 20.7 | 32.7 |
| 6 | 3 | 28 | 150 | 258 | 109 | 32 | 3.53 | 56x16 | 24 | 1091 | Borderline | 2.9 | 6 | 37.6 | 20 | 20.7 | 40.7 |
| 7 | 4 | 28 | 150 | 258 | 109 | 32 | 3.53 | 56x16 | 24 | 1324 | Strengthening layer | 2.8 | 7 | 38.6 | 24 | 20.7 | 44.7 |
| Lane 3 | | | | | | | | | | | | | | | | | |
| 9 | 2 | 31 | 185 | 200 | 155 | 32 | 4.01 | 56x16 | 32 | 120 | Subgrade | 2.3 | 6 | 32.7 | 12 | 17.1 | 29.1 |
| 10 | 3 | 31 | 185 | 200 | 155 | 32 | 4.01 | 56x16 | 32 | 408 | Strengthening layer | 3.0 | 7 | 33.7 | 20 | 17.1 | 37.1 |
| 11 | 4 | 31 | 185 | 200 | 155 | 32 | 4.01 | 56x16 | 32 | 750 | -- | 3.0 | 7 | 37.6 | 24 | 17.1 | 41.1 |
| **Test Section II, XM18 Mat** | | | | | | | | | | | | | | | | | |
| Lane 1 | | | | | | | | | | | | | | | | | |
| 12 | 1 | 30 | 250 | 131 | 229 | -- | -- | 30x11.5 | 24 | 72 | Subgrade | 1.3 | 3.0 | 30.6 | 7 | 22.4 | 29.4 |
| 13 | 2 | 30 | 250 | 131 | 229 | -- | -- | 30x11.5 | 24 | 170 | Subgrade | 2.3 | 3.1 | 26.3 | 12 | 22.4 | 34.4 |
| 14 | 3 | 30 | 250 | 131 | 229 | -- | -- | 30x11.5 | 24 | 202 | Borderline | 1.4 | 3.4 | 34.7 | 17 | 22.4 | 39.4 |
| 15 | 4 | 30 | 250 | 131 | 229 | -- | -- | 30x11.5 | 24 | 202 | Strengthening layer | -- | 3.4 | 22.4 | 35 | 22.4 | 57.4 |
| Lane 2 | | | | | | | | | | | | | | | | | |
| 16 | | 34 | 185 | 193 | 182 | 32.5 | 4.21 | 44x16 | 28 | 32 | Subgrade | 1.4 | 3.3 | 35.1 | 7 | 29.5 | 36.5 |
| 17 | 2 | 34 | 185 | 193 | 182 | 32.5 | 4.21 | 44x16 | 28 | 60 | Subgrade | 1.7 | 3.1 | 35.8 | 12 | 29.5 | 41.5 |
| 18 | 3 | 34 | 185 | 193 | 182 | 32.5 | 4.21 | 44x16 | 28 | 141 | Borderline | 1.7 | 3.4 | 44.2 | 17 | 29.5 | 46.5 |
| 19 | 4 | 34 | 185 | 193 | 182 | 32.5 | 4.21 | 44x16 | 28 | 300 | Strengthening layer | -- | 3.7 | 29.5 | 35 | 29.5 | 64.5 |
| **Test Section III, XM28 Mat** | | | | | | | | | | | | | | | | | |
| Lane 1 | | | | | | | | | | | | | | | | | |
| 20 | 1 | 25 | 250 | 111 | 225 | -- | -- | 30x11.5 | 24 | 528 | Subgrade | 2.1 | 7 | 29.4 | 6 | 21.6 | 27.6 |
| 21 | 2 | 25 | 250 | 111 | 225 | -- | -- | 30x11.5 | 24 | 884 | Subgrade | 2.0 | 7 | 32.1 | 12 | 21.6 | 33.6 |
| Lane 2 | | | | | | | | | | | | | | | | | |
| 22 | 1 | 75 | 125 | 349 | 115 | -- | -- | 25.00x23 | 30 | 56 | Subgrade | 2.1 | 8 | 34.3 | 6 | 34.0 | 40.0 |
| 23 | 2 | 75 | 125 | 349 | 116 | -- | -- | 25.00x23 | 30 | 72 | Subgrade | 1.8 | 7 | 40.6 | 12 | 34.0 | 46.0 |
| 24 | 3 | 75 | 125 | 349 | 116 | -- | -- | 25.00x23 | 30 | 92 | Subgrade | 1.9 | 6 | 41.1 | 17 | 34.0 | 51.0 |
| **Test Section IV, XM13 Mat** | | | | | | | | | | | | | | | | | |
| 25 | -- | 40 | 125 | 338 | 112 | -- | -- | 25.00x28 | 30 | 348 | Subgrade | 1.8 | 7 | 41.1 | 15.5 | 40.0 | 55.5 |
| **Test Section V, AM2 Mat** | | | | | | | | | | | | | | | | | |
| 26 | -- | 24 | 250 | 111 | 22[illegible] | -- | -- | 30x11.5 | 24 | 230 | Subgrade | 3.7 | 5 | 20.6 | 6 | 18.5 | 24.5 |
| **B, Mat** | | | | | | | | | | | | | | | | | |
| 27* | -- | 25 | 100 | 232 | 108 | -- | -- | 56x16 | 24 | 302 | Subgrade | 4.6 | 37 | 17.6 | 6** | 17.5 | 23.5 |
| 28 | -- | 25 | 200 | 159 | 172 | -- | -- | 56x16 | 24 | 86 | Subgrade | 5.0 | 31 | 14.2 | 6 | 10.2 | 16.2 |
| 29 | -- | 25 | 300 | 112 | 223 | -- | -- | 56x16 | 24 | 70 | Subgrade | 4.7 | 66 | 11.8 | 6 | 7.2 | 13.2 |
| 30 | -- | 25 | 300 | 112 | 223 | -- | -- | 56x16 | 24 | 960 | Subgrade | 20 | 56 | 8.5 | 3 | 7.2 | 10.2 |
| 31 | -- | 25 | 300 | 112 | 224 | -- | -- | 56x16 | 24 | 450 | Subgrade | 10 | 83 | 12.9 | 6 | 7.2 | 13.2 |
| **M3 Mat** | | | | | | | | | | | | | | | | | |
| 32 | -- | 25 | 100 | 232 | 108 | -- | -- | 56x16 | 24 | 316 | Subgrade | 5.2 | 29 | 16.5 | 6 | 18.5 | 24.5 |
| 33 | -- | 25 | 200 | 160 | 172 | -- | -- | 56x16 | 24 | 227 | Subgrade | 4.8 | 37 | 14.9 | 6 | 11.2 | 17.2 |
| 34 | -- | 25 | 300 | 112 | 223 | -- | -- | 56x16 | 24 | 78 | Subgrade | 5.9 | 69 | 12.9 | 6 | 6.2 | 12.2 |
| 35 | -- | 50 | 100 | 479 | 104 | -- | -- | 56x16 | 24 | 40 | Subgrade | 2.6 | 33 | 20.5 | 6 | 21.5 | 27.5 |
| 36 | -- | 50 | 200 | 270 | 185 | -- | -- | 56x16 | 24 | 300 | Subgrade | 5.8 | 69 | 22.8 | 12 | 12.6 | 24.6 |
| 37 | -- | 50 | 300 | 187 | 267 | -- | -- | 56x16 | 24 | 40 | Subgrade | 4.3 | 89 | 19.2 | 12 | 8.4 | 20.4 |
| 38 | -- | 50 | 300 | 187 | 267 | -- | -- | 56x16 | 24 | 170 | Subgrade | 15 | 92 | 12.4 | 3 | 8.4 | 11.4 |
| 39 | -- | 50 | 300 | 187 | 267 | -- | -- | 56x16 | 24 | 400 | Subgrade | 16 | 72 | 13.[illegible] | [illegible] | 8.4 | 14.4 |
| **M9 Mat** | | | | | | | | | | | | | | | | | |
| 40 | -- | 25 | 100 | 232 | 108 | -- | -- | 56x16 | 24 | 160 | Subgrade | 4.2 | 27 | 16.9 | 6 | 17.5 | 23.5 |
| 41 | -- | 25 | 200 | 159 | 172 | -- | -- | 56x16 | 24 | 59 | Subgrade | 3.4 | 30 | 16.4 | 6 | 10.2 | 16.2 |
| 42 | -- | 25 | 300 | 112 | 223 | -- | -- | 56x16 | 24 | 359 | Subgrade | 4.5 | 100 | 15.5 | 12 | 7.2 | 19.2 |
| 43 | -- | 25 | 300 | 112 | 223 | -- | -- | 56x16 | 24 | 400 | Subgrade | 14 | 44 | 9.8 | 3 | 7.2 | 10.2 |
| 44 | -- | 25 | 300 | 112 | 223 | -- | -- | 56x16 | 24 | 600 | Subgrade | 17 | 100 | 9.5 | 6 | 7.2 | 13.2 |

Note: (t) = required flexible pavement thickness; ($t_{um}$) = actual thickness of strengthening layer; (TK) = mat thickness reduction; (TK + $t_{um}$) = effective thickness.

* Data for test numbers 27 through 44 were obtained from tables 2 and 3 of reference 2 (see Literature Cited at end of main text).

** Strengthening layer consisted of a high-quality, graded, crushed limestone.

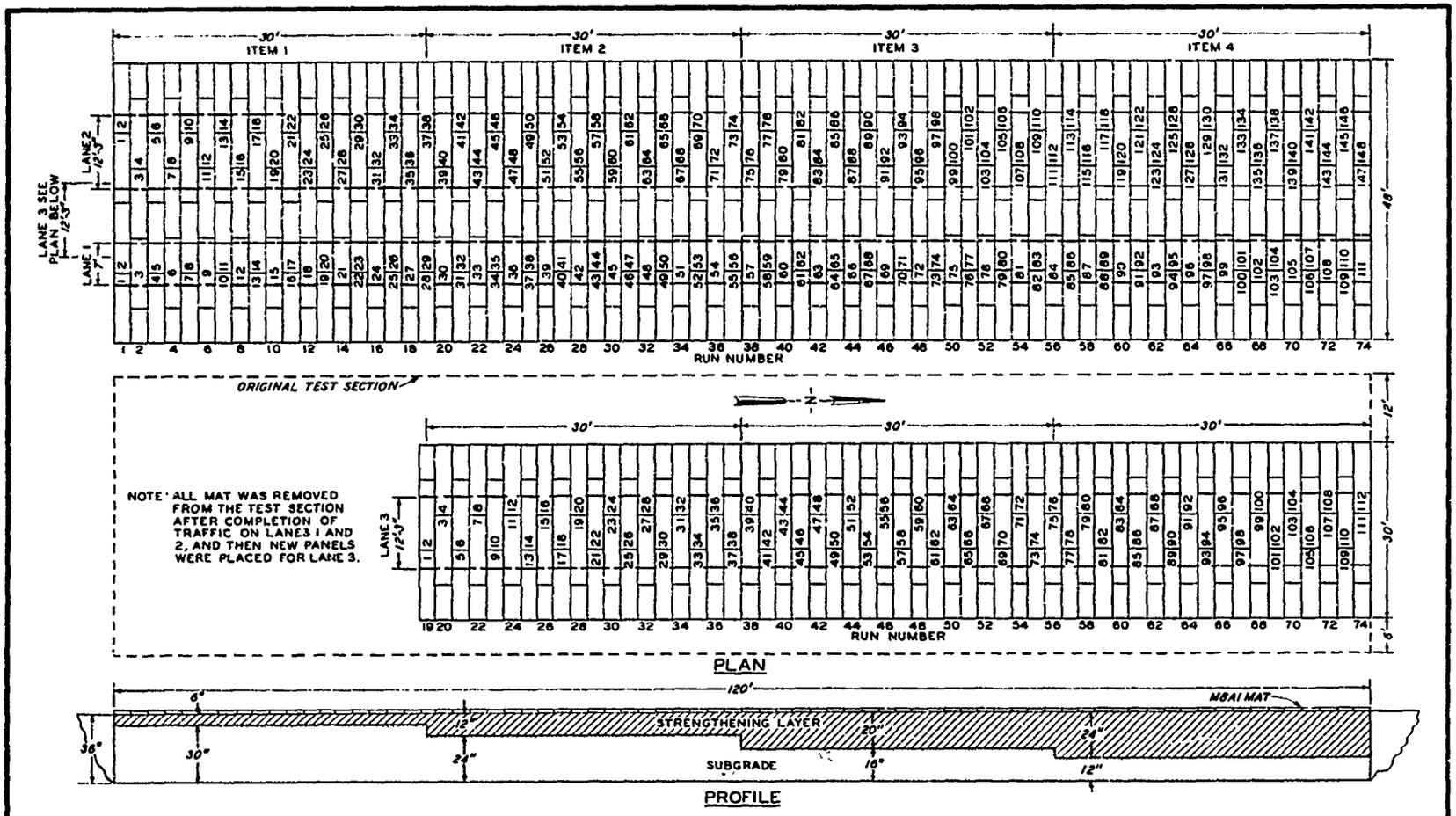


## PLAN AND PROFILE
TEST SECTION I

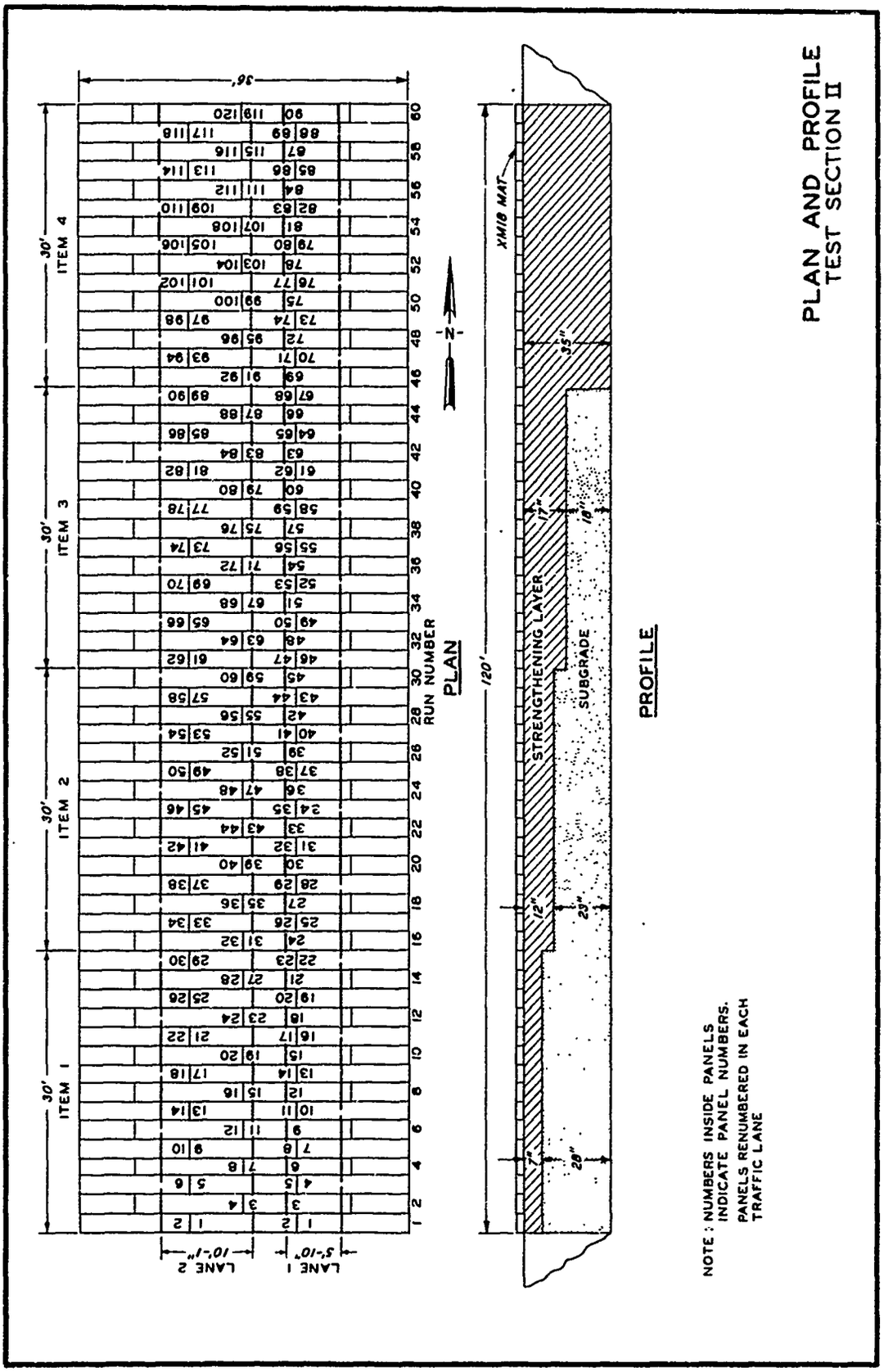
PLAN AND PROFILE
TEST SECTION II
PLAN
PROFILE
RUN NUMBER
LANE 1
LANE 2
ITEM 1
ITEM 2
ITEM 3
ITEM 4
30'
36'
120'
N
XM18 MAT
STRENGTHENING LAYER
SUBGRADE
35"
17"
12"
29"
7"
20"
NOTE : NUMBERS INSIDE PANELS
INDICATE PANEL NUMBERS.
PANELS RENUMBERED IN EACH
TRAFFIC LANE

PLATE 2

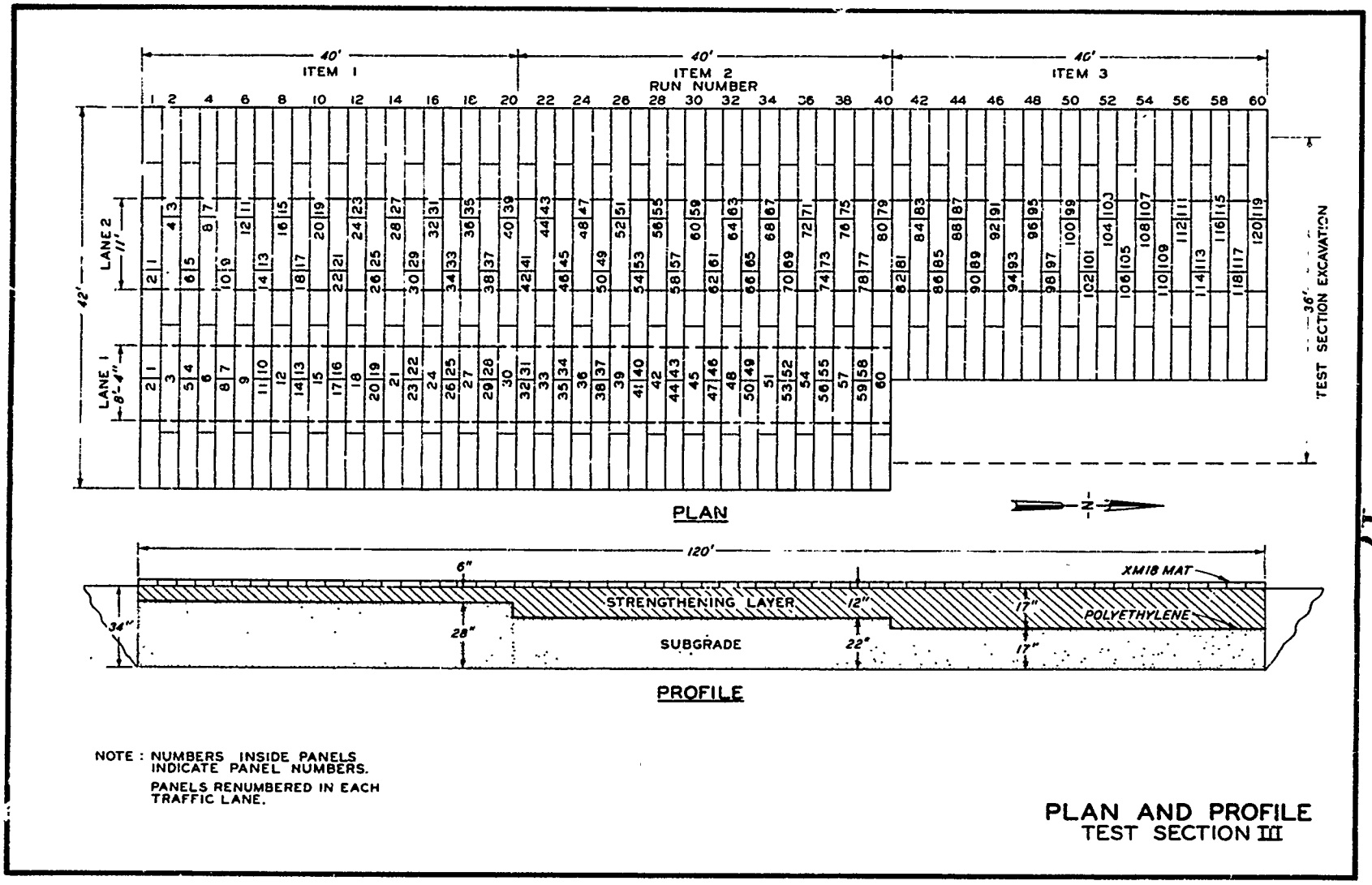


NOTE : NUMBERS INSIDE PANELS INDICATE PANEL NUMBERS.
PANELS RENUMBERED IN EACH TRAFFIC LANE.

PLAN AND PROFILE
TEST SECTION III

PLATE 3

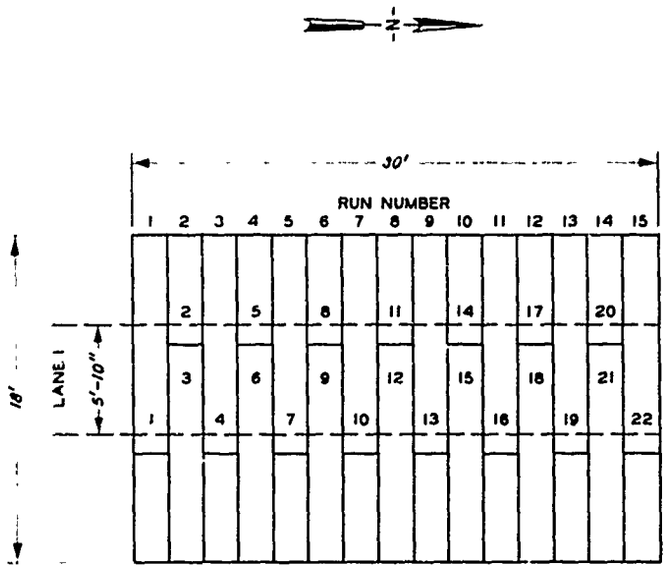


PLAN

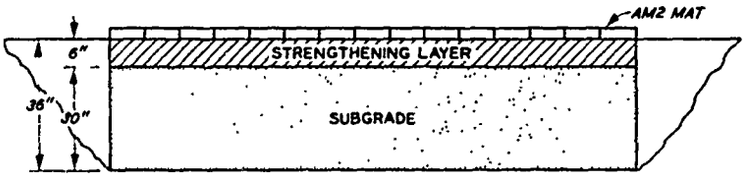


PROFILE

NOTE: NUMBERS INSIDE PANELS INDICATE PANEL NUMBERS.

PLAN AND PROFILE
TEST SECTION V

PLATE 5

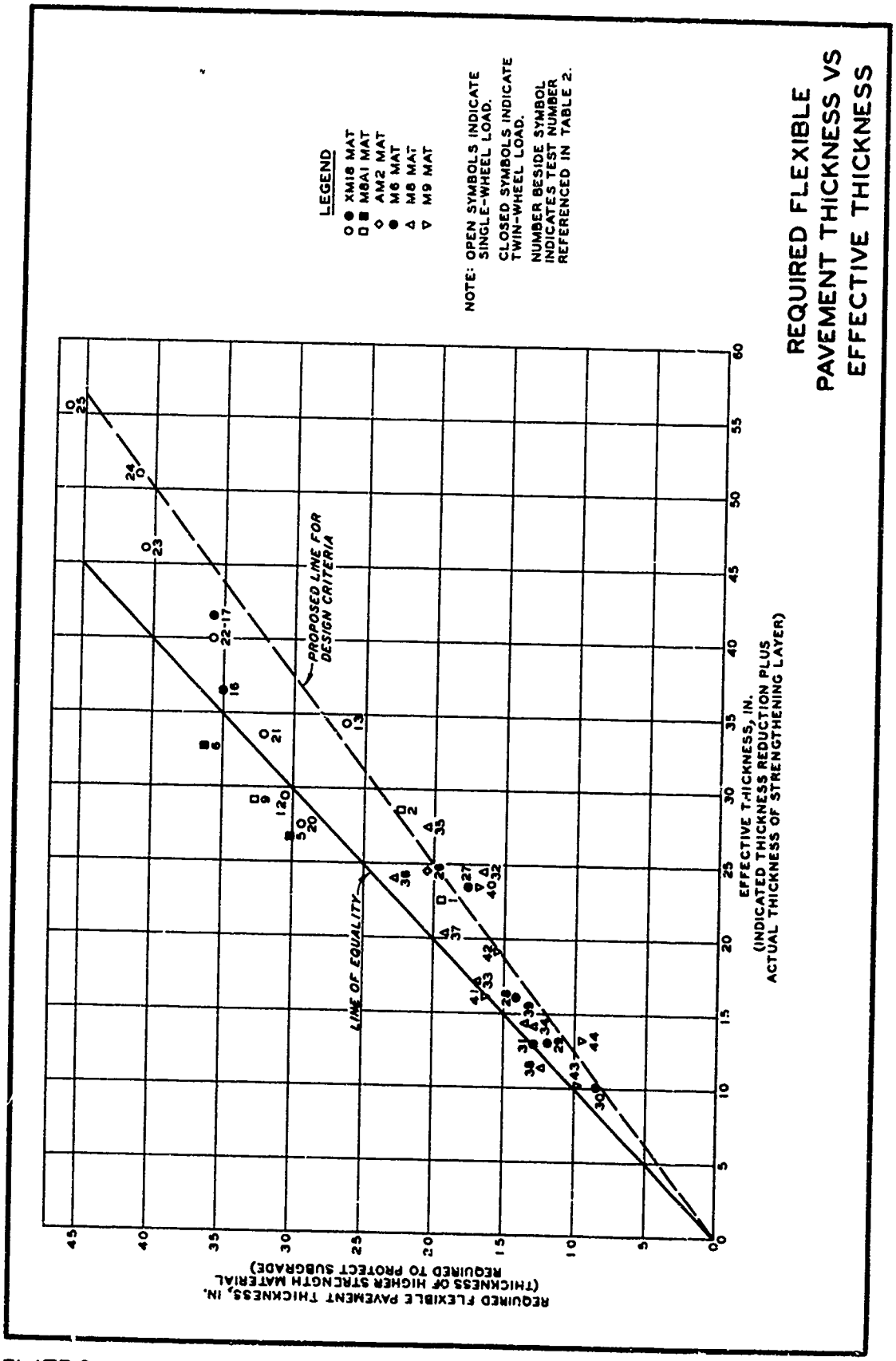
REQUIRED FLEXIBLE PAVEMENT THICKNESS VS EFFECTIVE THICKNESS
LEGEND
XM18 MAT
M8AI MAT
AM2 MAT
M6 MAT
M8 MAT
M9 MAT
NOTE: OPEN SYMBOLS INDICATE SINGLE-WHEEL LOAD.
CLOSED SYMBOLS INDICATE TWIN-WHEEL LOAD.
NUMBER BESIDE SYMBOL INDICATES TEST NUMBER REFERENCED IN TABLE 2.
PROPOSED LINE FOR DESIGN CRITERIA
LINE OF EQUALITY
REQUIRED FLEXIBLE PAVEMENT THICKNESS, IN. (THICKNESS OF HIGHER STRENGTH MATERIAL REQUIRED TO PROTECT SUBGRADE)
EFFECTIVE THICKNESS, IN. (INDICATED THICKNESS REDUCTION PLUS ACTUAL THICKNESS OF STRENGTHENING LAYER)

PLATE 6

# Appendix A: Traffic Tests

1. Five test sections were constructed and trafficked under controlled conditions to provide the performance data required to develop a method for determining soil thickness requirements for landing-mat-surfaced airfields. Details of the traffic tests are documented in this appendix.

## Test Section I

2. A plan and profile of test section I are shown in plate A1. The plan of lane 3 is shown separately in plate A1 for clarity. Traffic distribution patterns for lanes 1, 2, and 3 are shown in plate A2. A 31,000-lb single-wheel load utilizing a 56x16 tire with an inflation pressure of 185 psi was used to traffic lane 1. Lane 2 was trafficked with a 56,000-lb twin-wheel load utilizing 56x16 tires with an inflation pressure of 105 psi. After 612 coverages, the load was increased to 62,000 lb with an inflation pressure of 185 psi. Lane 3 was trafficked with a 62,000-lb twin-wheel load utilizing 56x16 tires with an inflation pressure of 185 psi. Soils and mat breakage data for the test section are summarized in tables A1 and A2, respectively.

### Lane 1

3. Item 1. A view of item 1 prior to traffic is shown in photograph A1. There was considerable permanent deformation of the mat with the application of traffic, and by 10 coverages, longitudinal deformation averaged about 1.9 in. Traffic was continued to 30 coverages, at which time item 1 was considered failed due to excessive roughness. At failure, three panels had cover-plate weld breaks. Photograph A2 shows permanent deformation of 3.2 in. at one location; average deformation was about 2.3 in. for the test item at 30 coverages. An overall view of item 1 at failure is shown in photograph A3.

4. Item 2. An overall view of item 2 prior to traffic is shown in photograph A4. Permanent deformation of the mat was observed immediately after application of traffic, and after 30 coverages, longitudinal deformation averaged 1.1 in. Mat breakage was first observed at approximately

70 coverages with the occurrence of locking-lug breaks. At 110 coverages, six locking lugs had broken, and permanent deformation and roughness had become excessive. Item 2 was considered failed at 110 coverages, and an overall view of the item at failure is shown in photograph A5.

5. Item 3. An overall view of item 3 prior to traffic is shown in photograph A6. Deformation of the mat, which did not deform so rapidly as that in items 1 and 2, averaged about 0.8 in. after 30 coverages. Deformation increased very slowly with increased traffic. Mat breakage was first observed at approximately 170 coverages with the occurrence of two locking-lug breaks. As traffic continued, mat breakage and deformation increased rapidly, and at 310 coverages, item 3 was considered failed. Deformation at failure averaged about 2 in. Failure was due primarily to mat breakage. An overall view of item 3 at failure is shown in photograph A7.

6. Item 4. An overall view of item 4 prior to traffic is shown in photograph A8. Permanent mat deformation developed slowly during the application of traffic. The first mat breakage, locking-lug breaks, was observed at approximately 230 coverages. Mat breakage progressed with increased traffic, and after 430 coverages, item 4 was considered failed due to excessive mat breakage. Photograph A9 shows a typical locking-lug break, and an overall view of item 4 at failure is shown in photograph A10.

7. Permanent deformation. Permanent deformation of each item in lane 1, as determined from level readings taken prior to and at intervals throughout the traffic test period, is shown in plate A3. The deformation values in plate A3 are averages of two readings taken in each item. Center-line profiles, illustrating deformation of the mat along the center line of each test item, are shown in plate A4.

8. Mat deflection. Deflections of the mat surface under static load were determined from level readings and are shown in plate A5. Deflections are shown for two panel locations prior to traffic and at failure of each test item.

Lane 2

9. Item 1. An overall view of item 1 prior to traffic is shown in photograph A11. Permanent mat deformation developed at a uniform rate with the application of traffic. After 120 coverages, the subgrade had deformed

sufficiently to consider item 1 failed. An overall view of item 1 at failure is shown in photograph A12.

10. Item 2. An overall view of item 2 prior to traffic is shown in photograph A13. Permanent deformation of the mat developed very slowly with the application of traffic. By 120 coverages, longitudinal deformation averaged about 1.0 in. Mat breakage was first observed at 360 coverages. Breakage developed slowly, and after 612 coverages, only three breaks were observed. At this time, item 2 was considered failed because of excessive roughness. An overall view of item 2 at failure is shown in photograph A14.

11. Item 3. An overall view of item 3 prior to traffic is shown in photograph A15. No apparent distress was observed in item 3 during 612 coverages. After 612 coverages, the test load was increased from 56,000 to 62,000 lb, and the tire inflation pressure was increased from 105 to 185 psi. Photograph A16 shows item 3 at 612 coverages prior to trafficking with the revised test load. The first sign of distress, a locking-lug break, was noted after an additional 192 coverages had been applied. After 312 additional coverages (924 coverages of mixed traffic), tire hazards had developed from excessive mat breakage, as shown in photograph A17, and item 3 was considered failed. An overall view of item 3 at failure is shown in photograph A18. Item 3 received a total of 924 coverages.

12. Item 4. An overall view of item 4 prior to traffic is shown in photograph A19. The mat showed no signs of distress by 612 coverages, and additional traffic was applied with the revised load described in the preceding paragraph. After an additional 288 coverages, the first mat break was observed. After 350 additional coverages, mat breakage began to develop rapidly, and after 432 additional coverages (1044 total coverages), item 4 had developed serious tire hazards and was considered failed. An overall view of item 4 at failure is shown in photograph A20. Item 4 received a total of 1044 coverages.

13. Permanent deformation. Permanent deformation of each item in lane 2, as determined from level readings taken prior to and at intervals throughout the traffic test period, is shown in plate A6. The deformation values are averages of two readings taken in each item. Center-line

profiles, illustrating deformation along the center line of each test item, are shown in plate A7.

14. Mat deflection. Deflections of the mat under static load were determined from level readings and are shown in plate A8. The deflections shown are for two panel locations prior to traffic and at failure of each test item.

Lane 3

15. After traffic had been completed on lanes 1 and 2, the M8A1 landing mat was removed from the test section, and new panels of M8A1 were placed so that lane 3 was positioned in the untrafficked area between lanes 1 and 2 as shown in plate A1. Item 1 was not trafficked in lane 3.

16. Item 2. An overall view of item 2 prior to traffic is shown in photograph A21. As traffic was applied, permanent deformation of the mat was fairly rapid, and after 120 coverages, item 2 was considered failed due to excessive roughness. There was no mat breakage at failure. An overall view of item 2 at failure is shown in photograph A22.

17. Item 3. An overall view of item 3 prior to traffic is shown in photograph A23. Permanent deformation developed slowly with continued traffic. The first mat breakage was observed at 228 coverages. Traffic was continued to 408 coverages, at which time item 3 was considered failed due to excessive roughness. An overall view of item 3 at failure is shown in photograph A24.

18. Item 4. An overall view of item 4 prior to traffic is shown in photograph A25. Mat deformation developed slowly, and the first mat breakage was observed at approximately 385 coverages. With increased traffic, roughness began to develop, and at 750 coverages, item 4 was failed due to excessive roughness and tire hazards caused by mat breakage. An overall view of item 4 at failure is shown in photograph A26.

19. Permanent deformation. Permanent deformation of each item in lane 3, as determined from level readings taken prior to and at intervals throughout the traffic test period, is shown in plate A9. The deformation values in plate A9 are averages of two readings taken in each item. Center-line profiles, illustrating deformation of the mat along the center line of each test item, are shown in plate A10.

20. Mat deflection. Deflections of the mat surface under static load were determined from level readings and are shown in plate A11. The deflections are shown for two locations prior to traffic and at failure of each test item.

## Test Section II

21. A plan and profile of test section II are shown in plate A12. Traffic distribution patterns and tire characteristics for lanes 1 and 2 are shown in plate A13. A 30,000-lb single-wheel load utilizing a 30x11.5 tire with an inflation pressure of 250 psi was used to traffic lane 1. Lane 2 was trafficked with a 70,000-lb twin-wheel load utilizing 44x16 tires with an inflation pressure of 185 psi. Soils and mat breakage data are summarized in tables A1 and A3, respectively.

### Lane 1

22. Item 1. An overall view of item 1 prior to traffic is shown in photograph A27. Mat roughness in item 1 was observed after three coverages, and after 12 coverages, dishing measured 0.75 in. in the transverse direction in one location, as shown in photograph A28. Photograph A29 shows longitudinal deformation of about 1 in., as measured on panel 13. By 32 coverages, the bottom lip of the overlapping end joint in panel 5 had sheared off, causing panel 4 to deflect under the wheel load. After 54 coverages, the C-rail of panel 4 was extensively damaged (see photograph A30), and panels 4 and 5 were replaced. After 72 coverages, item 1 was considered failed due to excessive roughness. An overall view of item 1 at failure is shown in photograph A31.

23. Item 2. An overall view of item 2 prior to traffic is shown in photograph A32. Permanent mat deformation was observed at approximately eight coverages. By 100 coverages, longitudinal deformation averaged about 1.7 in. After 170 coverages, item 2 was considered failed due to excessive roughness. Longitudinal deformation at failure averaged 1.8 in. No mat breakage was observed in item 2 throughout the period of traffic. An overall view of item 2 at failure is shown in photograph A33.

24. Item 3. An overall view of item 3 prior to traffic is shown in

photograph A34. Permanent mat deformation, observed initially after several coverages, increased slowly with continued traffic. By 100 coverages, longitudinal deformation averaged 1.0 in. The first sign of mat breakage, an internal rib failure, was observed at 142 coverages. After 202 coverages, item 3 was considered failed due to excessive roughness caused by subgrade deformation. An overall view of item 3 at failure is shown in photograph A35.

25. Item 4. An overall view of item 4 prior to traffic is shown in photograph A36. Permanent mat deformation developed slowly as traffic was applied. Longitudinal deformation averaged 1.3 in. after 100 coverages and increased to 2.5 in. by 202 coverages. After 202 coverages, item 4 was considered failed due to excessive deformation of the mat. At failure one panel was observed with internal rib failures, and one panel was observed with a damaged C-rail. An overall view of item 4 at failure is shown in photograph A37.

26. Permanent deformation. Permanent deformation of the mat for each test item in lane 1, as determined from level readings taken prior to and at intervals throughout the traffic test period, is shown in plate A14. Level readings were recorded from two locations in each test item, and the curves in plate A14 were plotted from average deformation measurements. Center-line profiles illustrating deformation of the mat along the center line of each test item are shown in plate A15.

27. Mat deflection. Deflections of the mat surface under static load were determined from level readings and are shown in plate A16. The deflections are shown for two panel locations prior to traffic and at failure of each test item.

Lane 2

28. Item 1. An overall view of item 1 prior to traffic is shown in photograph A38. Permanent deformation was observed after the first coverage and developed very rapidly with increased traffic. By 32 coverages, longitudinal deformation averaged 2.3 in., and item 1 was considered failed. At failure, three panels had disconnected along the C-rail and male connectors, as shown in photograph A39. The bottom lip of an overlapping end joint had also sheared in one panel. An overall view of item 1

at failure is shown in photograph A40.

29. Item 2. An overall view of item 2 prior to traffic is shown in photograph A41. Longitudinal deformation measured 1.13 in. after 32 coverages. Mat breakage was first observed after 48 coverages. The bottom lip of an overlapping end joint had sheared on one panel, and two panels had disconnected along the C-rail and male connectors. Item 2 was considered failed after 60 coverages due to excessive deformation and mat breakage. Photograph A42 shows a typical overlapping end-joint failure. An overall view of item 2 at failure is shown in photograph A43.

30. Item 3. An overall view of item 3 prior to traffic is shown in photograph A44. No serious mat damage occurred in item 3 during the first 60 coverages; however, longitudinal deformation averaged 1.2 in. The first mat failure occurred at 120 coverages, at which time two panels had disconnected along the C-rail and male connectors. By 144 coverages, excessive mat breakage, as shown in photograph A45, had occurred and longitudinal deformation had increased to 3.1 in., as shown in photograph A46. Failure of item 3 at this coverage level was attributed to excessive mat deformation and mat breakage caused by subgrade deformation. An overall view of item 3 at failure is shown in photograph A47.

31. Item 4. An overall view of item 4 prior to traffic is shown in photograph A48. Little deformation and no mat breakage were observed in item 4 prior to 144 coverages. At 228 coverages, the bottom lip of an overlapping end connector sheared. Permanent deformation started to develop very rapidly after 228 coverages, and after 300 coverages, item 4 was considered failed due to excessive longitudinal deformation (2.8 in., see photograph A49) and mat breakage. An overall view of item 4 at failure is shown in photograph A50.

32. Permanent deformation. Permanent deformation of the mat for each test item in lane 2, as determined from level readings taken prior to and at intervals throughout the traffic test period, is shown in plate A17. The plots in plate A17 show the differential deformation of the mat at failure. Center-line profiles, illustrating deformation along the center line of each test item, are shown in plate A18.

33. Mat deflection. Elastic deflections of the mat surface under

static load were determined from level readings and are shown in plate A19. The deflections are shown for two panel locations prior to traffic and at failure of each test item.

## Test Section III

34. A plan and profile of test section III are shown in plate A20. Traffic distribution patterns and tire characteristics for lanes 1 and 2 are shown in plate A21. A 25,000-lb single-wheel load utilizing a 30x11.5 tire with an inflation pressure of 250 psi was used to traffic lane 1. Lane 2 was trafficked with a 75,000-lb single-wheel load utilizing a 25.00x28 tire with an inflation pressure of 125 psi. Soils and mat breakage data are summarized in tables A1 and A3, respectively.

### Lane 1

35. Item 1. A view of item 1 prior to traffic is shown in photograph A51. The first sign of mat breakage, noted at 42 coverages, was a weld crack along the underlapping end joint of panel 29. At 200 coverages, the weld crack had progressed along the width of the panel; however, the panel was not considered a tire hazard at this time (see photograph A52). At this coverage level, similar weld cracks had also developed in panels 28 (adjacent to panel 29) and 14. As traffic continued, top skin tears developed parallel to the C-rail in panels 28 and 29, and at 314 coverages, the panels were considered failed and were replaced. A surface depression, indicative of an internal rib failure, had also developed in panel 30; however, the damage was slight and did not warrant removal of the panel. Portions of panels 28, 29, and 30 are shown in photograph A53.

36. Traffic was resumed after replacement of failed panels 28 and 29, and at 374 coverages, five additional panels showed evidence of internal rib failures. The rib failures developed slowly with continued traffic, but no serious damage occurred until 500 coverages had been completed. At this point, the mat began to deteriorate very rapidly. The top lip of the underlapping end joint of panel 14 sheared off at 526 coverages, and at 528 coverages, the locking bar between panels 13 and 14 was forced from the panels, as shown in photograph A54. Item 1 was considered failed at

528 coverages due to excessive roughness and mat breakage. An overall view of item 1 at failure is shown in photograph A55.

37. Item 2. A view of item 2 prior to traffic is shown in photograph A56. No distress was noted in item 2 until surface depressions, indications of internal rib failures, developed in panels 51 and 54 at 400 coverages. At 477 coverages, a top skin tear developed at a location corresponding to an internal rib failure in panel 51. Photograph A57 shows the skin tear at 528 coverages. Panels 51 and 54 were considered failed at 569 coverages and were replaced. Several additional panels had developed evidence of internal rib failures at this time; however, the damage was slight, and the panels were not considered hazardous to tires during aircraft operations. At 720 coverages, top skin tears and depressions from internal rib failures in panel 48 became a serious tire hazard, as shown in photograph A58. The top lip of the underlapping end joint in panel 47 had also sheared off at this time, and both panels were replaced. Traffic was continued to 884 coverages before the entire test item was considered failed. Photographs A59 and A60, respectively, show depressions from internal rib failures and top skin tears of typical failed panels. Failure of item 2 was attributed to excessive mat breakage (rib failures and skin tears). An overall view of item 2 at failure is shown in photograph A61.

38. Permanent deformation. Permanent deformation of the mat, as determined from level readings taken prior to and at the end of traffic, is shown in plate A22. Since the mat was laid in a staggered pattern, an end joint in every other run of mat was located on the center line of the traffic lane. In adjacent runs, the center of a panel was located on the center line of the traffic lane. Plate A22 shows the average cross section for both conditions for each test item of the test lane. These data indicate that the deformation across the traffic lane was generally about the same regardless of where the joint was located. Subgrade deformation at failure is shown in plate A23. Center-line profiles, illustrating deformation of the mat along the center line of each test item, are shown in plate A24.

39. Mat deflection. Deflections of the mat surface under static load were determined from level readings and are shown in plate A25. The

deflections shown are for two panel locations prior to traffic and at failure of each test item.

Lane 2

40. Item 1. An overall view of item 1 prior to traffic is shown in photograph A62. Evidence of internal rib failures developed in 18 panels at approximately 11 coverages. At 16 coverages, the top lip of the overlapping end joint sheared off in panel 17. The resulting failure, as shown in photograph A63, was a tire hazard and the panel was replaced. At 48 coverages, a similar failure occurred in panel 29. Panel 32 was also failed at 48 coverages due to internal rib failures. The panels were replaced, and traffic was continued to 56 coverages, at which time the entire test item was considered failed. Failure of the test item was attributed chiefly to the failure of the end joints, although approximately 50 percent of all of the panels had internal rib failures. Typical mat failure is shown in photograph A64. An overall view of item 1 at failure is shown in photograph A65.

41. Item 2. A view of item 2 prior to traffic is shown in photograph A66. Depressions caused by internal rib failures were first noted at 16 coverages. The damage was slight, however, and did not present a hazard to continued operation. At 28 coverages, the bottom lip of the overlapping end joint of panel 41 sheared off. Five additional panels were damaged in a similar manner after 60 coverages. These failures in turn led to C-rail failures of the panels in the adjacent runs. Traffic was stopped at 72 coverages, and item 2 was considered failed due to excessive roughness and mat breakage. An overall view of item 2 at failure is shown in photograph A67.

42. Item 3. An overall view of item 3 prior to traffic is shown in photograph A68. Breakage was first noted at approximately 16 coverages, at which time depressions that indicated internal rib failures developed. The damaged ribs, however, did not present a tire hazard throughout the period of traffic. The first major distress occurred at 22 coverages when the bottom lip of the overlapping end joint sheared on panels 101 and 113. A similar break occurred in panel 97 at 48 coverages, as shown in photograph A69. In photograph A69, it can be seen that the panel adjacent to panel 97 is

depressed. This depression resulted from support loss caused by the failed overlapping end joint. Traffic was continued to 92 coverages, and although no panels were replaced during the traffic test period, the entire test item was failed at 92 coverages due to roughness and tire hazards caused by end-joint failures. An overall view of item 3 at failure is shown in photograph A70.

43. Permanent deformation. Permanent deformation of the mat, determined from level readings taken prior to and at the end of traffic, is plotted in plate A26 as the differential deformation at failure. The average cross section for each test item is shown in plate A26. Cross sections of subgrade deformation for items 1, 2, and 3 are shown in plate A27. Center-line profiles, illustrating deformation along the center line of each test item, are shown in plate A28.

44. Mat deflection. Deflections of the mat surface under static load were determined from level readings and are shown in plate A29. The deflections are shown for two locations.

## Test Section IV

45. A plan and profile of test section IV are shown in plate A30. The test section consisted of only one test item and was trafficked with a 60,000-lb single-wheel load utilizing a 25.00x28 tire with an inflation pressure of 125 psi. The traffic distribution pattern and tire characteristics for the test section are shown in plate A31. Soils and mat breakage data are summarized in tables A1 and A3, respectively.

46. An overall view of the test section prior to traffic is shown in photograph A71. A depression caused by the failure of an internal rib was the first sign of mat breakage. After 42 coverages, damaged ribs were apparent in 18 panels. The damage was slight, however, and traffic was continued. After approximately 190 coverages, it was observed that the bottom lip of the overlapping end joint had completely sheared off panel 33. A similar break was noted in panel 1 after 216 coverages. After 232 coverages, panel 33 was considered a tire hazard for further aircraft operation and was replaced. Panel 35, in the run adjacent to the run containing

panel 33, also had extensive C-rail damage and was replaced after 232 coverages. After 298 coverages, two additional panels were failed and replaced due to the failure of the bottom lip of the overlapping end joint and damaged C-rails. Traffic was continued until completion of 348 coverages, at which time the test section was considered failed due to excessive mat breakage. Photographs A72 and A73 show typical views of top skin tears at failure. An overall view of the test section at failure is shown in photograph A74.

47. Permanent deformation of the mat was determined from level readings taken prior to and at the end of traffic. Plate A32 shows the differential deformation at failure. A cross section of the subgrade deformation at failure is shown in plate A33. A center-line profile, illustrating deformation along the center line of the test section, is shown in plate A34.

48. Deflections of the mat surface under static load were determined from level readings and are shown in plate A35. The deflections are shown for two locations prior to traffic and at failure of the test section.

## Test Section V

49. A plan and profile of test section V are shown in plate A36. The test section consisted of one test item and was surfaced with one-, two-, and three-piece AM2 landing mat and was trafficked with a 25,000-lb single-wheel load utilizing a 30x11.5 tire with an inflation pressure of 250 psi. The traffic distribution pattern and tire characteristics for the test section are shown in plate A37. Soils and mat breakage data are presented in tables A1 and A3, respectively.

50. An overall view of the test section prior to traffic is shown in photograph A75. Mat breakage was first observed at approximately 75 coverages, with end-joint weld breaks occurring in three panels. By 100 coverages, the breaks averaged about 5 in. in length. After 120 coverages, two additional panels developed similar weld breaks, and after 140 coverages, the end joint of one panel had completely sheared off. The panel was replaced, and traffic was continued. A similar failure occurred after 210 coverages. By 330 coverages, a total of 10 panels had failed due to weld

breaks. In four of these panels, the end connector had completely sheared off. A typical weld break is shown in photograph A76. Traffic was stopped at 330 coverages, and the test section was considered failed due to excessive mat breakage. Photograph A77 shows an overall view of test section V at failure.

51. Permanent deformation of the mat was determined from level readings taken prior to and at the end of traffic. Cross-section plots showing the differential deformation at failure are shown in plate A38. A center-line profile, showing the differential deformation at failure along the center line of the test section, is shown in plate A39.

52. Deflections of the mat surface under static load were determined from level readings and are shown in plate A40. The deflections are shown for two locations prior to traffic and at failure of the test section.

Table A1

Summary of CBR, Water Content, and Dry Density Data

| Lane | Test Item | Traffic Coverages | Depth in. | CBR | Water Content % | Dry Density pcf |
|---|---|---|---|---|---|---|
| | | | **Test Section I** | | | |
| 1 | 1 | 0 | 0 | 5 | 27.9 | 91.3 |
| | | | 8 | 1.5 | 32.9 | 84.1 |
| | | | 12 | 2.9 | 32.5 | 86.? |
| | | 30 | 0 | 6 | 27.5 | 93.6 |
| | | | 8 | 2.0 | 33.1 | 84.3 |
| | | | 14 | 2.6 | 31.8 | 86.4 |
| | 2 | 0 | 0 | 5 | 26.9 | 92.4 |
| | | | 6 | 9 | 26.4 | 93.5 |
| | | | 14 | 2.5 | 32.5 | 86.7 |
| | | | 20 | 3.5 | 32.0 | 88.0 |
| | | 110 | 0 | 6 | 25.7 | 93.7 |
| | | | 6 | 6 | 26.7 | 94.8 |
| | | | 14 | 2.7 | 31.6 | 87.5 |
| | | | 20 | 2.6 | 31.5 | 87.4 |
| | 3 | 0 | 0 | 6 | 27.2 | 93.9 |
| | | | 8 | 8 | 26.3 | 96.7 |
| | | | 14 | 9 | 25.6 | 95.4 |
| | | | 22 | 3.3 | 28.8 | 89.2 |
| | | | 28 | 2.3 | 32.8 | 87.8 |
| | | 310 | 0 | 7 | 25.1 | 93.8 |
| | | | 8 | 8 | 25.4 | 95.7 |
| | | | 14 | 8 | 25.1 | 94.9 |
| | | | 22 | 4.7 | 28.8 | 91.3 |
| | | | 28 | 2.3 | 31.4 | 87.3 |
| | 4 | 0 | 0 | 5 | 27.5 | 95.3 |
| | | | 6 | 7 | 26.6 | 92.5 |
| | | | 12 | 6 | 25.7 | 94.6 |
| | | | 18 | 6 | 26.3 | 92.7 |
| | | | 26 | 2.4 | 31.6 | 86.6 |
| | | | 30 | 3.1 | 28.5 | 89.5 |
| 1 | 4 | 430 | 0 | 8 | 24.5 | 96.5 |
| | | | 6 | 6 | 25.6 | 95.4 |
| | | | 12 | 8 | 24.3 | 94.7 |
| | | | 18 | 6 | 26.8 | 93.2 |
| | | 26 | 26 | 3.1 | 31.2 | 88.9 |
| | | | 30 | 4.1 | 29.5 | 91.8 |
| 2 | 1 | 0 | 0 | 5 | 27.7 | 93.4 |
| | | | 8 | 1.9 | 33.6 | 83.6 |
| | | | 14 | 3.0 | 32.5 | 86.4 |
| | | 120 | 0 | 4.9 | 27.4 | 92.9 |
| | | | 8 | 2.1 | 30.9 | 83.9 |
| | | | 14 | 2.2 | 32.5 | 86.0 |
| | 2 | 0 | 0 | 5 | 26.9 | 92.3 |
| | | | 6 | 6 | 27.7 | 95.1 |
| | | | 14 | 2.5 | 33.0 | 84.3 |
| | | | 20 | 3.9 | 30.8 | 87.6 |
| | | 612 | 0 | 7 | 25.9 | 95.9 |
| | | | 6 | 5 | 26.8 | 93.5 |
| | | | 14 | 2.1 | 32.4 | 85.9 |
| | | | 20 | 2.7 | 31.8 | 87.5 |
| | 3 | 0 | 0 | 4.7 | 28.3 | 93.0 |
| | | | 8 | 5 | 26.7 | 94.7 |
| | | | 14 | 6 | 25.9 | 91.6 |
| | | | 22 | 2.7 | 29.4 | 88.3 |
| | | | 28 | 3.2 | 31.0 | 88.7 |
| | | 924 | 0 | 6 | 27.7 | 93.9 |
| | | | 8 | 9 | 25.6 | 95.4 |
| | | | 14 | 7 | 27.2 | 92.1 |
| | | | 22 | 3.2 | 30.6 | 87.6 |
| | | | 28 | 2.4 | 32.6 | 87.2 |
| | 4 | 0 | 0 | 6 | 27.8 | 95.7 |
| | | | 6 | 6 | 26.6 | 93.9 |
| | | | 12 | 8 | 25.3 | 93.6 |
| | | | 18 | 8 | 27.0 | 91.7 |
| | | | 26 | 2.0 | 33.3 | 85.7 |
| | | | 30 | 3.0 | 30.6 | 88.1 |
| 2 | 4 | 1044 | 0 | 7 | 26.4 | 94.9 |
| | | | 6 | 6 | 27.1 | 93.9 |
| | | | 14 | 8 | 25.6 | 94.3 |
| | | | 26 | 2.9 | 30.6 | 89.2 |
| | | | 30 | 3.4 | 29.5 | 91.7 |
| 3 | 2 | 0 | 0 | 5 | 26.9 | 92.4 |
| | | | 6 | 7 | 27.0 | 94.3 |
| | | | 14 | 2.5 | 32.7 | 85.5 |
| | | | 20 | 3.7 | 31.4 | 87.8 |
| | | 120 | 0 | 8 | 25.1 | 96.4 |
| | | | 6 | 5 | 27.9 | 94.3 |
| | | | 14 | 1.9 | 32.1 | 86.3 |
| | | | 20 | 1.9 | 31.8 | 86.7 |
| | 3 | 0 | 0 | 5 | 27.7 | 93.5 |
| | | | 6 | 7 | 26.5 | 95.2 |
| | | | 14 | 9 | 25.8 | 93.5 |
| | | | 22 | 3.0 | 29.1 | 88.7 |
| | | | 28 | 2.7 | 31.9 | 88.2 |
| | | | **Test Section I (Continued)** | | | |
| 3 (Cont'd) | | 408 | 0 | 8 | 25.4 | 95.0 |
| | | | 8 | 8 | 25.2 | 96.0 |
| | | | 22 | 3.4 | 28.9 | 87.4 |
| | | | 28 | 2.9 | 30.9 | 88.0 |
| | 4 | 0 | 0 | 6 | 27.7 | 95.5 |
| | | | 6 | 6 | 26.6 | 93.2 |
| | | | 12 | 7 | 25.5 | 94.1 |
| | | | 18 | 7 | 26.7 | 92.2 |
| | | | 26 | 2.2 | 32.5 | 86.1 |
| | | | 30 | 3.1 | 29.6 | 88.8 |
| | | 750 | 0 | 8 | 25.4 | 94.1 |
| | | | 8 | 8 | 25.8 | 95.6 |
| | | | 16 | 6 | 27.2 | 92.8 |
| | | | 26 | 2.5 | 31.7 | 87.8 |
| | | | 30 | 4.0 | 30.0 | 88.5 |
| | | | **Test Section II** | | | |
| 1 | 1 | 0 | 0 | 2.9 | 32.3 | 84.5 |
| | | | 8 | 1.1 | 38.7 | 78.8 |
| | | | 16 | 1.0 | 39.8 | 78.5 |
| | | | 24 | 1.8 | 38.7 | 78.1 |
| | | 72 | 0 | 3.2 | 32.3 | 86.2 |
| | | | 8 | 1.3 | 35.1 | 80.2 |
| | | | 16 | 0.9 | 37.6 | 78.4 |
| | | | 24 | 1.7 | 38.9 | 78.5 |
| | 2 | 0 | 0 | 2.3 | 33.5 | 84.4 |
| | | | 6 | 3.2 | 32.6 | 85.4 |
| | | | 12 | 2.2 | 34.8 | 80.2 |
| | | | 18 | 2.3 | 35.5 | 81.5 |
| | | | 24 | 2.0 | 37.6 | 80.7 |
| | | 170 | 0 | 3.0 | 34.1 | 86.5 |
| | | | 6 | 3.9 | 32.2 | 86.6 |
| | | | 14 | 2.8 | 35.3 | 80.6 |
| | | | 22 | 2.2 | 37.0 | 82.2 |
| | 3 | 0 | 0 | 2.8 | 33.5 | 84.8 |
| | | | 8 | 3.5 | 32.1 | 86.9 |
| | | | 16 | 3.2 | 32.9 | 86.9 |
| | | | 24 | 1.4 | 38.8 | 78.6 |
| | | 202 | 0 | 3.5 | 31.6 | 86.8 |
| | | | 6 | 2.9 | 32.8 | 87.1 |
| | | | 12 | 4.2 | 31.0 | 85.8 |
| | | | 20 | 1.1 | 39.9 | 77.3 |
| | | | 26 | 1.? | 37.3 | 82.2 |
| | 4 | 0 | 0 | 3.1 | 7 | 84.5 |
| | | | 6 | 3.3 | .7 | 87.6 |
| | | | 12 | 3.5 | .1 | 82.2 |
| | | | 18 | 4.1 | 31.8 | 85.4 |
| | | | 0 | 3.6 | 32.5 | 84.9 |
| | | | 6 | 2.9 | 32.5 | 85.8 |
| | | | 12 | 3.4 | 32.4 | 85.2 |
| 2 | 1 | 0 | | 2.5 | 32.6 | 83.4 |
| | | | | 1.3 | 35.1 | 78.8 |
| | | | 16 | 0.8 | 40.5 | 76.7 |
| | | | 24 | 1.6 | 35.9 | 79.7 |
| | | 32 | 0 | 4.1 | 31.2 | 84.8 |
| | | | 8 | 2.0 | 34.1 | 80.0 |
| | | | 16 | 1.0 | 38.9 | 78.5 |
| | | | 24 | 1.7 | 37.6 | 80.1 |
| | 2 | 0 | 0 | 2.1 | 33.8 | 83.3 |
| | | | 6 | 2.8 | 33.1 | 84.2 |
| | | | 12 | 1.6 | 39.0 | 79.2 |
| | | | 18 | 2.3 | 36.7 | 79.2 |
| | | | 24 | 2.? | 38.2 | 79.9 |
| | | 60 | 0 | 3.8 | 30.8 | 87.7 |
| | | | 6 | 3.3 | 31.1 | 89.6 |
| | | | 14 | 1.4 | 35.6 | 80.9 |
| | | | 22 | 1.2 | 38.3 | 79.1 |
| | 3 | 0 | 0 | 2.2 | 32.2 | 84.7 |
| | | | 8 | 3.2 | 32.0 | 84.8 |
| | | | 16 | 2.0 | 33.7 | 80.9 |
| | | | 24 | 2.0 | 37.4 | 79.2 |
| | | 114 | 0 | 3.6 | 31.3 | 87.4 |
| | | | ? | 3.3 | 30.5 | 87.2 |
| | | | 12 | 6.0 | 29.1 | 90.0 |
| | | | 20 | 1.4 | 40.2 | 77.1 |
| | | | 26 | 1.3 | 35.1 | 84.3 |
| | 4 | 0 | 0 | 2.3 | 33.9 | 83.6 |
| | | | 6 | 3.4 | 31.1 | 86.6 |
| | | | 12 | 3.4 | 31.8 | 86.3 |
| | | | 18 | 3.8 | 31.9 | 85.3 |
| | | | 0 | 4.5 | 29.8 | 87.3 |
| | | | 6 | 4.2 | 30.5 | 87.6 |
| | | | 12 | 4.1 | 30.9 | 88.2 |
| | | | **Test Section III** | | | |
| 1 | 1 | 0 | 0 | 8 | 26.7 | 93.2 |
| | | | 6 | 1.5 | 34.3 | 83.7 |
| | | | 12 | 1.9 | 34.7 | 83.6 |
| | | | 18 | 2.8 | 34.8 | 83.1 |
| | | 528 | 0 | 6 | 26.8 | 94.0 |
| | | | 6 | 1.8 | 34.4 | 84.6 |
| | | | 12 | 1.9 | 34.8 | 84.2 |
| | | | 18 | 2.7 | 34.4 | 83.9 |
| | 2 | 0 | 0 | 8 | 26.0 | 93.0 |
| | | | 6 | 4.0 | 28.4 | 90.7 |
| | | | 12 | 1.5 | 35.2 | 82.4 |
| | | | 18 | 1.6 | 35.9 | 81.7 |
| | | | 24 | 1.8 | 35.5 | 82.2 |
| | | 528 | 0 | 9 | 25.5 | 94.7 |
| | | | 6 | 7 | 27.8 | 91.5 |
| | | | 12 | 2.5 | 34.4 | 83.0 |
| | | | 18 | 2.1 | 34.4 | 82.4 |
| | | | 24 | 1.9 | 34.3 | 82.2 |
| 2 | 1 | 0 | 0 | 8 | 25.7 | 93.2 |
| | | | 6 | 1.5 | 34.3 | 83.7 |
| | | | 12 | 1.9 | 34.7 | 83.6 |
| | | | 16 | 2.8 | 34.5 | 83.1 |
| | | 56 | 0 | 7 | 25.5 | 94.0 |
| | | | 6 | 2.3 | 33.8 | 84.6 |
| | | | 12 | 2.2 | 33.8 | 83.9 |
| | | | 18 | 1.8 | 34.6 | 82.6 |
| 2 | 2 | 0 | 0 | 8 | 26.0 | 93.0 |
| | | | 6 | 4.0 | 28.4 | 90.7 |
| | | | 12 | 1.5 | 35.2 | 82.4 |
| | | | 18 | 1.6 | 35.9 | 81.7 |
| | | | 24 | 1.8 | 35.5 | 82.2 |
| | | 72 | 0 | 1.0 | 25.1 | 96.5 |
| | | | 6 | 5.4 | 27.9 | 92.2 |
| | | | 12 | 2.1 | 35.7 | 82.6 |
| | | | 18 | 1.6 | 36.6 | 81.4 |
| | | | 24 | 2.0 | 33.1 | 84.7 |
| | 3 | 0 | 0 | 8 | 26.4 | 92.0 |
| | | | 5 | 5 | 29.0 | 89.7 |
| | | | 11 | 6 | 27.2 | 93.2 |
| | | | 17 | 1.9 | 31.5 | 87.0 |
| | | | 23 | 2.1 | 33.3 | 84.5 |
| | | 92 | 0 | 8 | 25.7 | 92.6 |
| | | | 5 | 4.6 | 29.4 | 89.9 |
| | | | 11 | 4.1 | 29.0 | 90.8 |
| | | | 17 | 1.8 | 35.8 | 82.2 |
| | | | 23 | 1.9 | 34.5 | 83.4 |
| | | | **Test Section IV** | | | |
| | | 0 | 0 | 8 | 26.4 | 92.0 |
| | | | 5 | 5 | 29.0 | 89.7 |
| | | | 11 | 6 | 27.2 | 93.2 |
| | | | 17 | 1.9 | 31.5 | 87.0 |
| | | | 23 | 2.1 | 33.3 | 84.5 |
| | | 348 | 0 | 8 | 26.6 | 93.4 |
| | | | 5 | 6 | 29.1 | 89.6 |
| | | | 11 | 6 | 28.4 | 89.3 |
| | | | 17 | 1.7 | 36.1 | 82.5 |
| | | | 23 | 1.9 | 34.7 | 83.3 |
| | | | **Test Section V** | | | |
| | | 0 | 0 | 4.2 | 29.9 | 90.3 |
| | | | 6 | 2.0 | 28.6 | 90.9 |
| | | | 12 | 3.4 | 25.8 | 93.7 |
| | | | 18 | 3.4 | 25.7 | 90.2 |
| | | | 0 | 5.9 | 28.8 | 90.- |
| | | | 6 | 3.6 | 27.1 | 93.- |
| | | | 12 | 5.3 | 29.1 | 90.2 |
| | | | 18 | 5.0 | 29.4 | 93.6 |

Table A2

Summary of Traffic Test Results

Test Section I

| Lane | Test Item | Rated CBR Strengthening Layer | Rated CBR Subgrade | Traffic Coverages | Mat Breakage: Locking Lug Break | Mat Breakage: Rolled Edge Break | Mat Breakage: Bayonet Shear | Mat Breakage: Cover-Plate Weld Break | Maximum Mat Deflection, in.: On Joint | Maximum Mat Deflection, in.: Center of Panel | Rating of Item at Failure |
|---|---|---|---|---|---|---|---|---|---|---|---|
| 1 | 1 | [illegible] | 2.3 | 0 | 0 | 0 | 0 | 0 | 1.60 | 1.80 | |
| | | | | 30 | 0 | 0 | 0 | 3 | 2.55 | 2.60 | Subgrade failure |
| | 2 | [illegible] | [illegible] | 0 | 0 | 0 | 0 | 0 | 1.58 | 1.50 | |
| | | | | 110 | 6 | 1 | 0 | 0 | 1.65 | 1.65 | |
| | 3 | 8 | 3.2 | 0 | 0 | 0 | 0 | 0 | 1.20 | 1.15 | |
| | | | | 310 | 18 | 6 | 1 | 6 | 1.45 | 1.60 | |
| | [illegible] | 7 | 3.2 | 0 | 0 | 0 | 0 | 0 | 0.85 | 1.00 | |
| | | | | 430 | 6 | 0 | 0 | 2 | 1.15 | 1.20 | |
| 2 | 1 | 5 | 2.3 | 0 | 0 | 0 | 0 | 0 | 1.55 | 1.80 | |
| | | | | 120 | 0 | 0 | 0 | 0 | 2.60 | 3.20 | Subgrade failure |
| | 2 | 6 | 2.8 | 0 | 0 | 0 | 0 | 0 | 1.30 | 1.10 | |
| | | | | [illegible]12 | 2 | 0 | 0 | 1 | 1.70 | 1.75 | Subgrade failure |
| | 3 | [illegible] | 2.9 | 0 | 0 | 0 | 0 | 0 | 1.20 | 1.05 | |
| | | | | [illegible]12 | 0 | 0 | 0 | 0 | 1.05 | 1.00 | |
| | | | | 924 | 12 | 0 | 0 | 0 | 1.75 | 1.58 | |
| | 4 | 7 | 2.8 | 0 | 0 | 0 | 0 | 0 | 0.90 | 0.80 | |
| | | | | 612 | 0 | 0 | 0 | 0 | 0.95 | 0.80 | |
| | | | | 104[illegible] | 7 | 0 | 0 | 0 | 1.65 | 1.45 | |
| 3 | 2 | 6 | 2.9 | 0 | 0 | 0 | 0 | 0 | 1.60 | 1.90 | Subgrade failure |
| | | | | 120 | 0 | 0 | 0 | 0 | 2.1 | 2.00 | |
| | [illegible] | 7 | 3.0 | 0 | 0 | 0 | 0 | 0 | 1.20 | 1.40 | |
| | | | | 408 | 7 | 0 | 0 | 0 | 1.82 | 1.80 | |
| | 4 | 7 | 3.0 | 0 | 0 | 0 | 0 | 0 | [illegible]20 | 1.35 | |
| | | | | 750 | 6 | 0 | 0 | 0 | [illegible]0 | [illegible]50 | |

Table A3

Summary of Traffic Test Results

| Lane | Test Item | Rated CBR Strengthening Layer | Rated CBR Subgrade | Traffic Coverages | Mat Breakage: Internal Rib Failures | Mat Breakage: Bottom Lip Sheared from Overlapping End Joint | Mat Breakage: C-Rail Failure | Mat Breakage: End-Joint Weld Break | Mat Breakage: Top Pin Shears | Mat Breakage: Sheared End Joint | Mat Deflection, in.: On Joint | Mat Deflection, in.: On Lug Point | Mat Deflection, in.: Center of Panel | Rating of Item at Failure |
|---|---|---|---|---|---|---|---|---|---|---|---|---|---|---|
| **Test Section II** | | | | | | | | | | | | | | |
| 1 | 1 | 3.0 | 1.3 | 0 | 0 | 0 | 0 | 0 | 0 | 0 | 1.55 | 1.62 | -- | |
| | | | | 72 | 1 | 1 | 1 | 0 | 0 | 0 | 1.69 | 1.28 | -- | Subgrade failure |
| | 2 | 3.1 | 2.3 | 0 | 0 | 0 | 0 | 0 | 0 | 0 | 1.35 | 0.98 | -- | |
| | | | | 170 | 0 | 0 | 0 | 0 | 0 | 0 | 1.40 | 1.20 | -- | Subgrade failure |
| | 3 | 3.4 | 1.4 | 0 | 0 | 0 | 0 | 0 | 0 | 0 | 1.15 | 0.90 | -- | |
| | | | | 202 | 1 | 0 | 0 | 1 | 0 | 0 | 1.20 | 1.25 | -- | |
| | [illegible] | 3.4 | -- | 0 | 0 | 0 | 0 | 0 | 0 | 0 | 1.15 | 0.78 | -- | |
| | | | | 202 | 1 | 0 | 1 | 0 | 0 | 0 | 1.05 | 0.90 | -- | |
| 2 | 1 | 3.3 | 1.4 | 0 | 0 | 0 | 0 | 0 | 0 | 0 | 3.20 | -- | 3.25 | |
| | | | | 32 | 0 | 1 | 0 | 0 | 0 | 3 | 3.85 | -- | 3.45 | Subgrade failure |
| | 2 | 3.1 | 1.7 | 0 | 0 | 0 | 0 | 0 | 0 | 0 | 2.15 | -- | 2.40 | |
| | | | | 60 | 0 | 2 | 1 | 0 | 0 | 2 | 3.20 | -- | 3.70 | Subgrade failure |
| | 3 | 3.4 | 1.7 | 0 | 0 | 0 | 0 | 0 | 0 | 0 | 2.00 | -- | 2.35 | |
| | | | | 140 | 0 | 1 | 0 | 0 | 0 | 1 | 2.85 | -- | 2.90 | |
| | 4 | 3.7 | -- | 0 | 0 | 0 | 0 | 0 | 0 | 0 | 1.90 | -- | 1.60 | |
| | | | | 300 | 0 | 1 | 0 | 2 | 0 | 0 | 2.55 | -- | 2.40 | |
| **Test Section III** | | | | | | | | | | | | | | |
| 1 | 1 | 7 | 2.1 | 0 | 0 | 0 | 0 | 0 | 0 | 0 | 1.04 | | 0.98 | |
| | | | | 528 | 9 | 0 | 0 | 3 | 3 | 0 | 1.14 | | 1.06 | Subgrade failure |
| | 2 | 7 | 2.0 | 0 | 0 | 0 | 0 | 0 | 0 | 0 | 0.68 | | 0.68 | |
| | | | | 528 | [illegible] | 6 | 0 | 1 | 0 | 0 | -- | | -- | |
| | | | | 884 | 14 | 0 | 8 | 1 | 14 | 0 | 1.08 | | 0.94 | Subgrade failure |
| 2 | 1 | 8 | 2.1 | 0 | 0 | 0 | 0 | 0 | 0 | 0 | 2.05 | | 2.50 | |
| | | | | [illegible]6 | 23 | 6 | 6 | 0 | 0 | 1 | 2.80 | | 3.18 | Subgrade failure |
| | 2 | 7 | 1.8 | 0 | 0 | 0 | 0 | 0 | 0 | 0 | 1.88 | | 1.98 | |
| | | | | 72 | 22 | 6 | 9 | 1 | 0 | 0 | 2.57 | | 2.72 | Subgrade failure |
| | 3 | [illegible] | 2.0 | 0 | 0 | 0 | 0 | 0 | 0 | 0 | 1.40 | | 1.58 | |
| | | | | 92 | 19 | 7 | 7 | 0 | 0 | 0 | 2.32 | | 2.42 | Subgrade failure |
| **Test Section IV** | | | | | | | | | | | | | | |
| | | 7 | 1.8 | 0 | 0 | 0 | 0 | 0 | 0 | 0 | 1.23 | | 1.28 | |
| | | | | 348 | 22 | 10 | 11 | 2 | 3 | 0 | 1.68 | | 1.63 | Subgrade failure |
| **Test Section V** | | | | | | | | | | | | | | |
| | | 5 | 3.7 | 0 | 0 | 0 | 0 | 0 | 0 | 0 | 0.61 | | 0.62 | |
| | | | | 330 | 0 | 0 | 0 | 6 | 0 | 4 | 0.75 | | 0.61 | Subgrade failure |

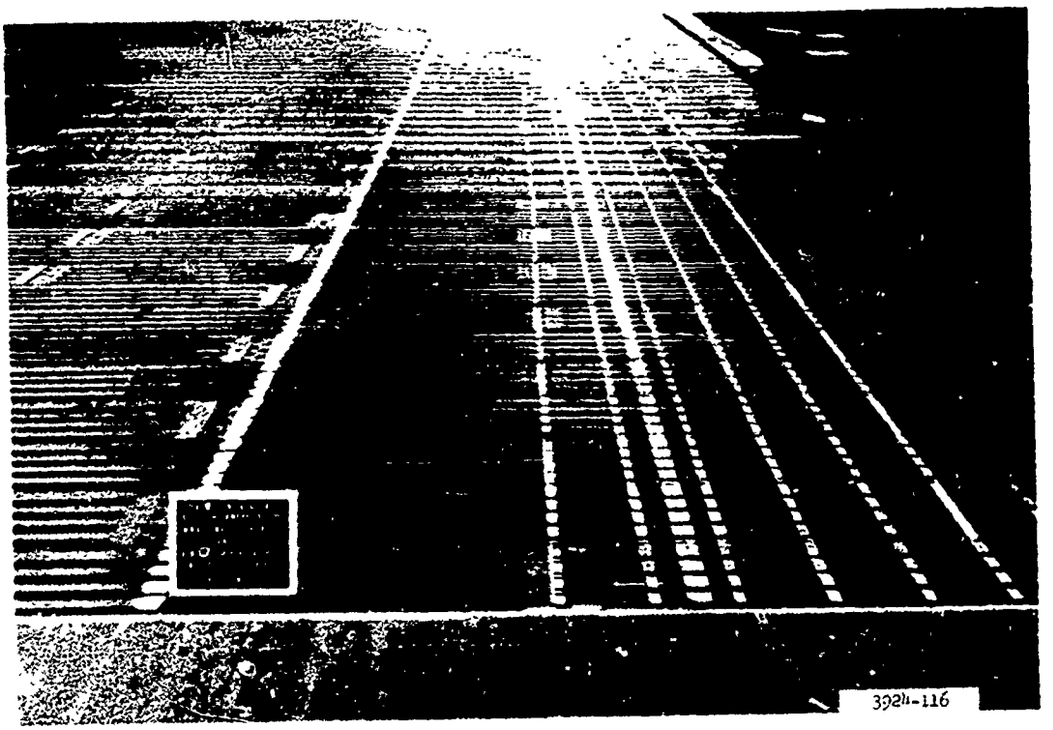


Photograph A1. Test section I, lane 1, item 1, prior to traffic

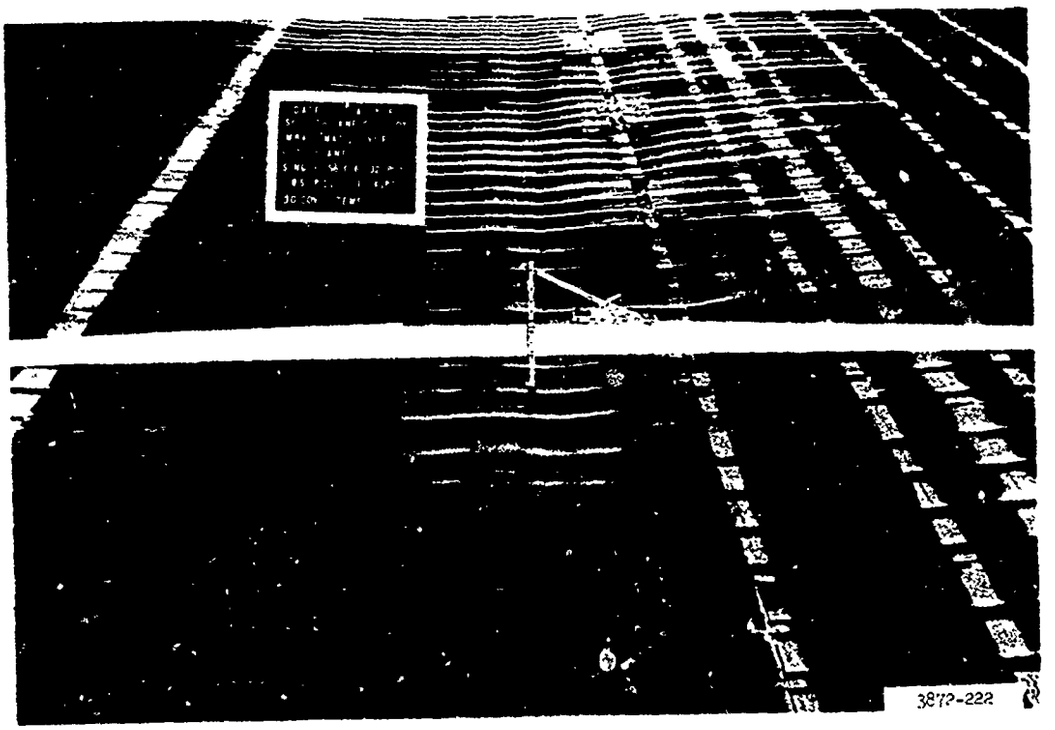


Photograph A2. Deformation of 3.2 in. in test section I, lane 1, item 1, after failure at 30 coverages

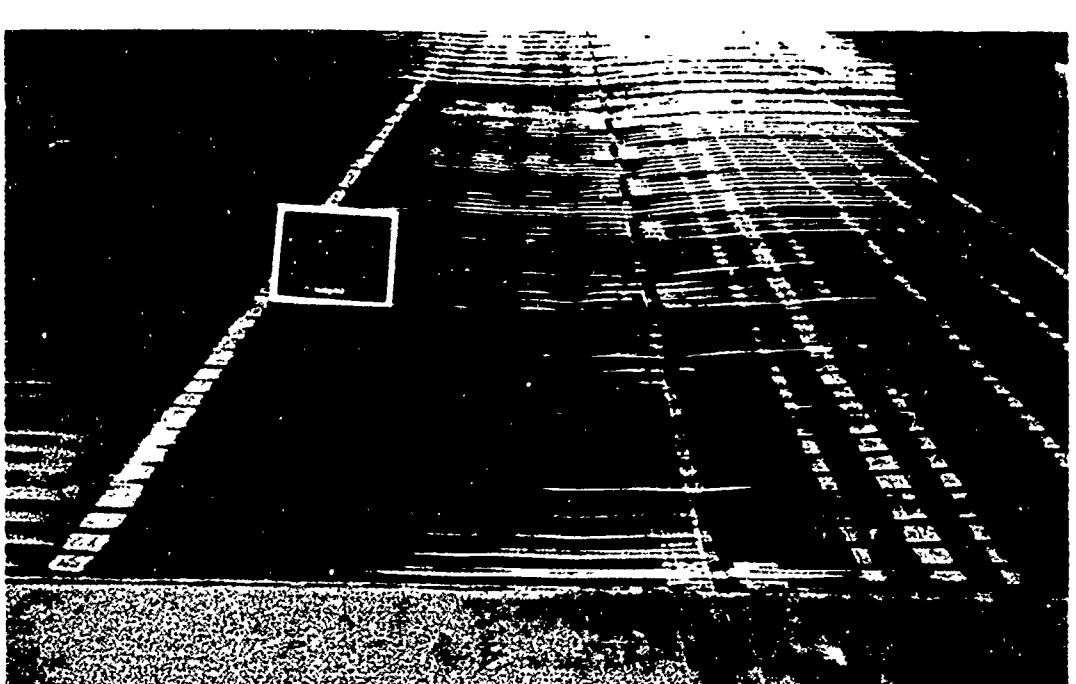

Photograph A3. Test section I, lane 1, item 1, after failure at 30 coverages

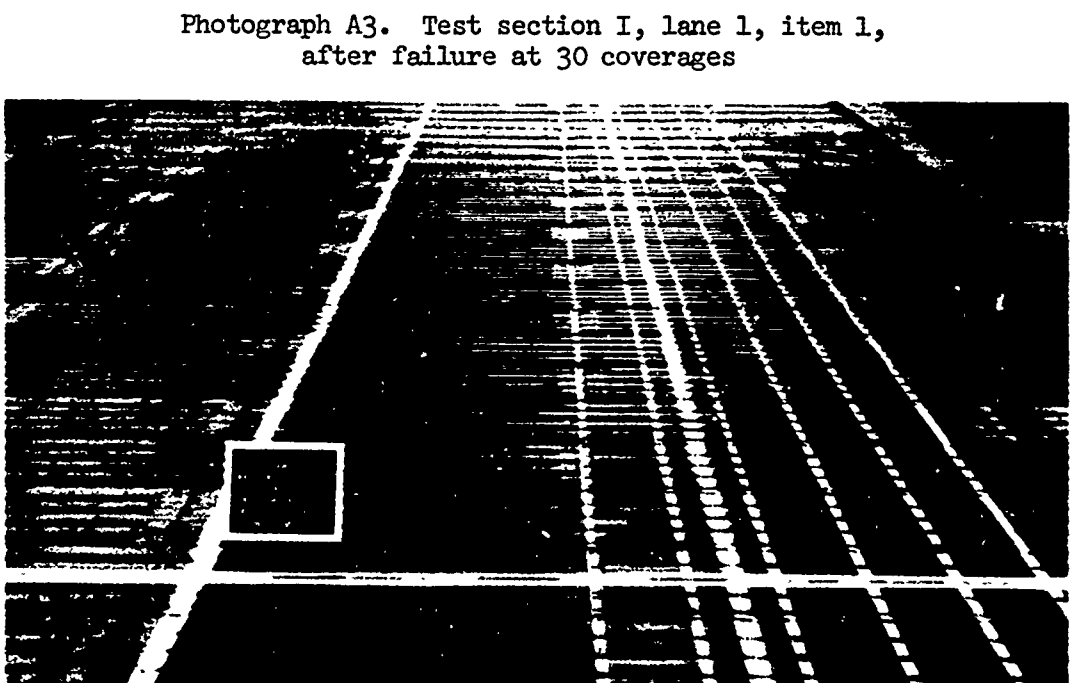

Photograph A4. Test section I, lane 1, item 2, prior to traffic

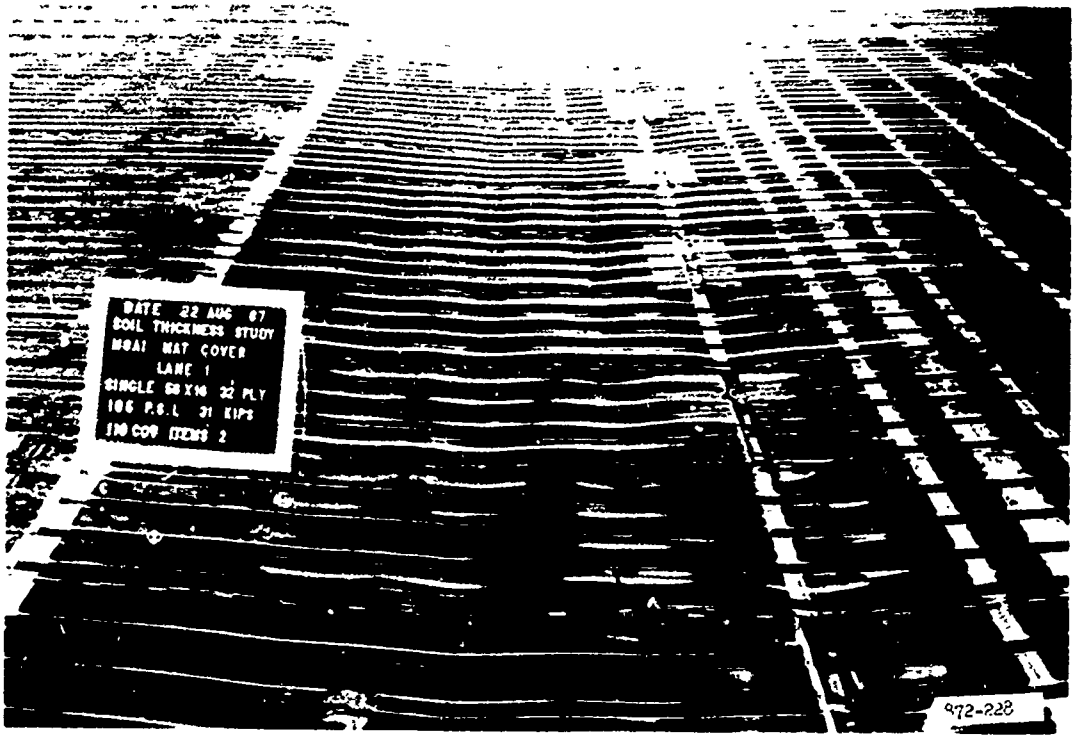


Photograph A5. Test section I, lane 1, item 2, after failure at 110 coverages

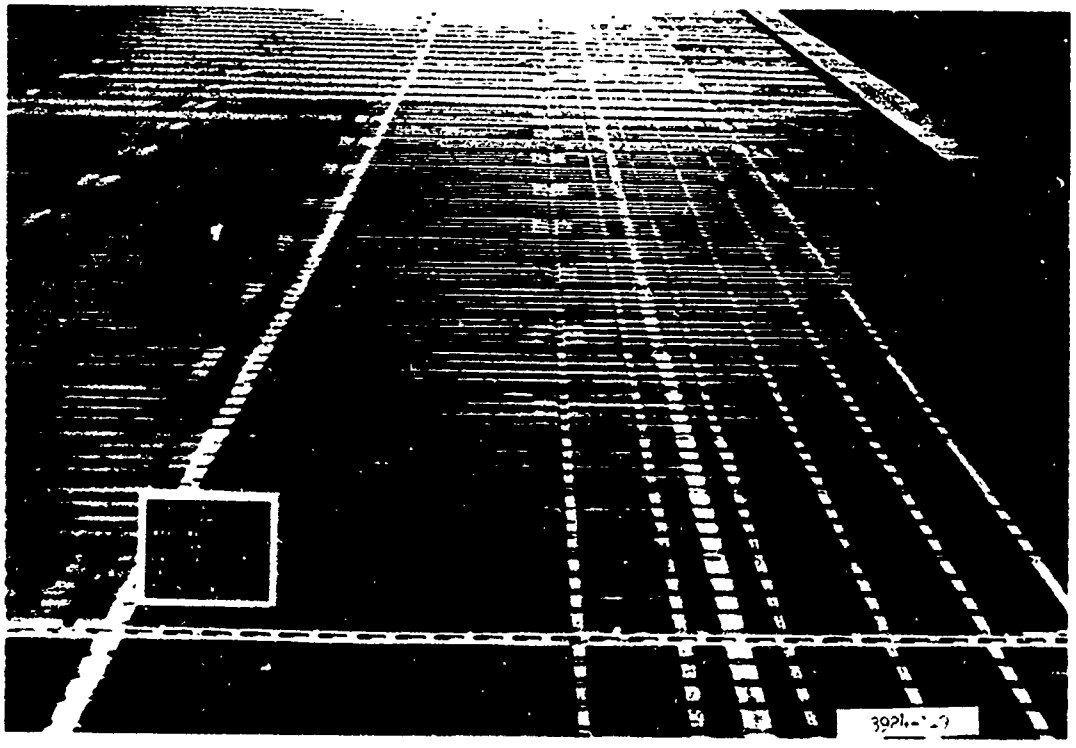

Photograph A6. Test section I, lane 1, item 3, prior to traffic

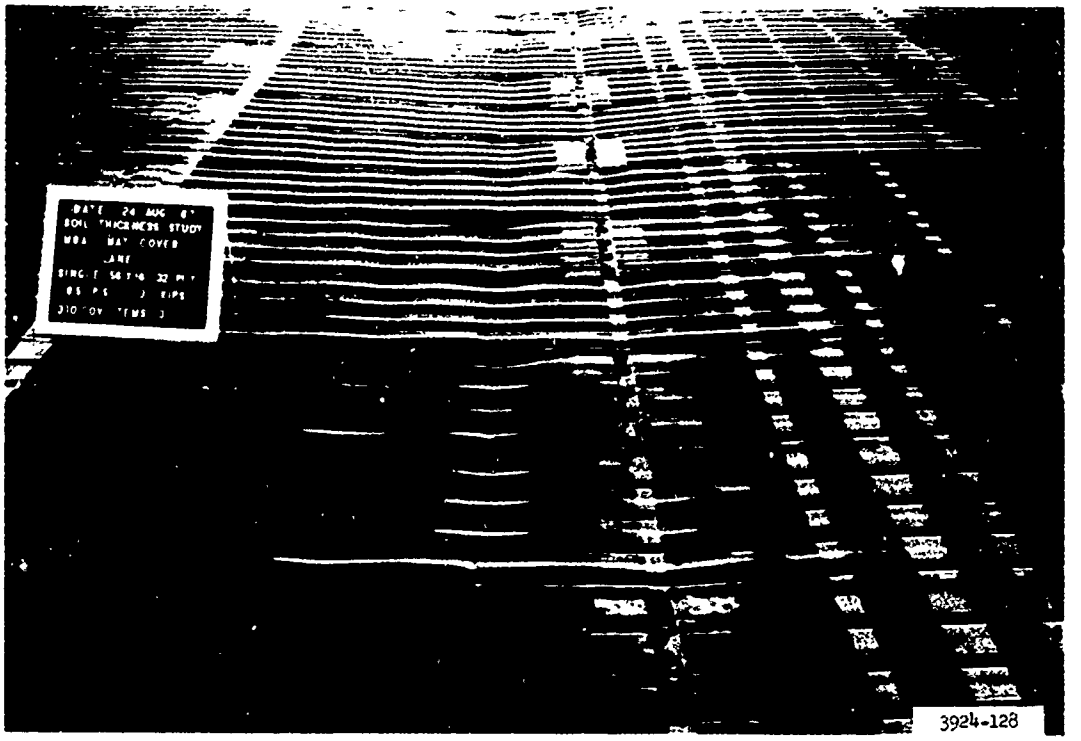


Photograph A7. Test section I, lane 1, item 3, after failure at 310 coverages

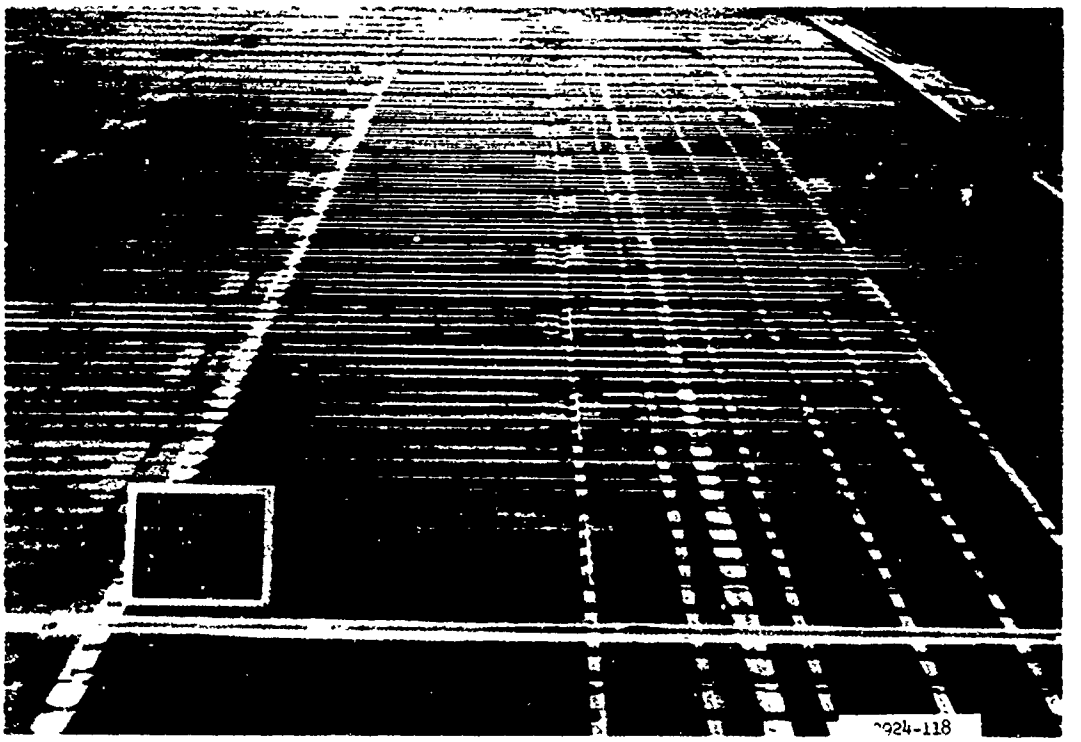


Photograph A8. Test section I, lane 1, item 4, prior to traffic

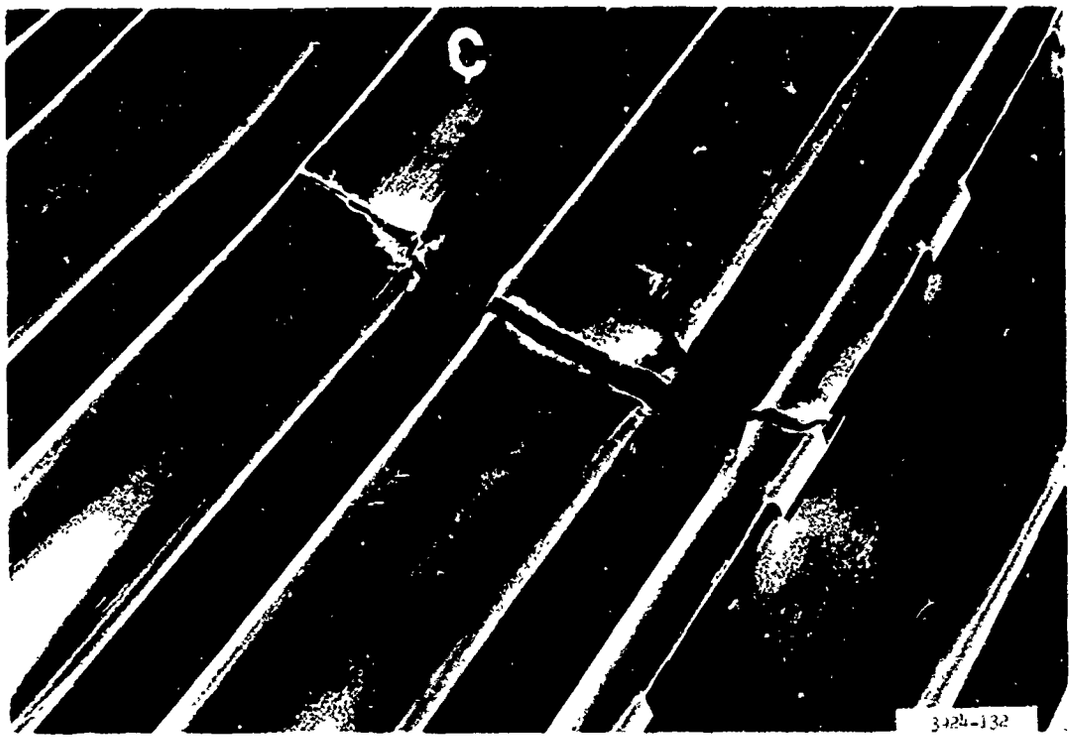


Photograph A9. Typical locking-lug break

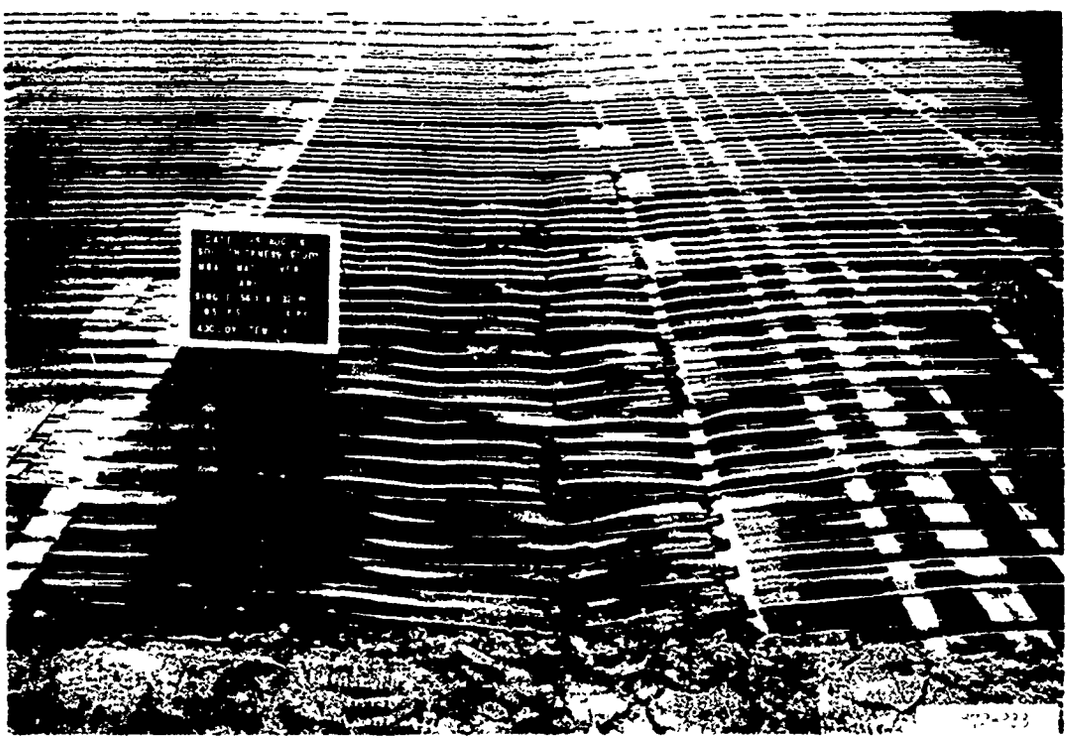

Photograph A10. Test section I, lane 1, item 4,
after failure at 430 coverages

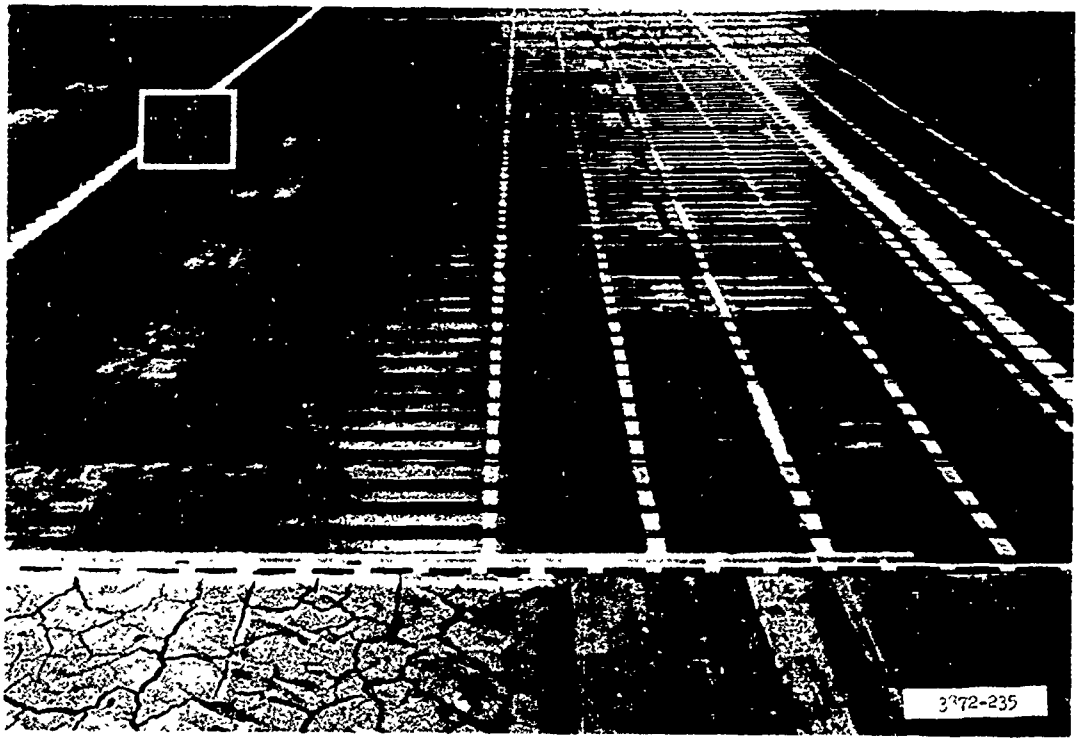


Photograph A11. Test section I, lane 2, item 1, prior to traffic

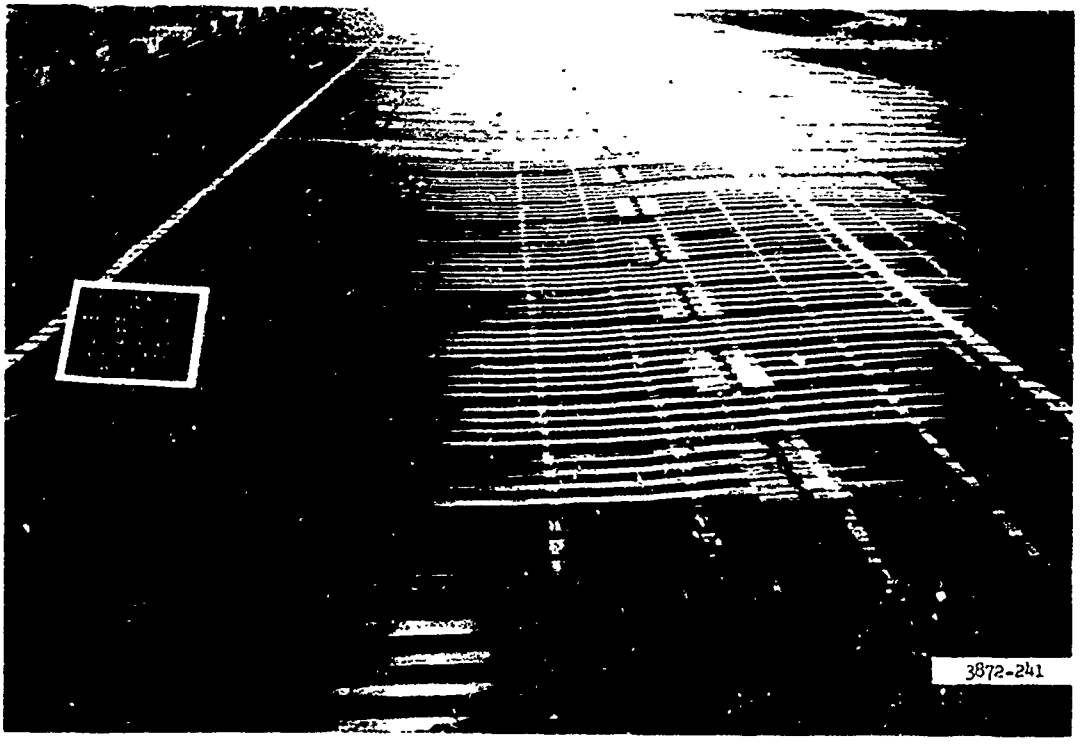


Photograph A12. Test section I, lane 2, item 1,
after failure at 120 coverages

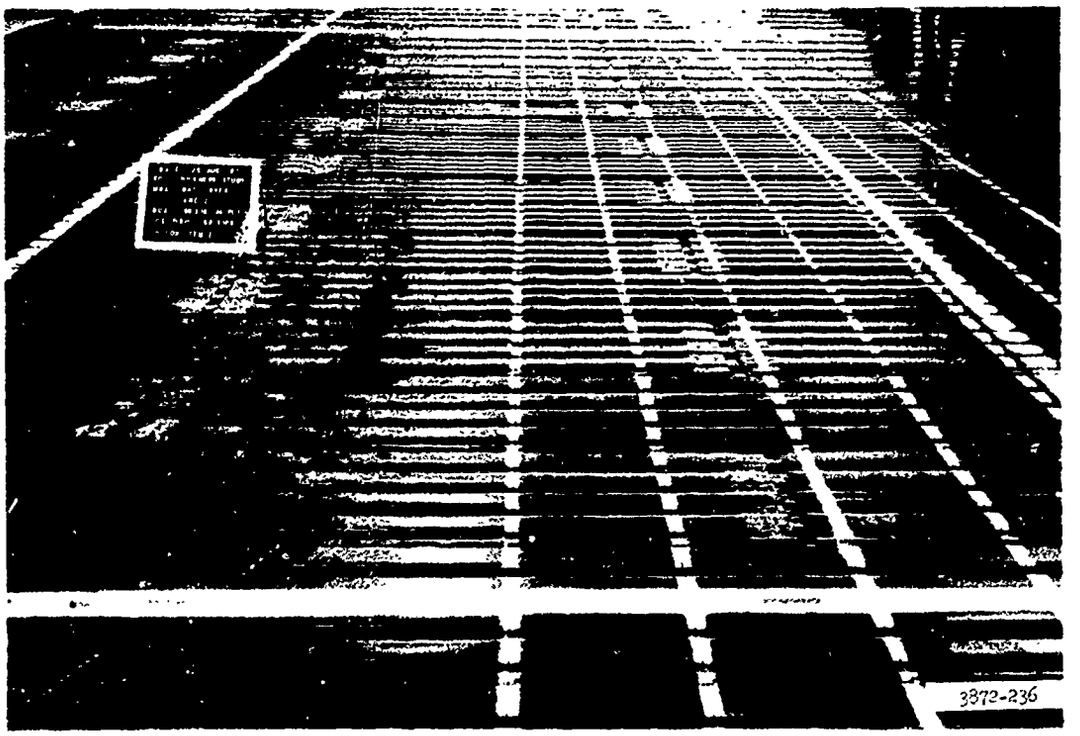


Photograph A13. Test section I, lane 2, item 2, prior to traffic

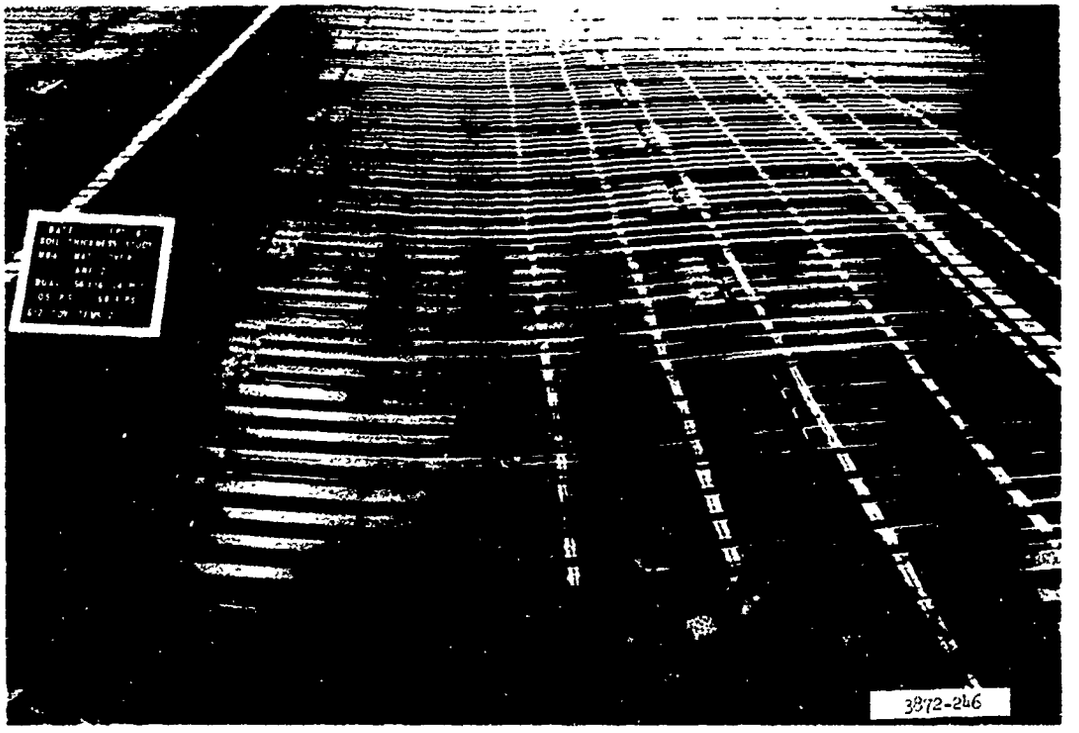


Photograph A14. Test section I, lane 2, item 2,
after failure at 612 coverages

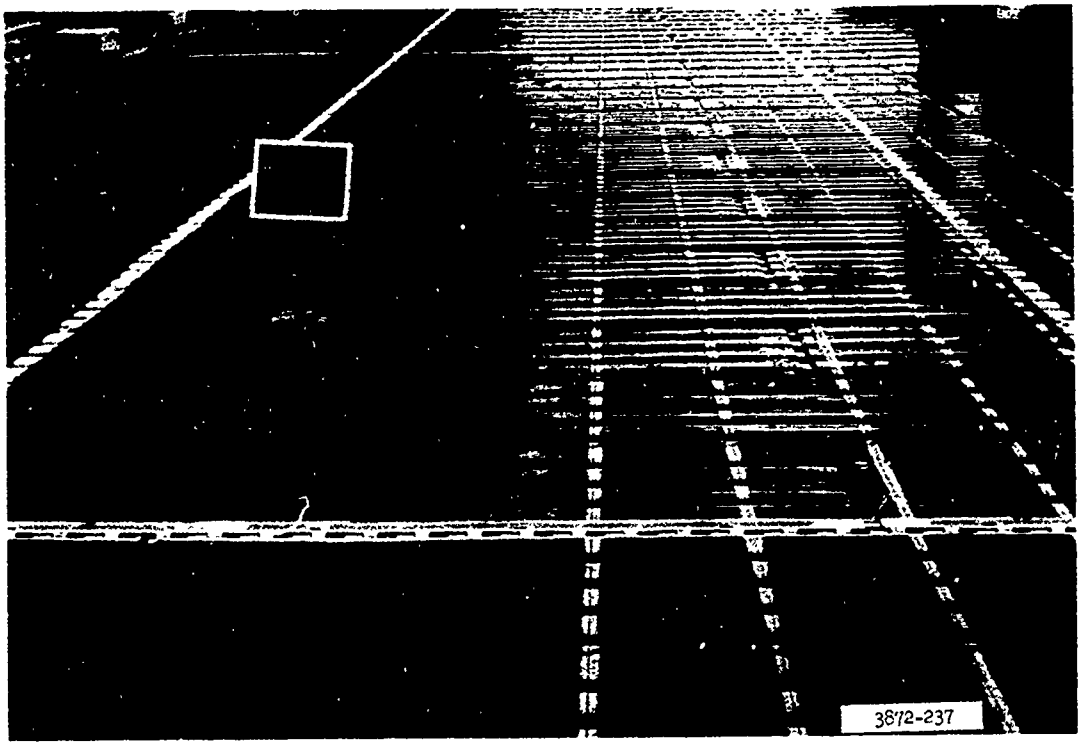


Photograph A15. Test section I, lane 2, item 3, prior to traffic

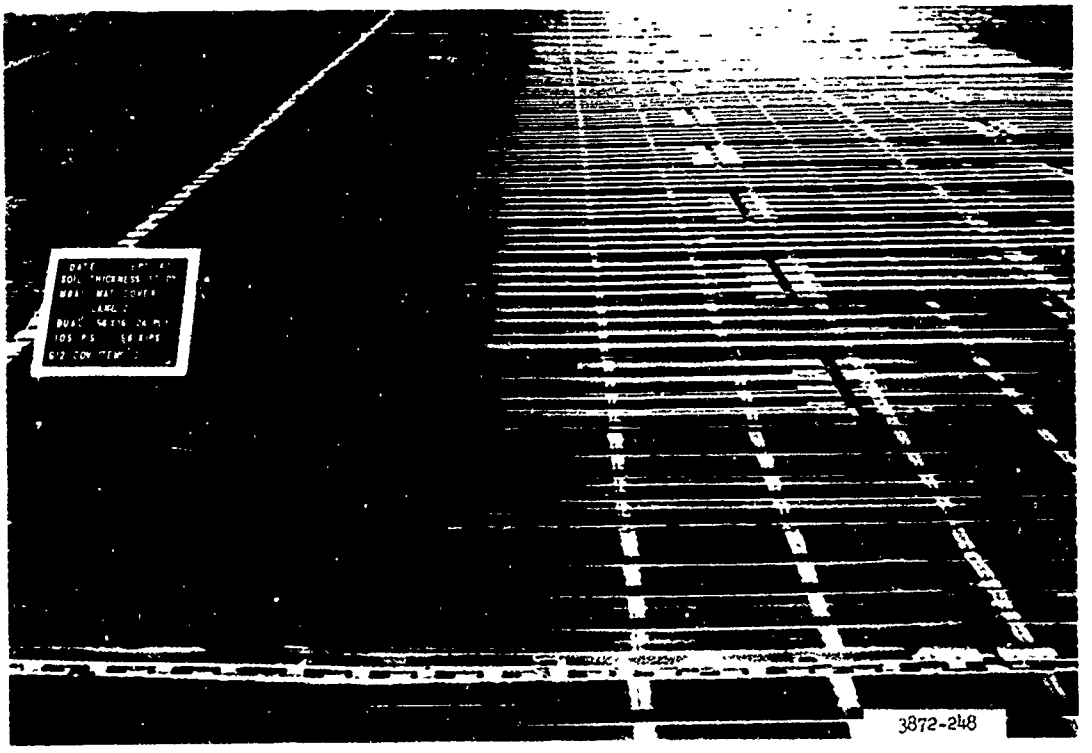


Photograph A16. Test section I, lane 2, item 3, after 612 coverages with initial test load


Photograph A17. Typical mat breakage after a total of 924 coverages of mixed traffic in test section I, lane 2, item 3

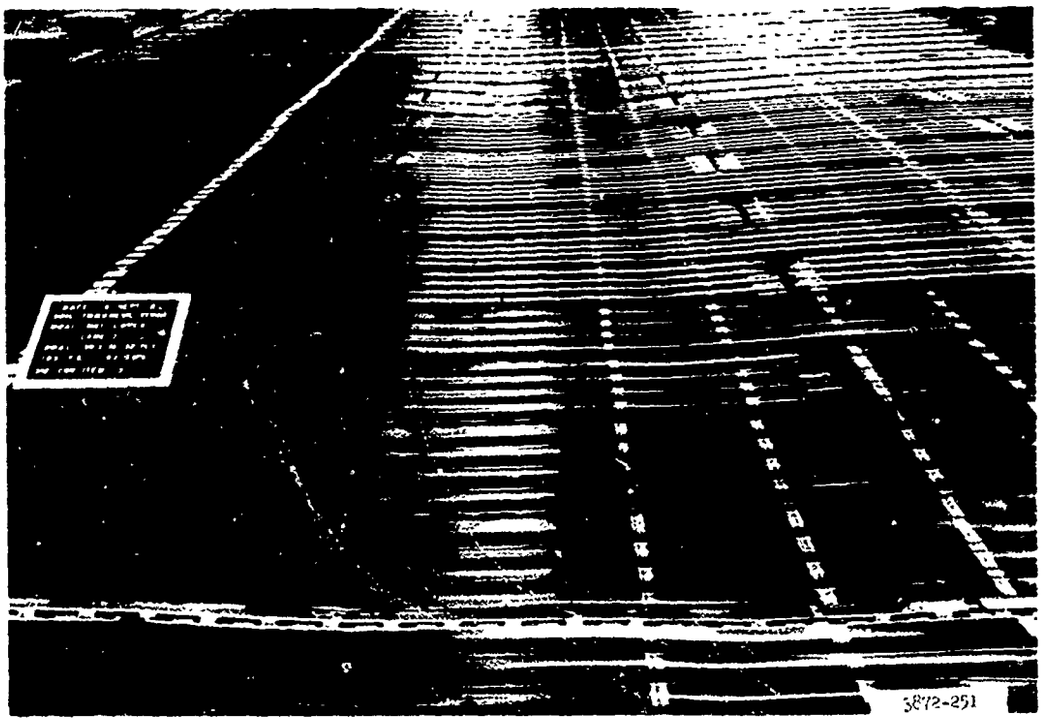


Photograph A18. Test section I, lane 2, item 3, after failure at 924 coverages of mixed traffic

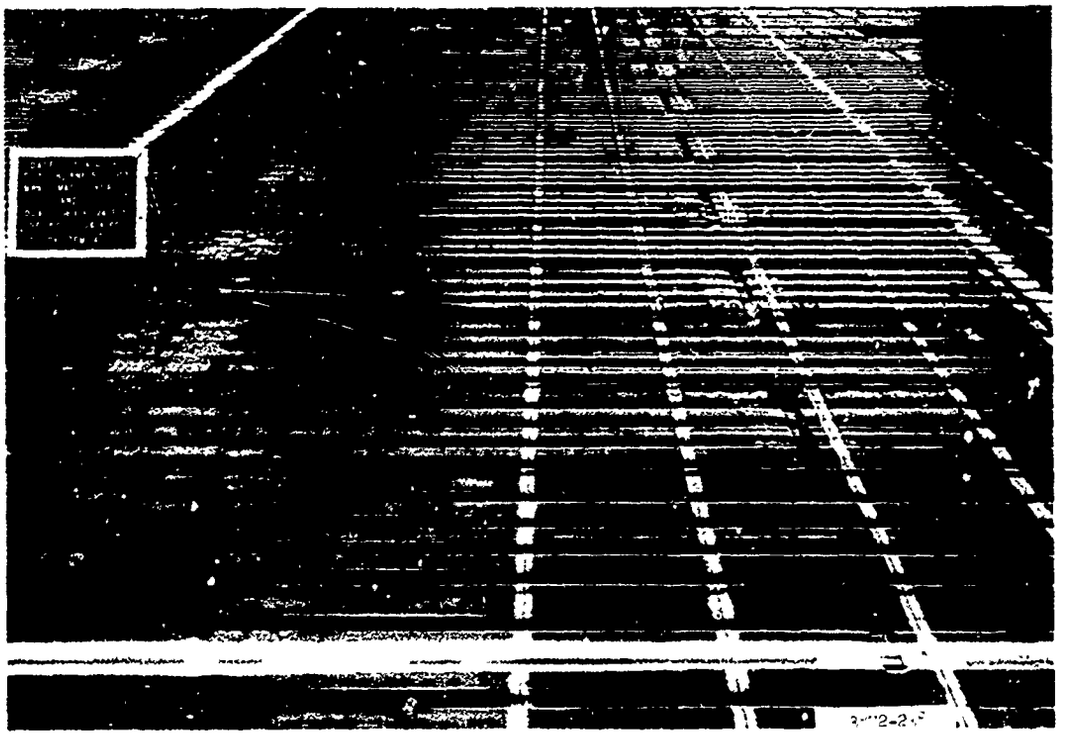

Photograph A19. Test section I, lane 2, item 4, prior to traffic

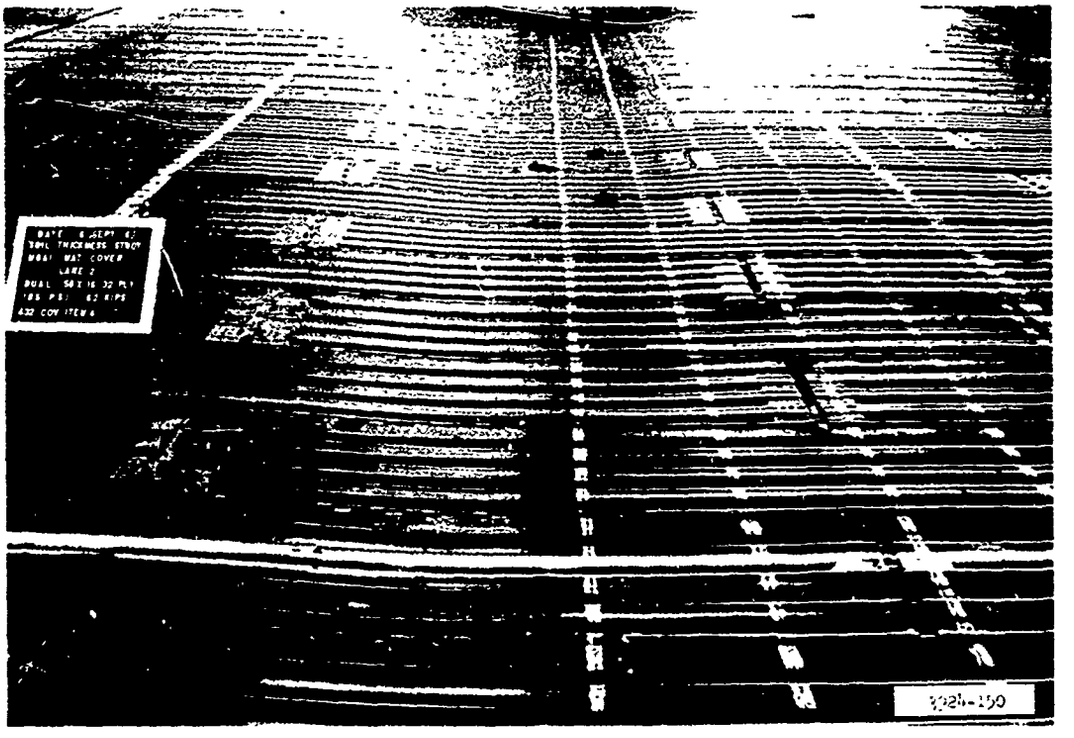

Photograph A20. Test section I, lane 2, item 4, after failure at 1044 coverages of mixed traffic

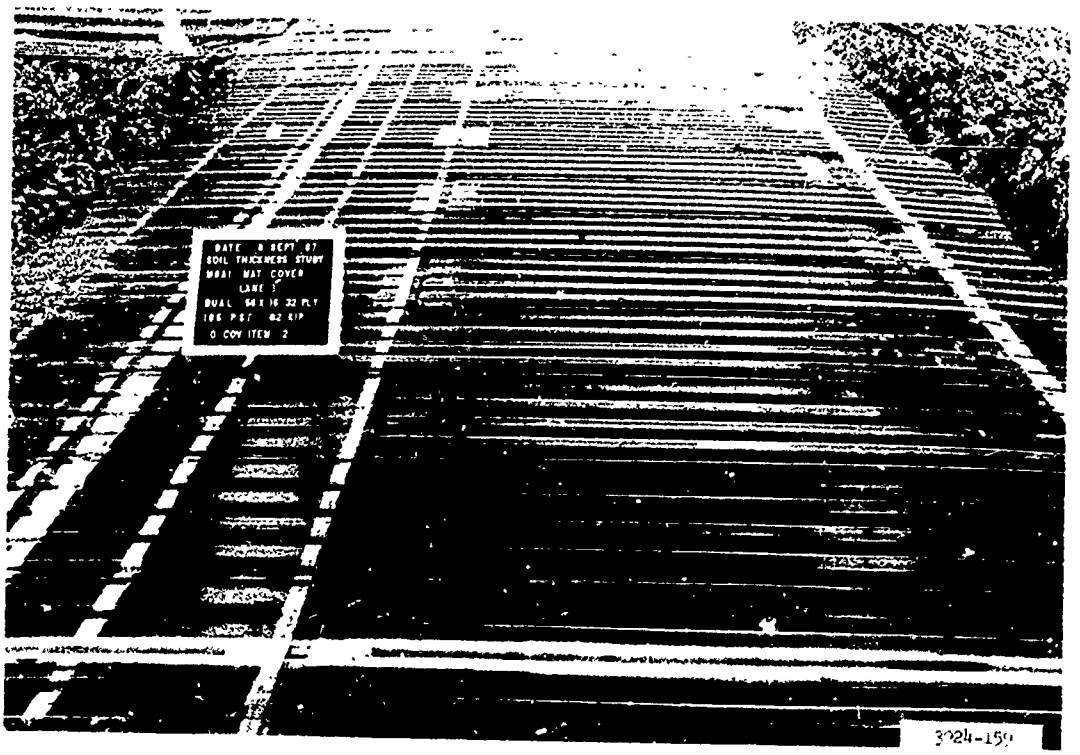


Photograph A21. Test section I, lane 3, item 2, prior to traffic

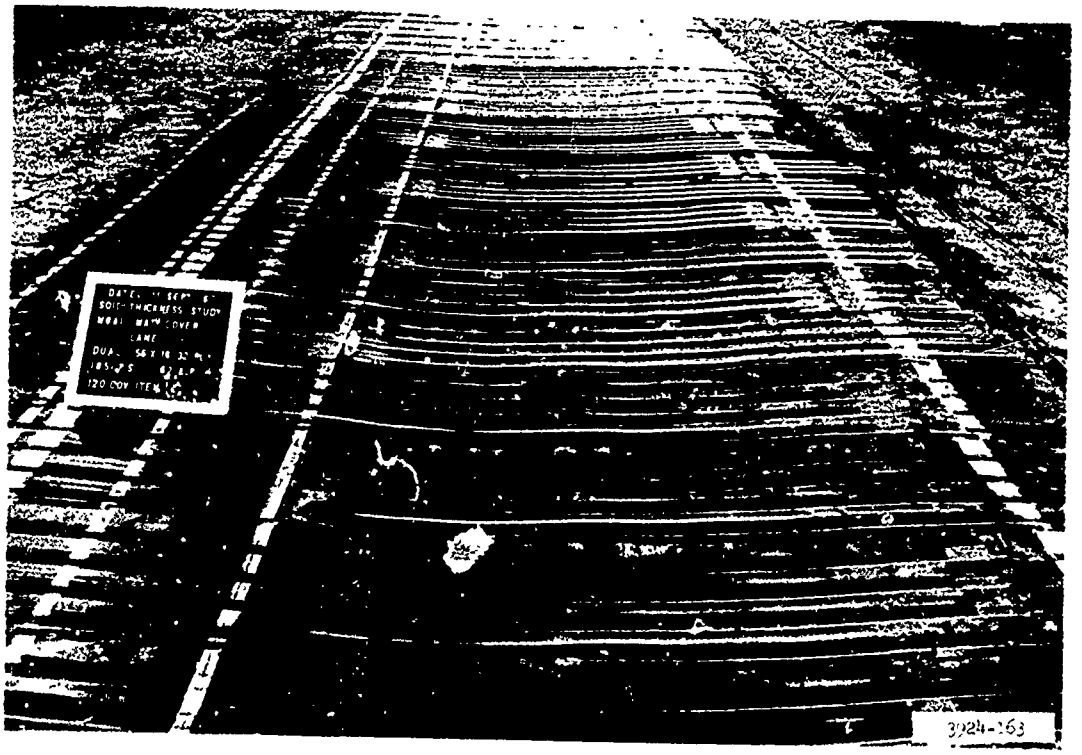


Photograph A22. Test section I, lane 3, item 2, after failure at 120 coverages


Photograph A23. Test section I, lane 3, item 3, prior to traffic

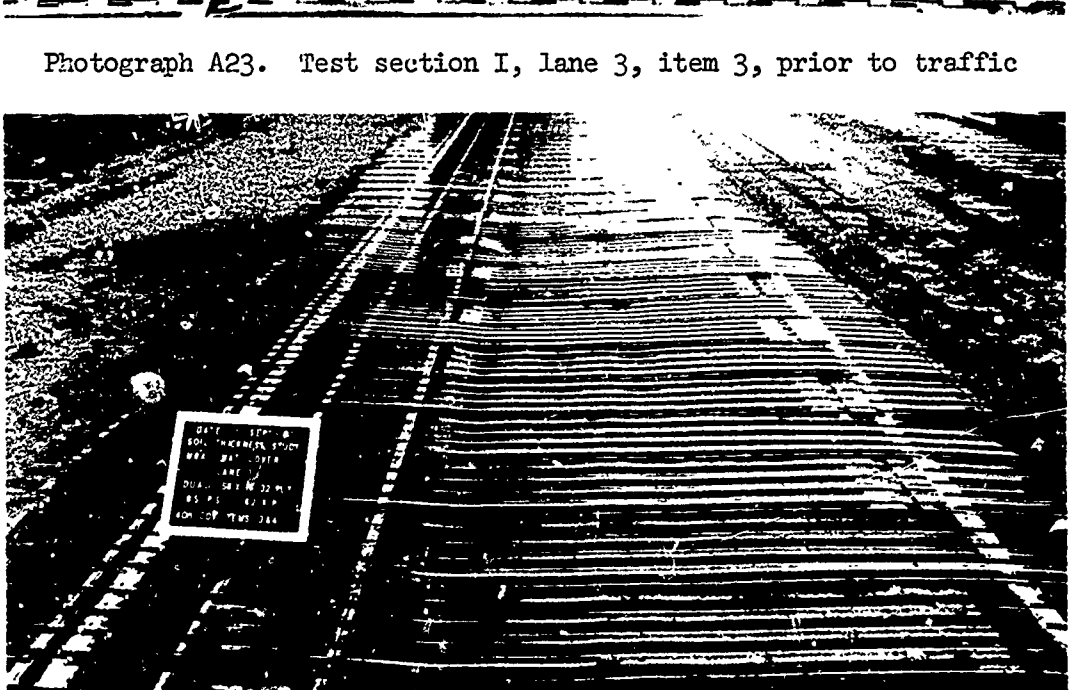


Photograph A24. Test section I, lane 3, item 3, after failure at 408 coverages

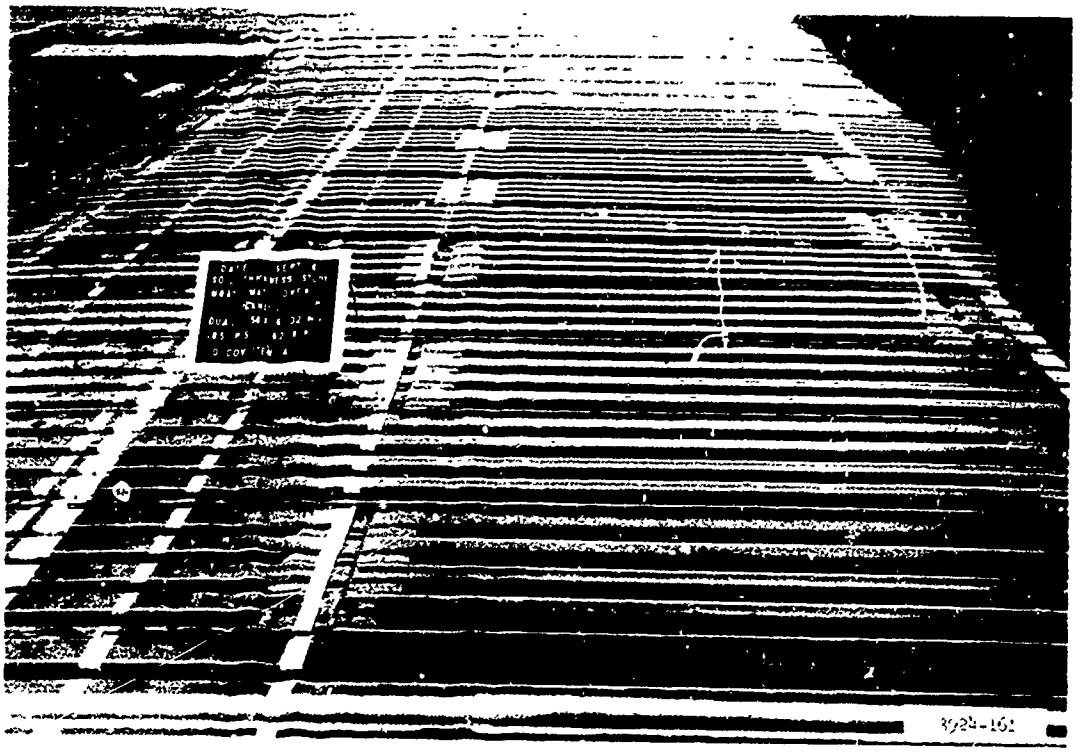

Photograph A25. Test section I, lane 3, item 4, prior to traffic

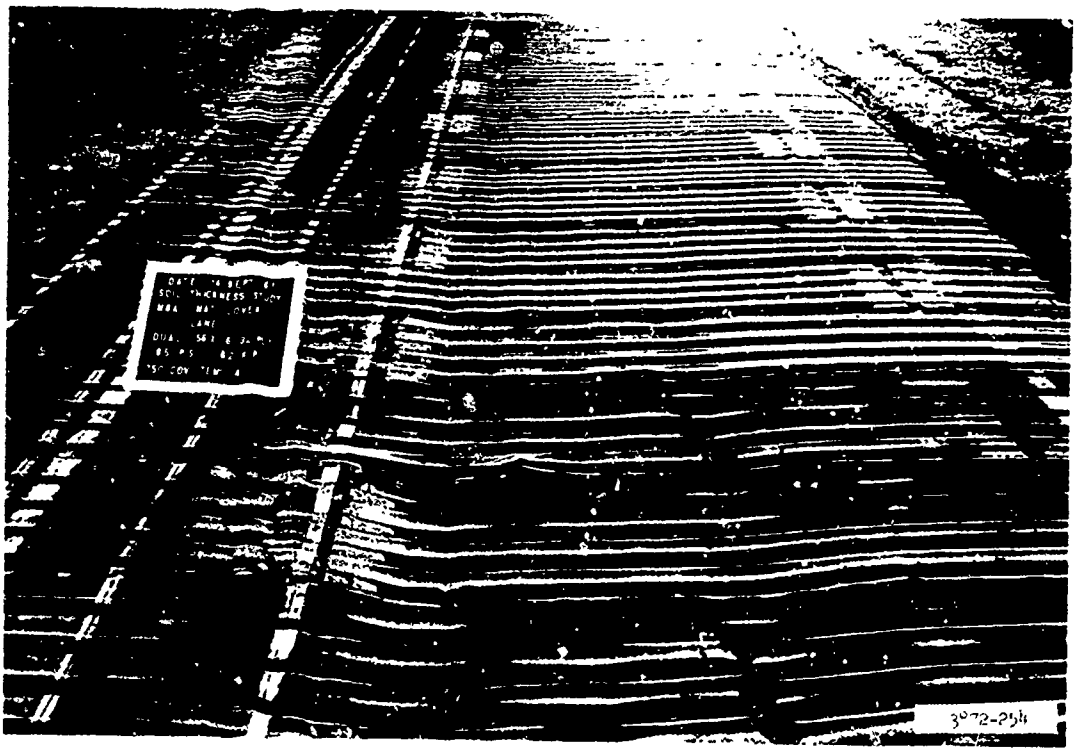

Photograph A26. Test section I, lane 3, item 4, after failure at 750 coverages

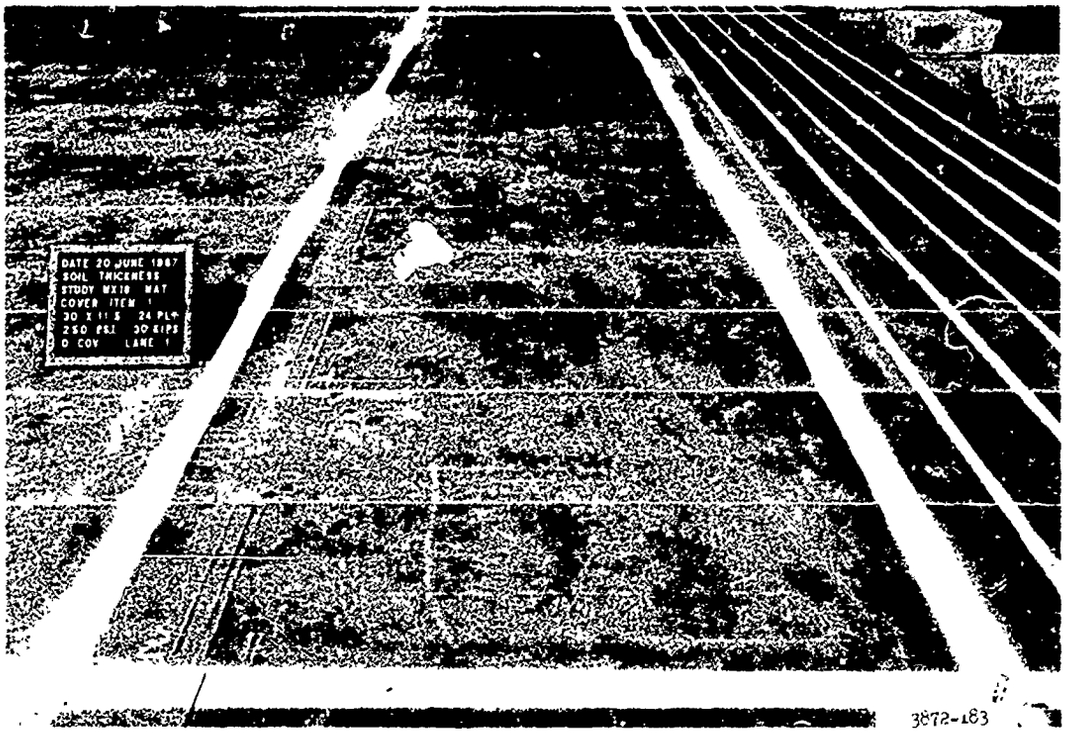


Photograph A27. Test section II, lane 1, item 1, prior to traffic

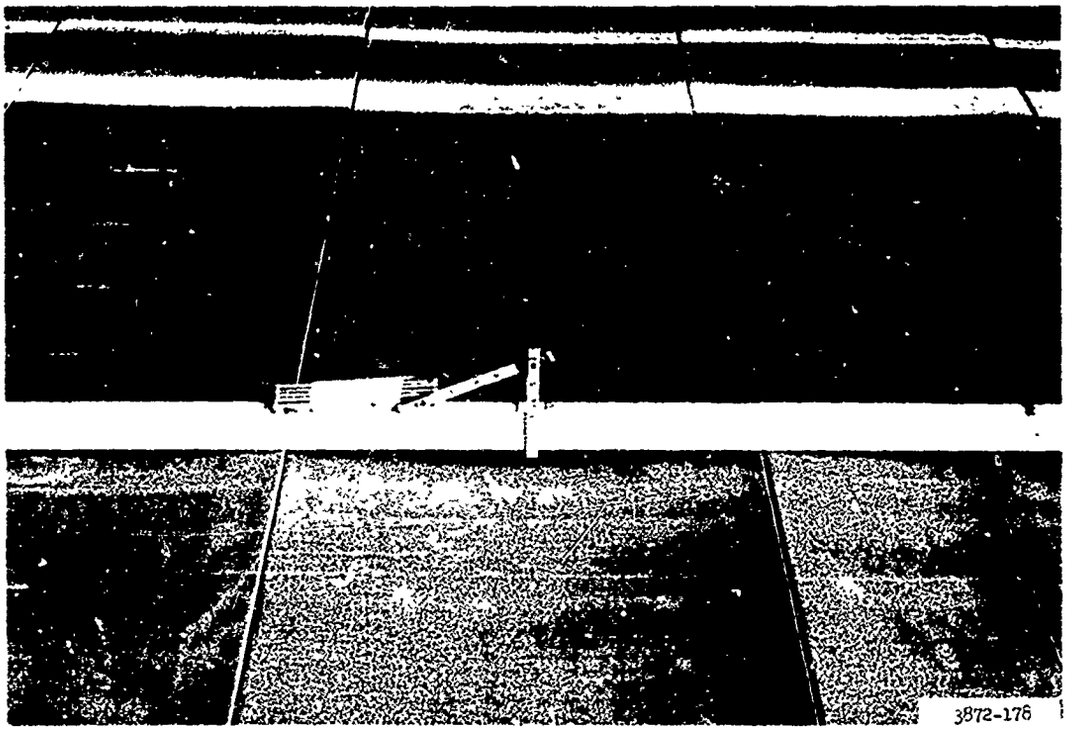


Photograph A28. Dishing of 0.75 in. in test section II, lane 1, item 1, after 12 coverages

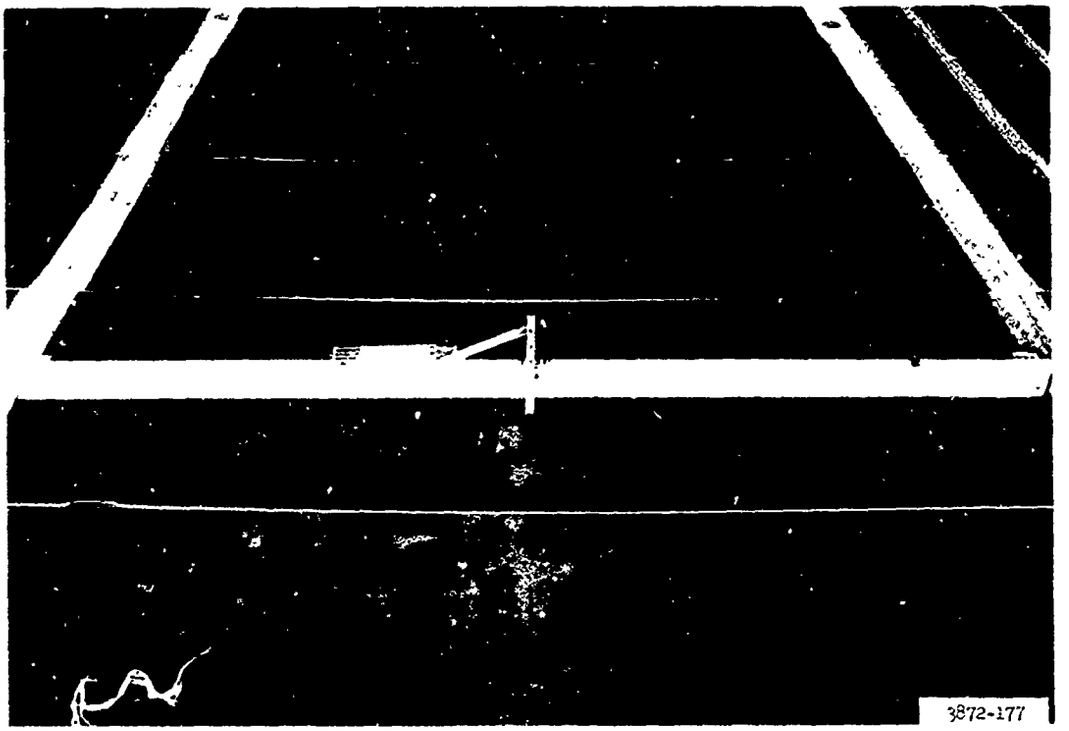


Photograph A29. Longitudinal deformation of 1 in. in test section II, lane 1, item 1, after 12 coverages

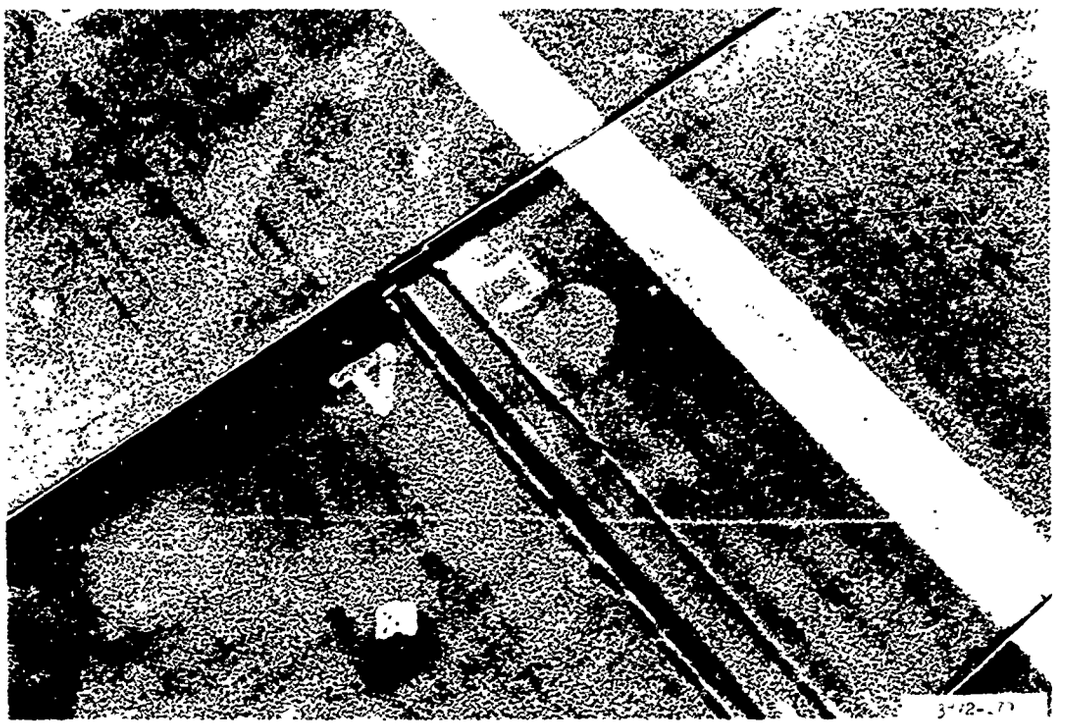

Photograph A30. Damaged C-rail of panel 4, test section II, lane 1, item 1, after 54 coverages

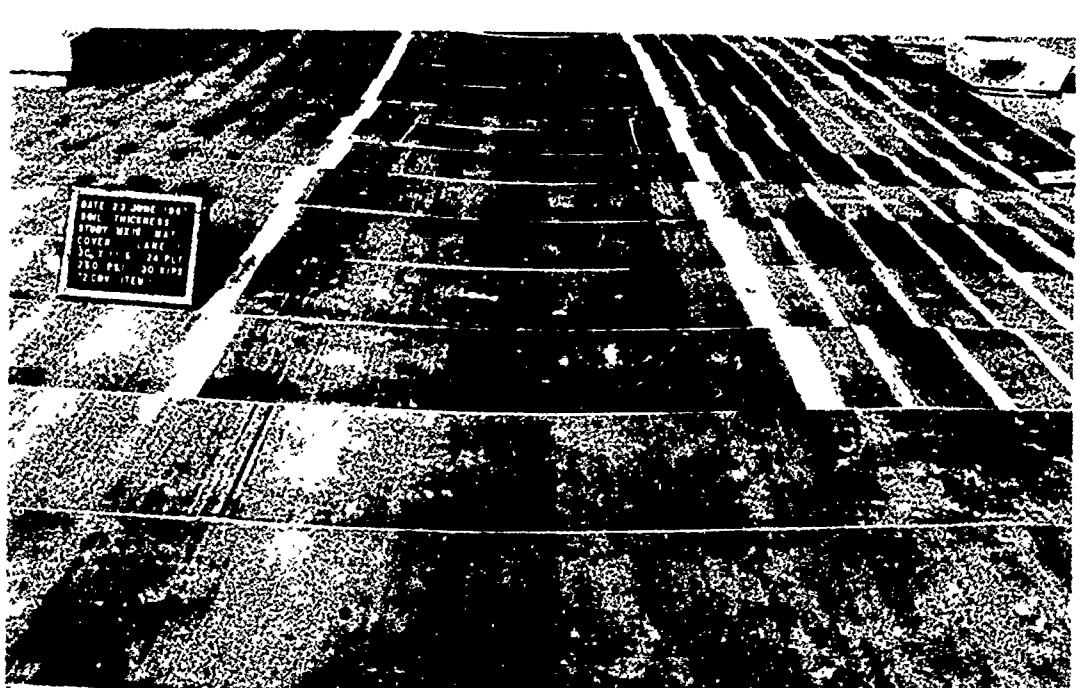


Photograph A31. Test section II, lane 1, item 1, after failure at 72 coverages

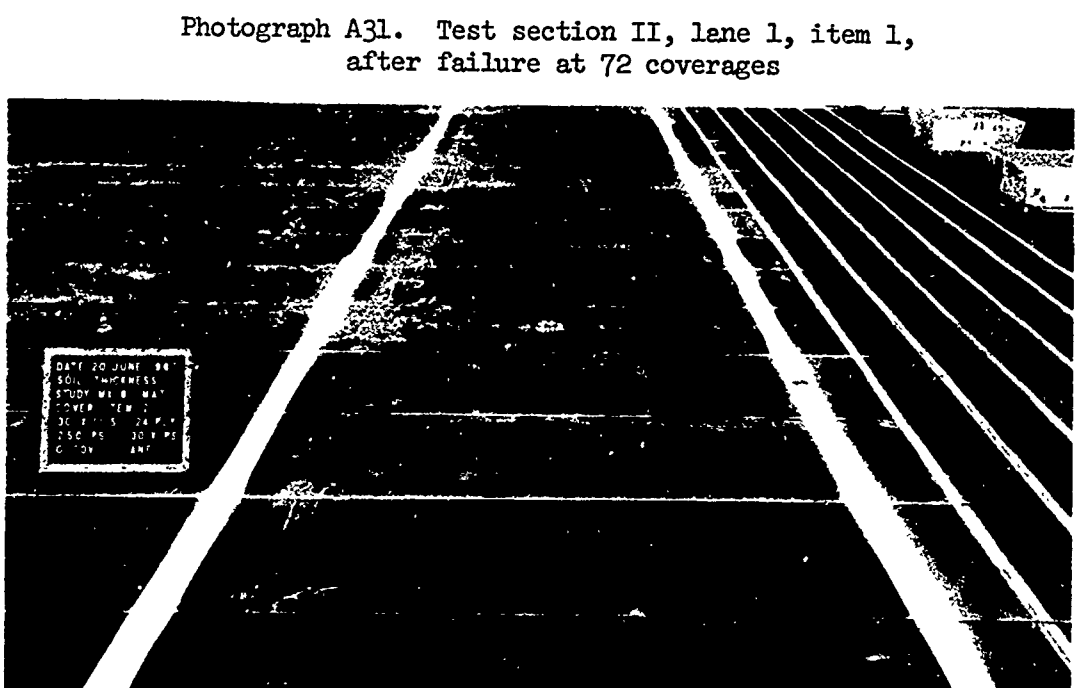


Photograph A32. Test section II, lane 1, item 2, prior to traffic

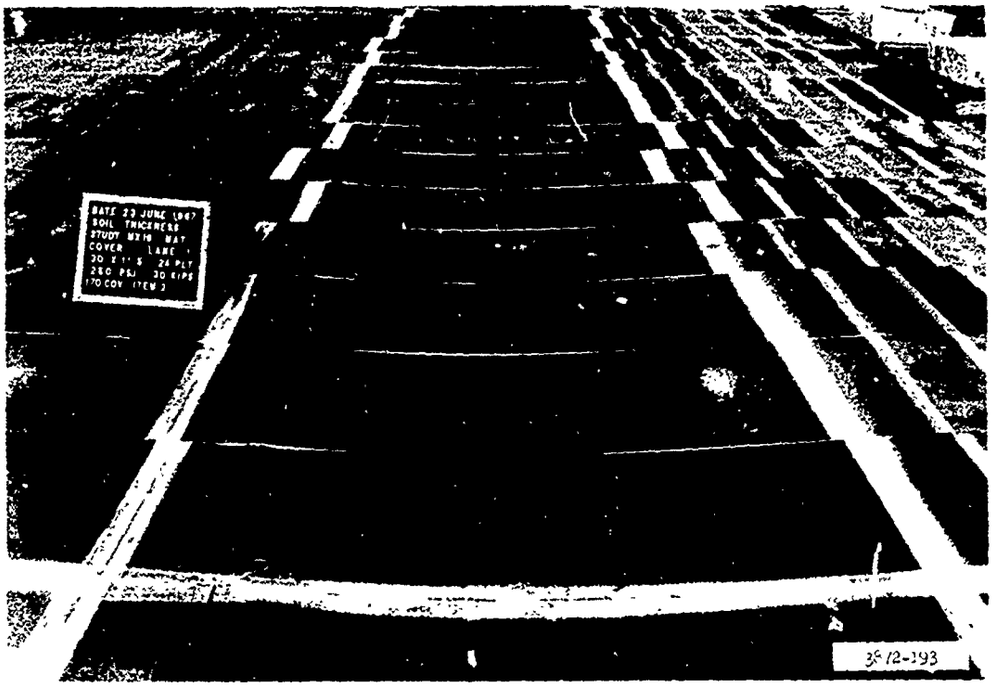


Photograph A33. Test section II, lane 1, item 2, after failure at 170 coverages

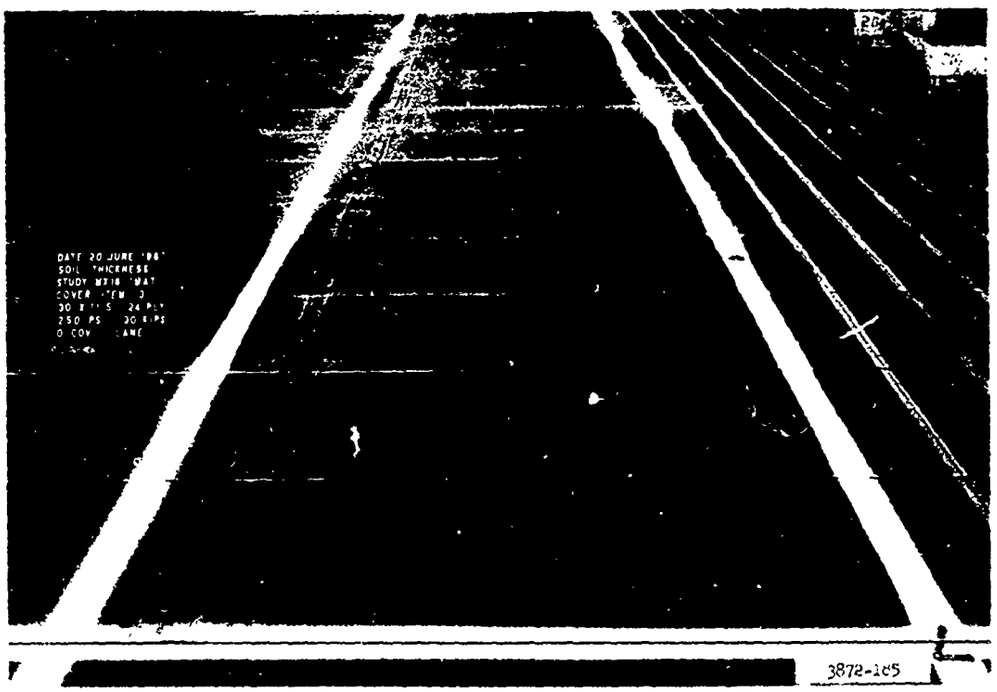


Photograph A34. Test section II, lane 1, item 3, prior to traffic

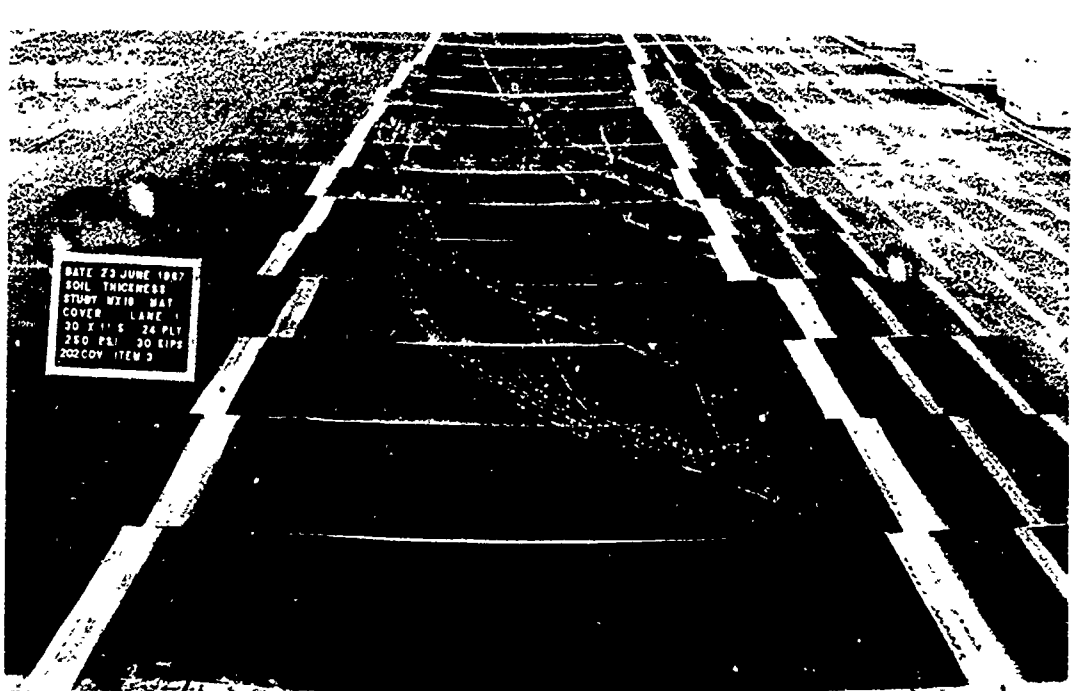


Photograph A35. Test section II, lane 1, item 3, after failure at 202 coverages

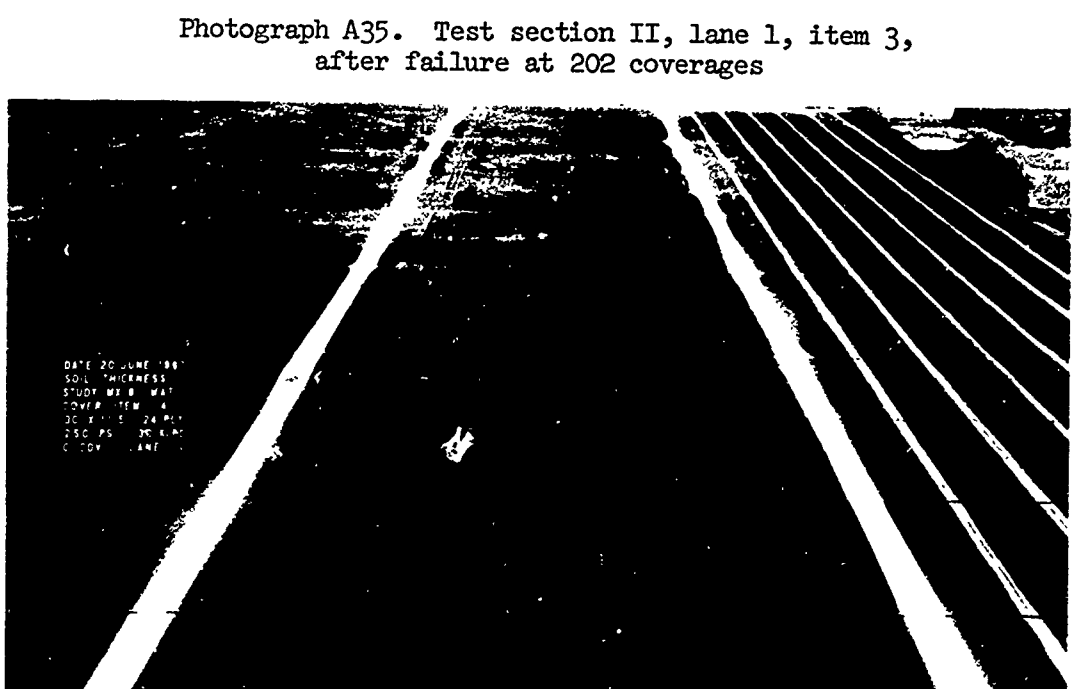

Photograph A36. Test Section II lane 1, item 4, prior to traffic

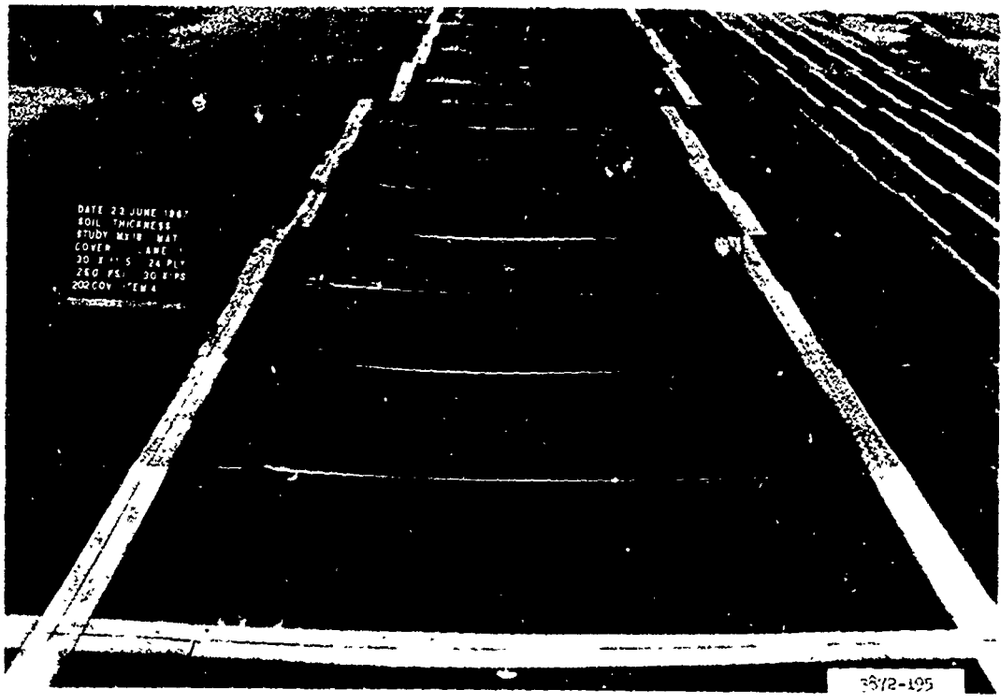

Photograph A37. Test section II, lane 1, item 4, after failure at 202 coverages

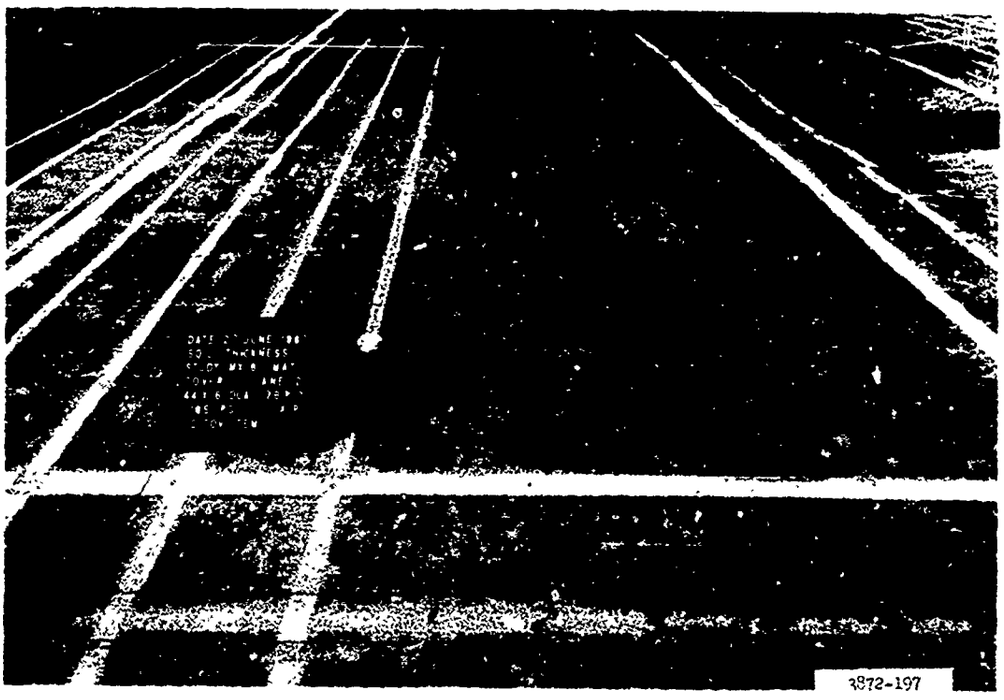

Photograph A38. Test section II, lane 2, item 1, prior to traffic

Photograph A39. Panels disconnected along C-rail and male connectors

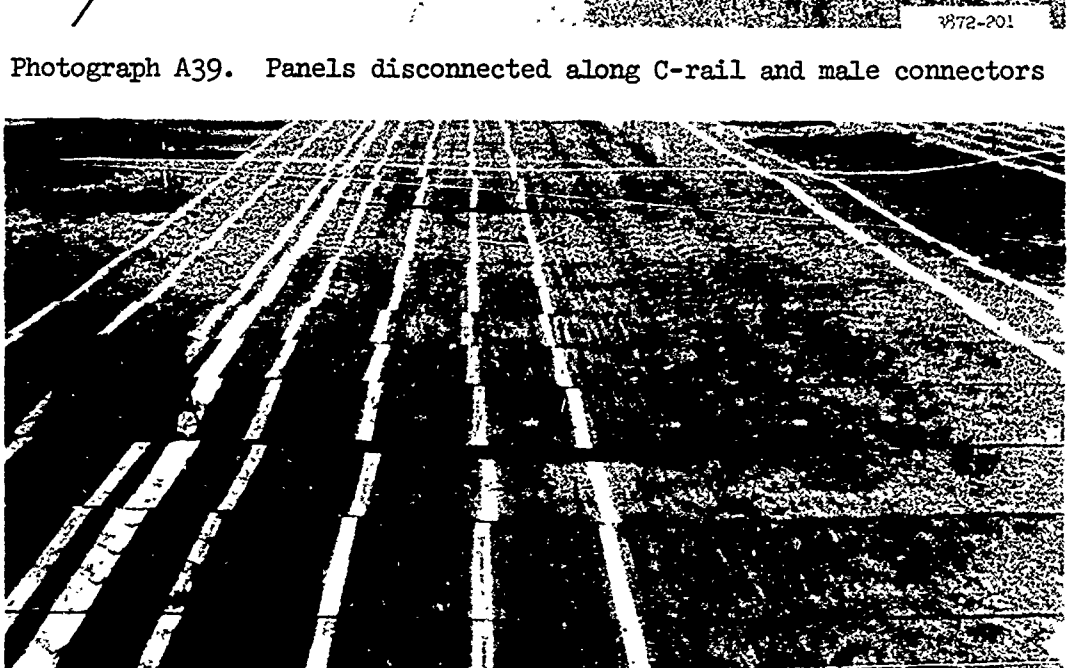

Photograph A40. Test section II, lane 2, item 1, after failure at 32 coverages

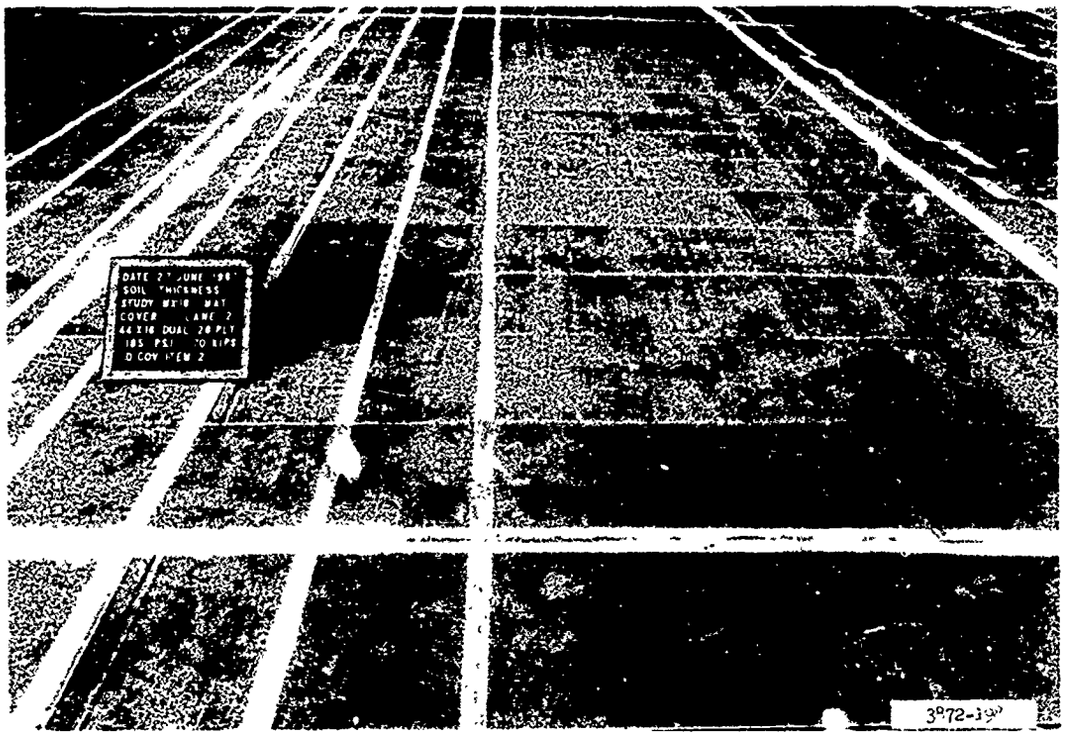


Photograph A41. Test section II, lane 2, item 2, prior to traffic

Photograph A42. Typical end-joint failure

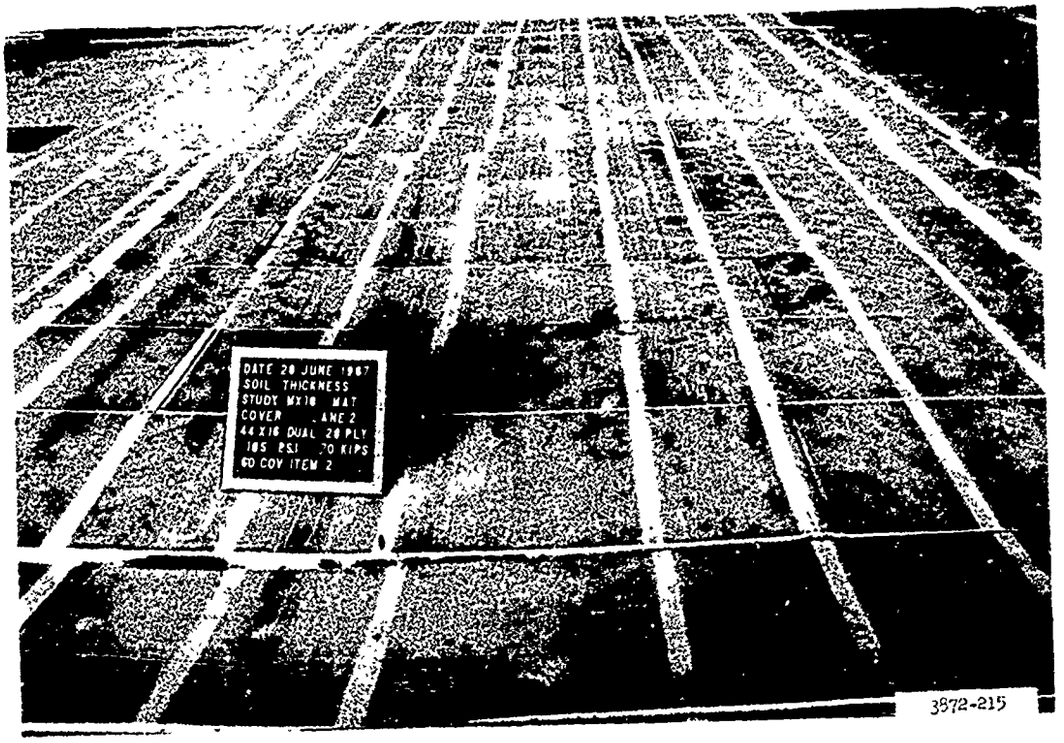


Photograph A43. Test section II, lane 2, item 2, after failure at 60 coverages

Photograph A44. Test section II, lane 2, item 3, prior to traffic


Photograph A45. Typical longitudinal and end-joint failure

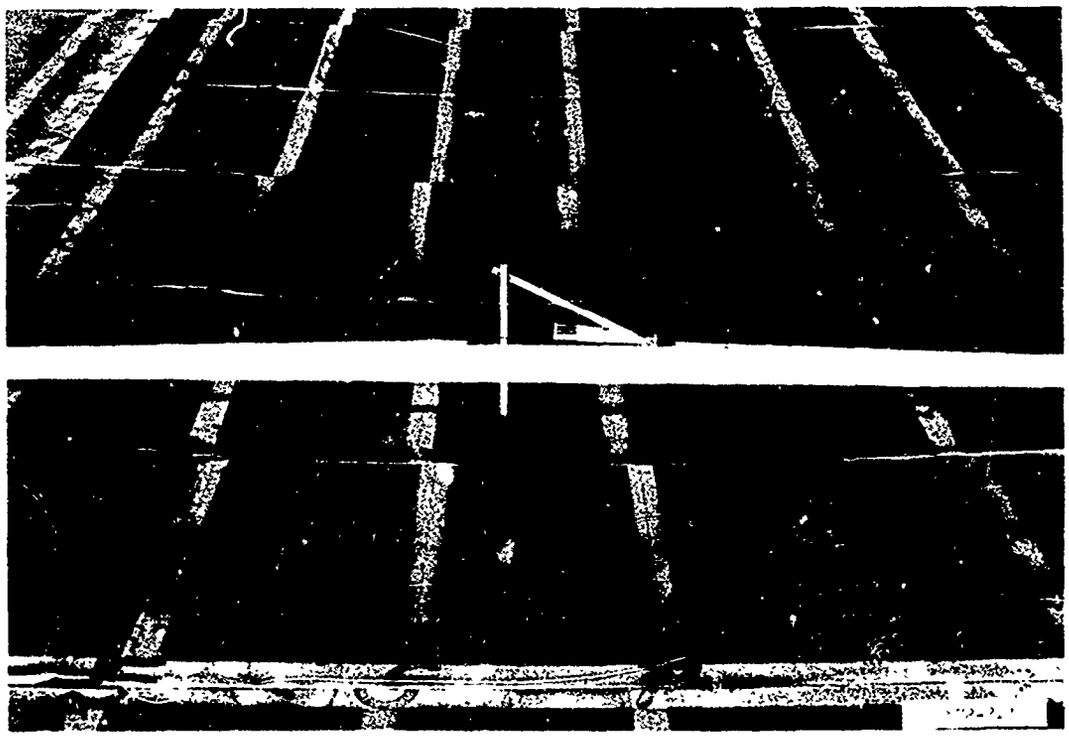

Photograph A46. Longitudinal deformation of 3.1 in. after 144 coverages

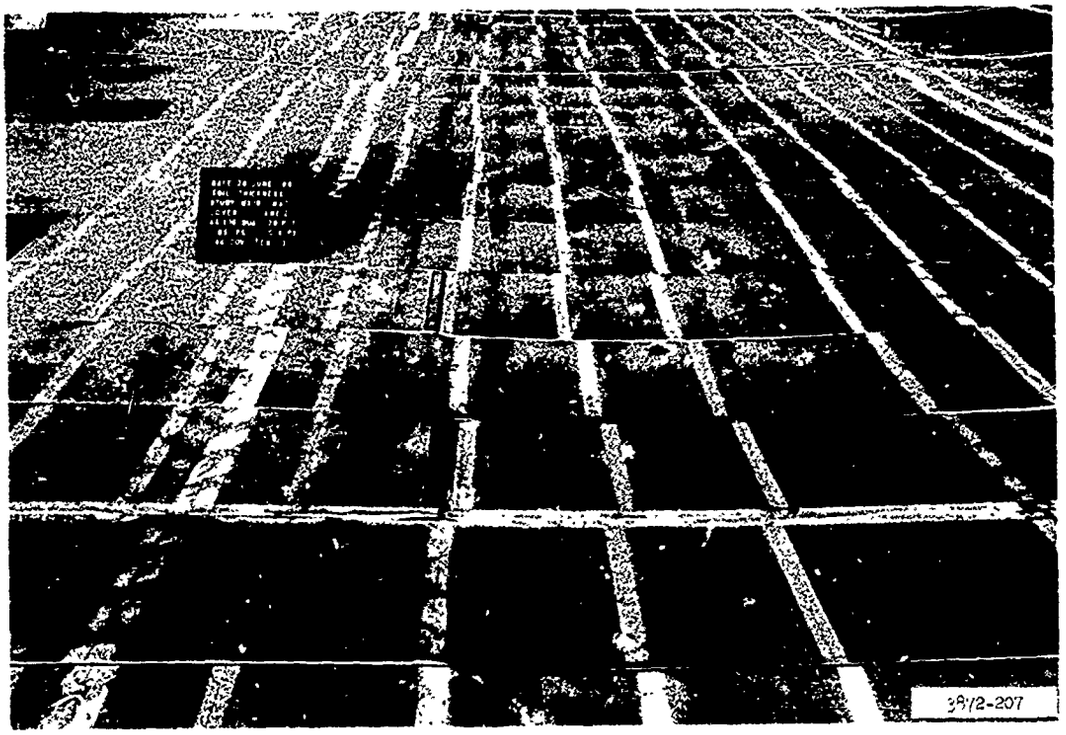


Photograph A47. Test section II, lane 2, item 3, after failure at 144 coverages

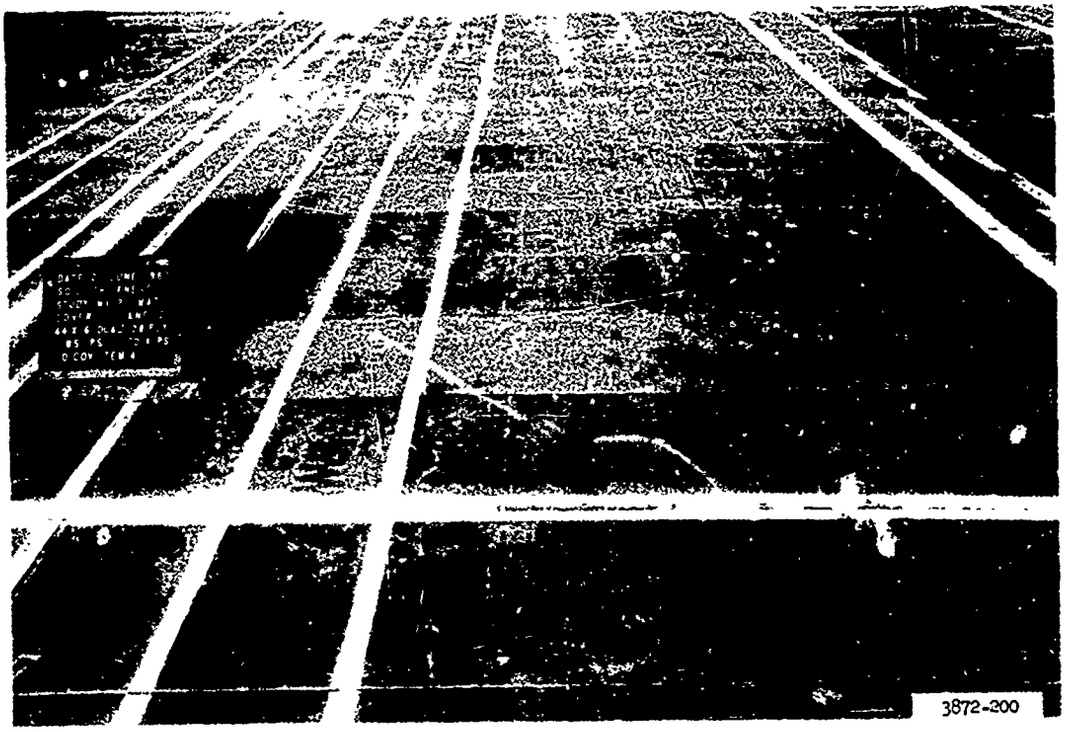


Photograph A48. Test section II, lane 2, item 4, prior to traffic


Photograph A49. Longitudinal deformation of 2.8 in. after 300 coverages


Photograph A50. Test section II, lane 2, item 4,
after failure at 300 coverages

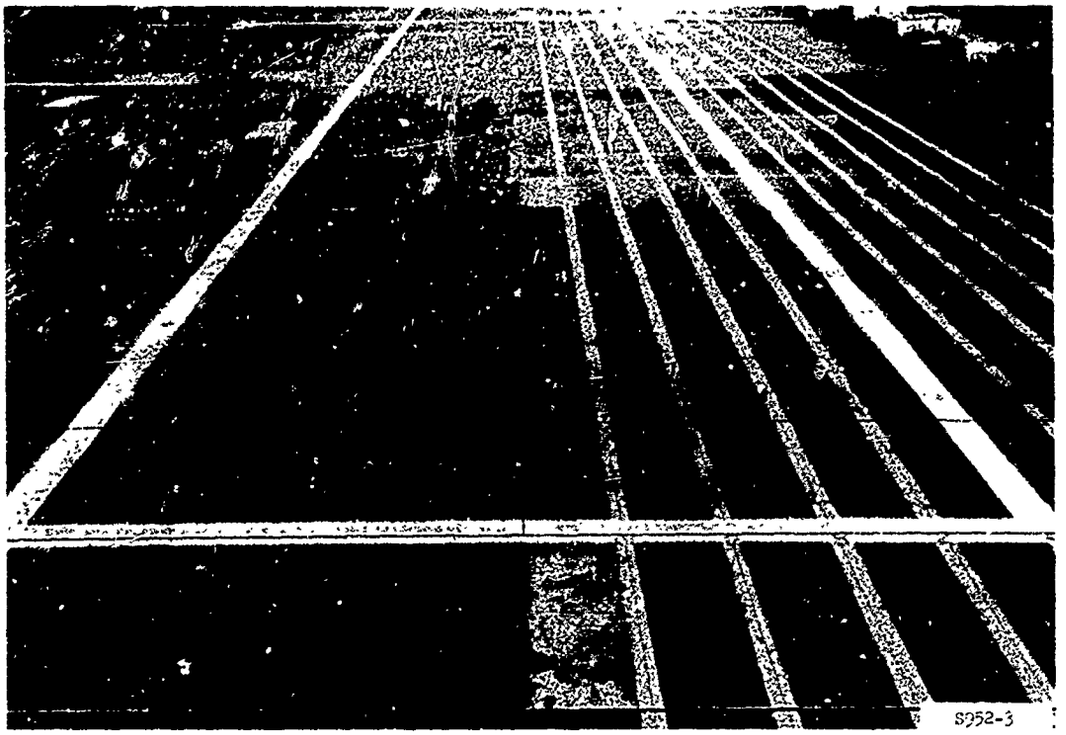


Photograph A51. Test section III, lane 1, item 1, prior to traffic

Photograph A52. Weld crack along underlapping end joint after 200 coverages

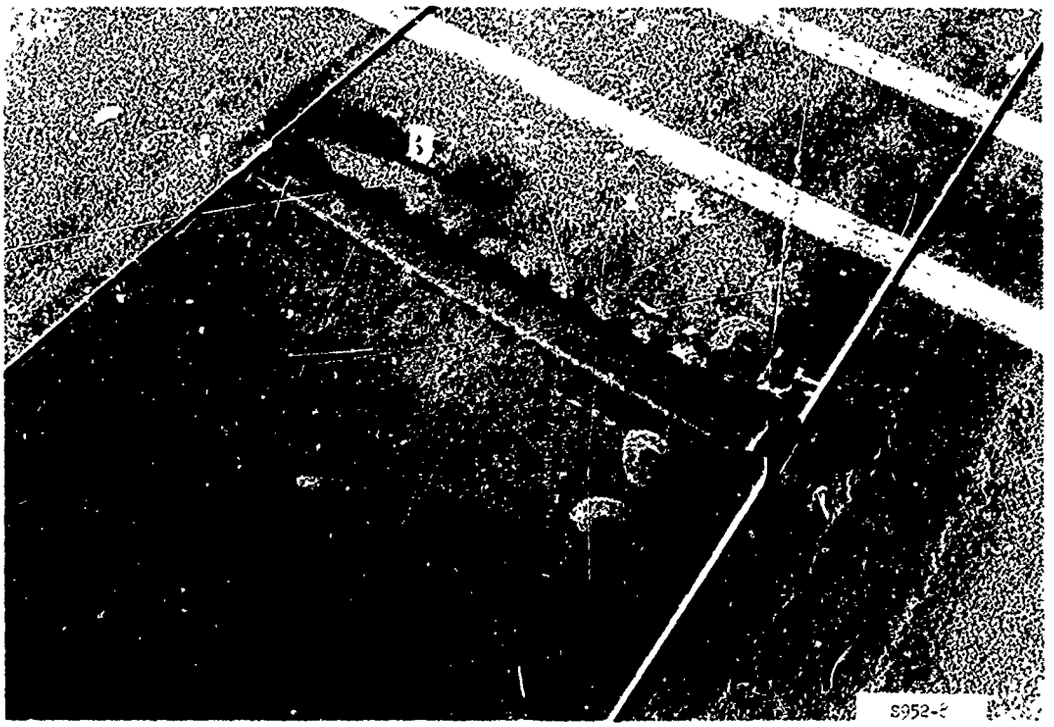

Photograph A53. Top skin tears and end-joint failure after 314 coverages

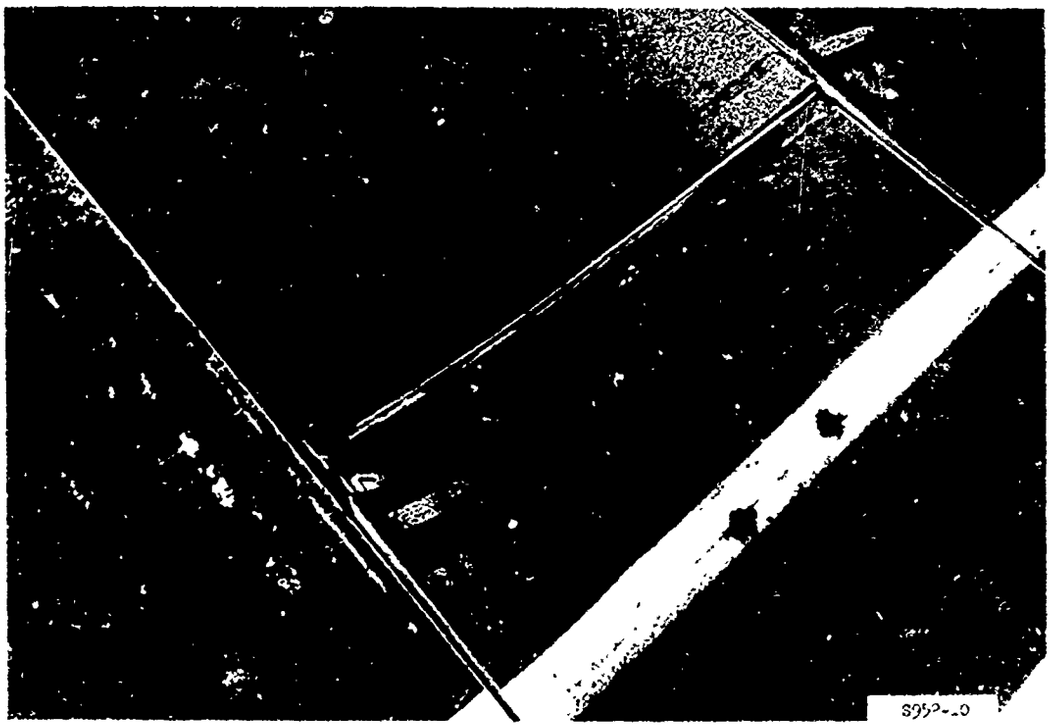

Photograph A54. Locking bar forced from end joint after 528 coverages

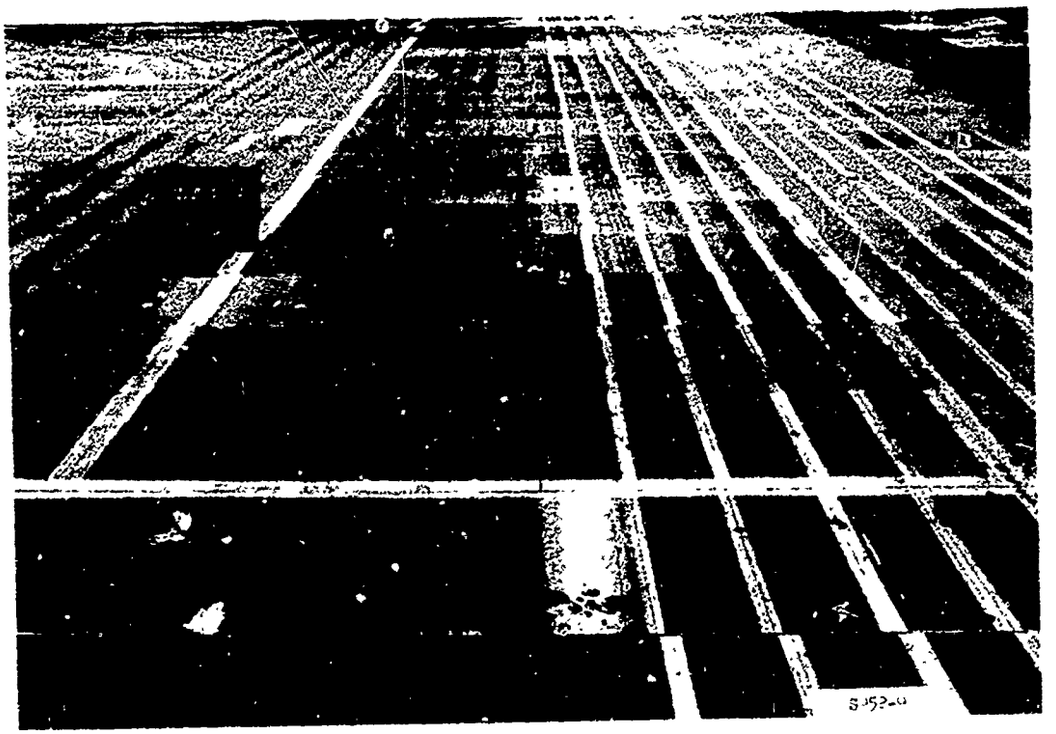

Photograph A55. Test section III, lane 1, item 1, after failure at 528 coverages


Photograph A56. Test section III, lane 1, item 2, prior to traffic

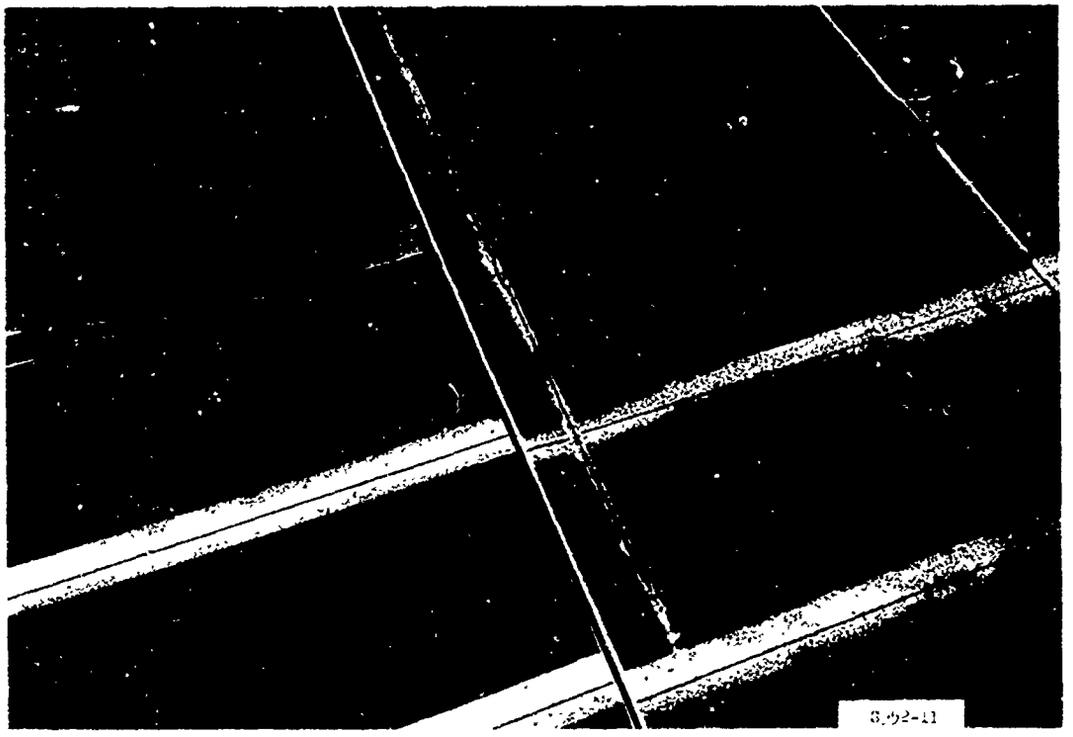

Photograph A57. Top skin tear after 528 coverages

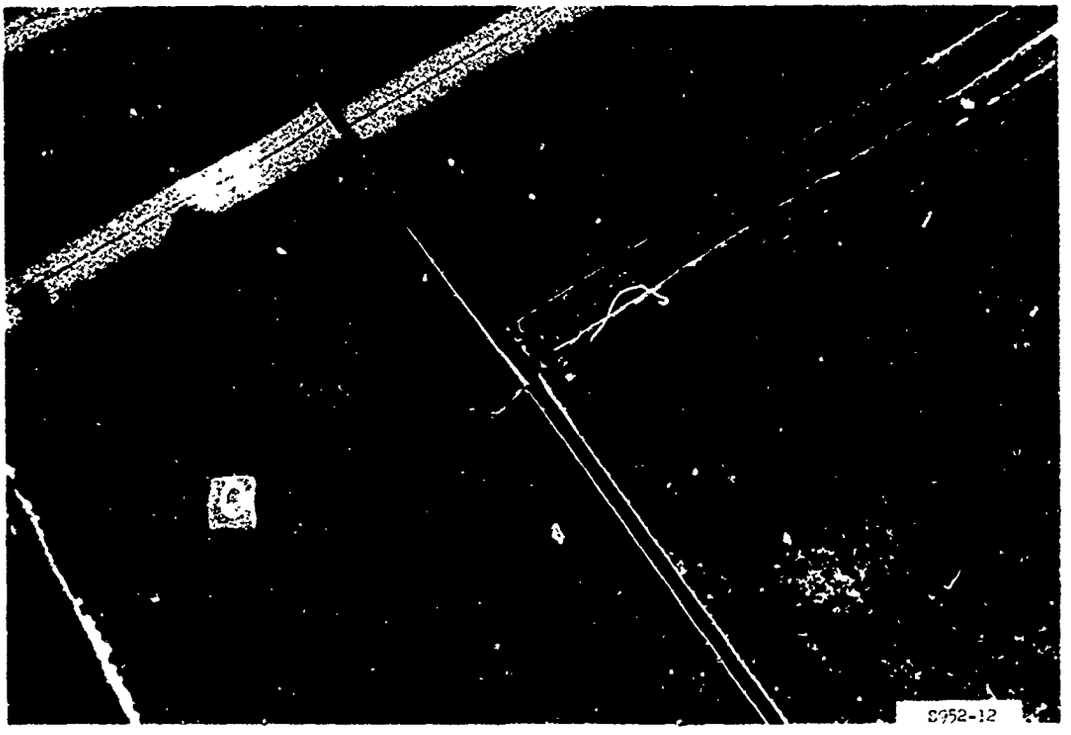

Photograph A58. Internal rib failures and top skin tear after 720 coverages

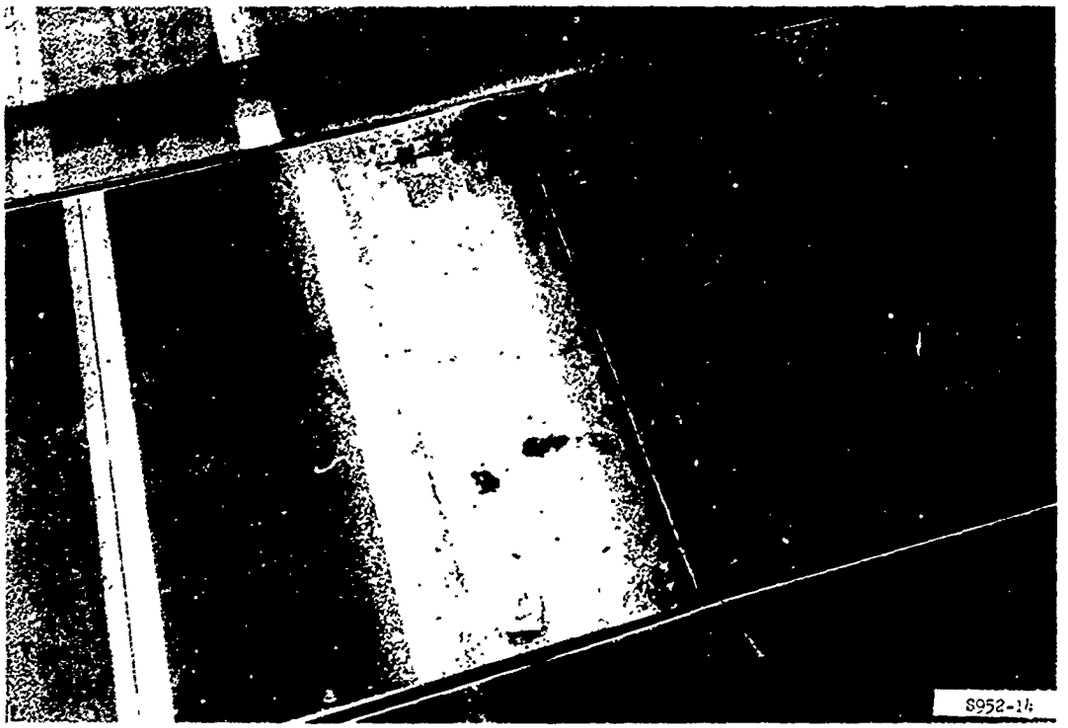


Photograph A59. Typical internal rib failures after 884 coverages

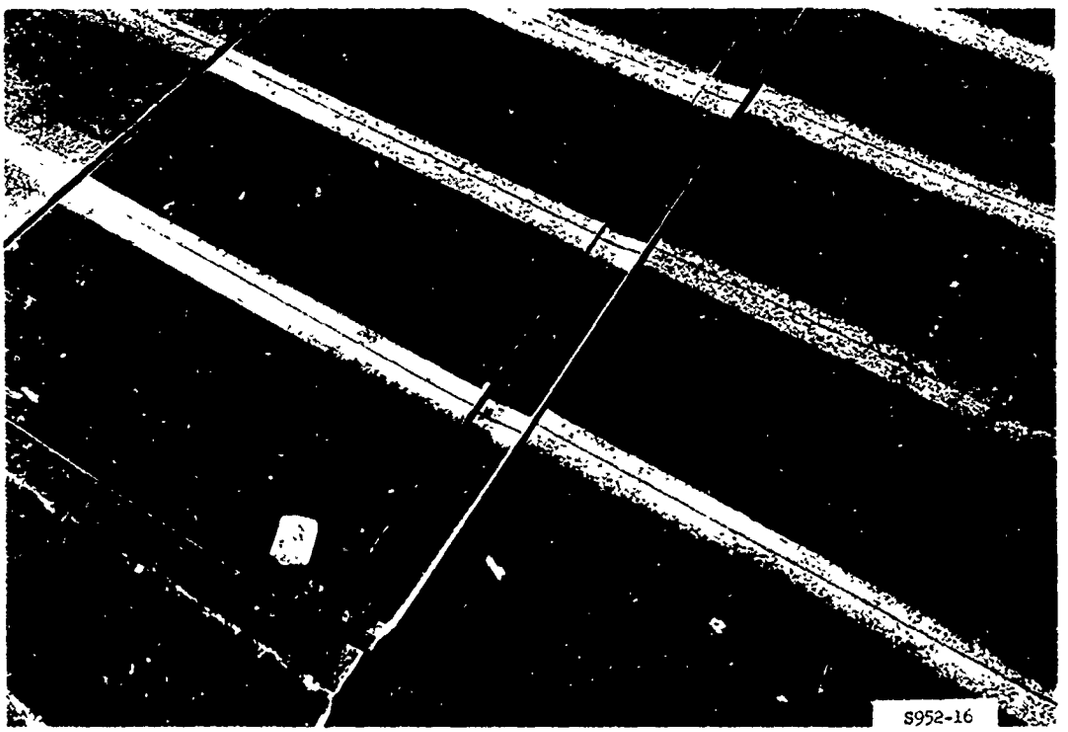


Photograph A60. Top skin tear along C-rail after 884 coverages

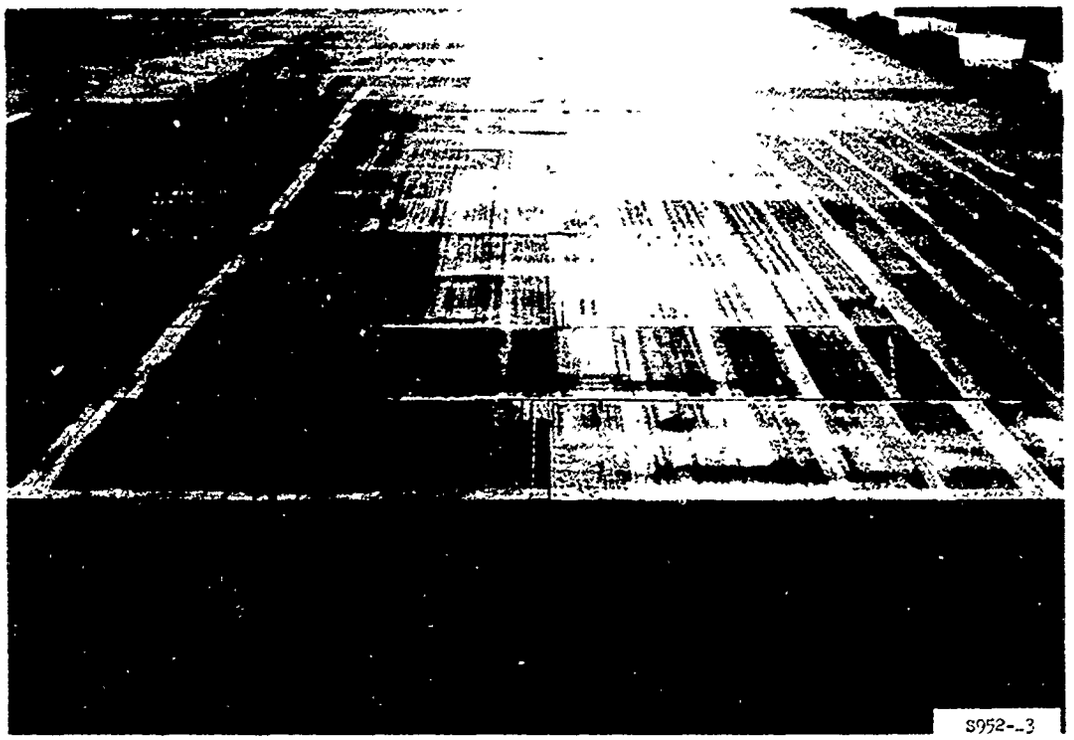


Photograph A61. Test section III, lane 1, item 2, after failure at 884 coverages

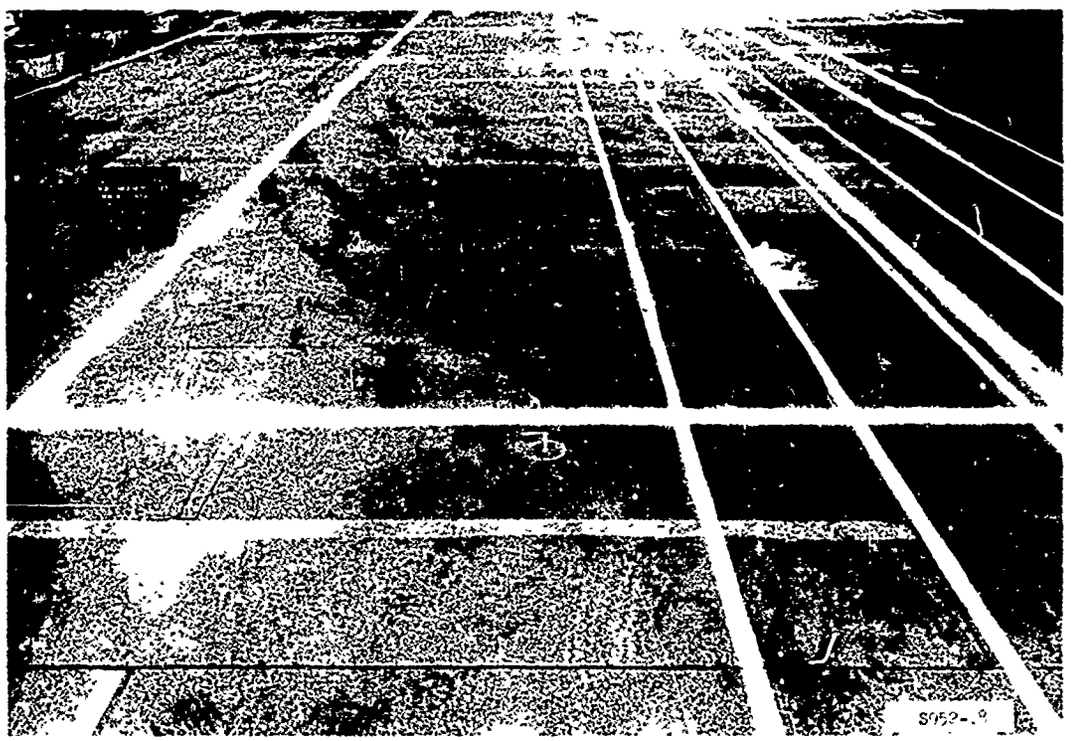


Photograph A62. Test section III, lane 2, item 1, prior to traffic

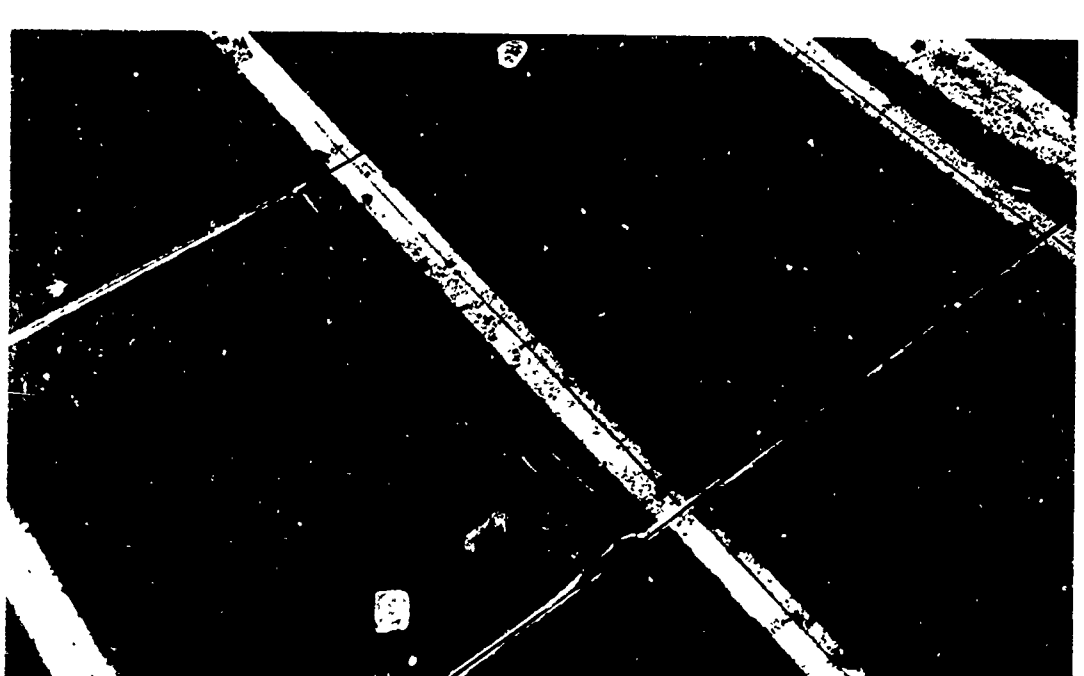


Photograph A63. Top lip of overlapping end joint sheared after 16 coverages

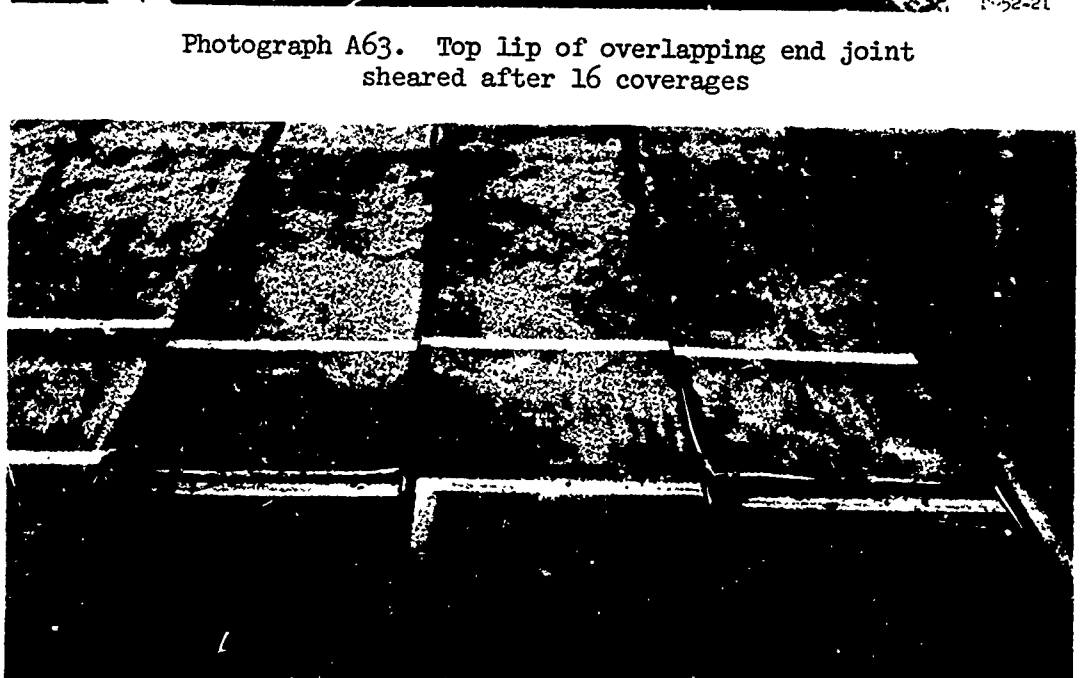


Photograph A64. Typical end-joint failure after 56 coverages

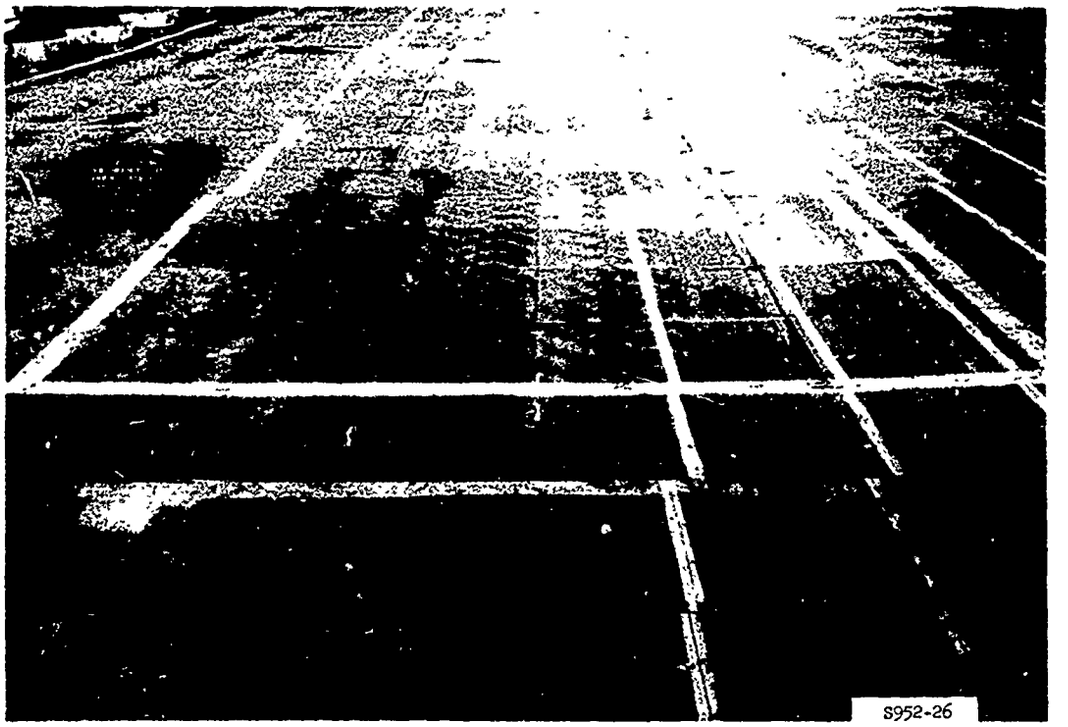


Photograph A65. Test section III, lane 2, item 1, after failure at 56 coverages

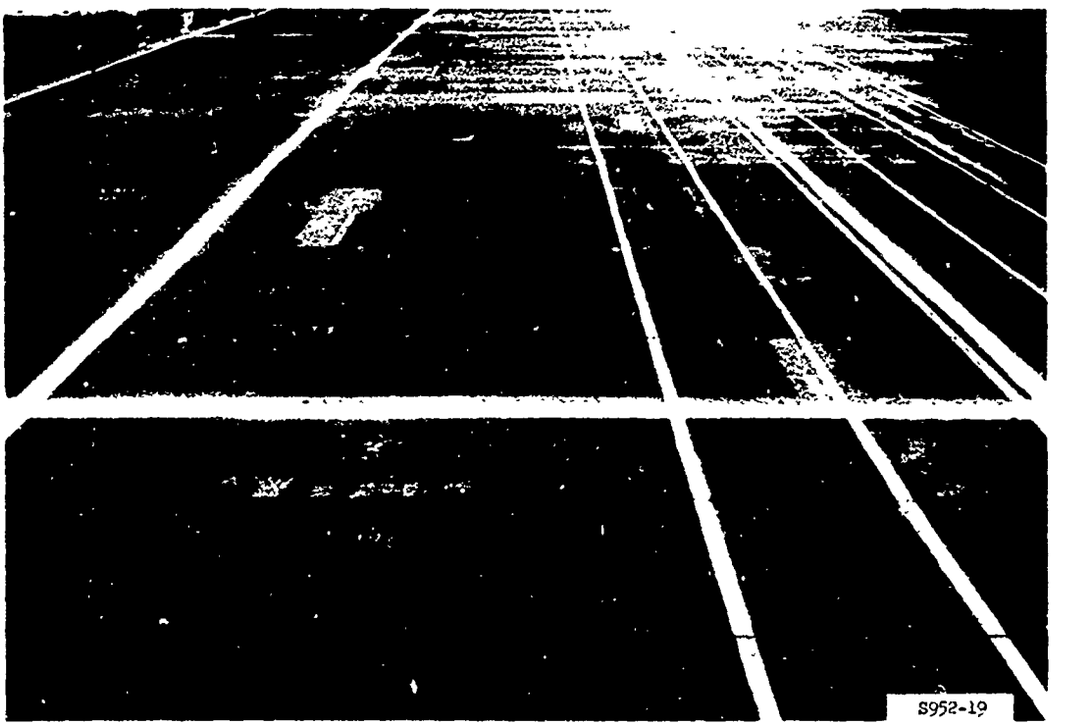


Photograph A66. Test section III, lane 2, item 2, prior to traffic

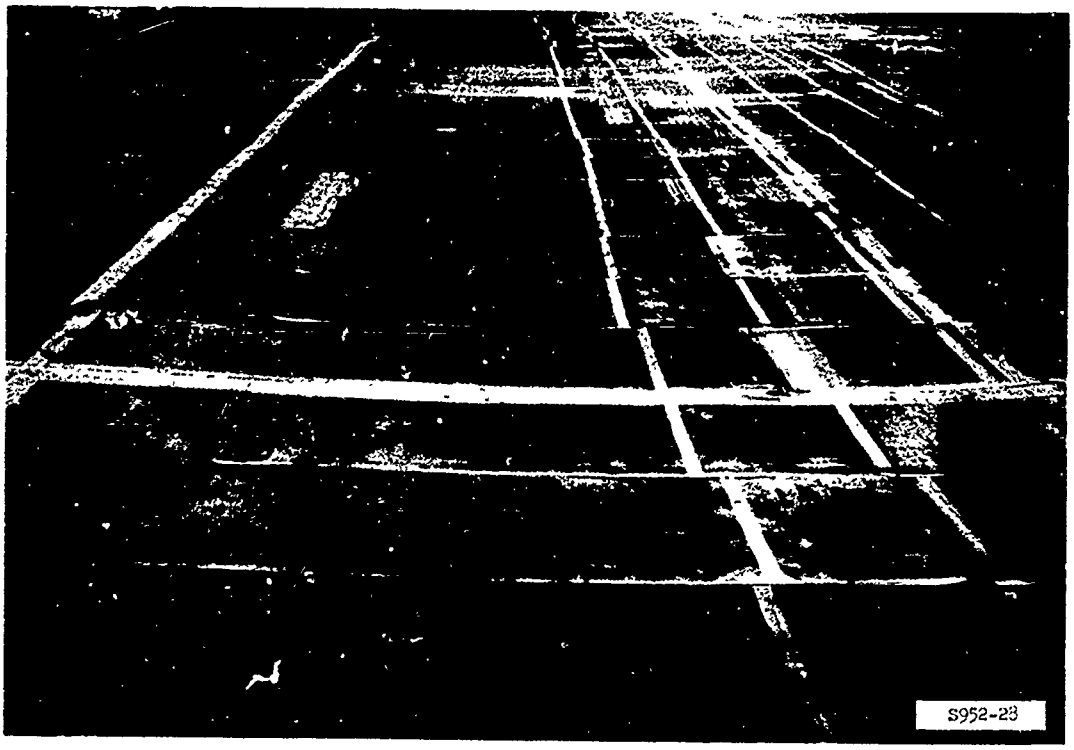


Photograph A67. Test section III, lane 2, item 2, after failure at 72 coverages

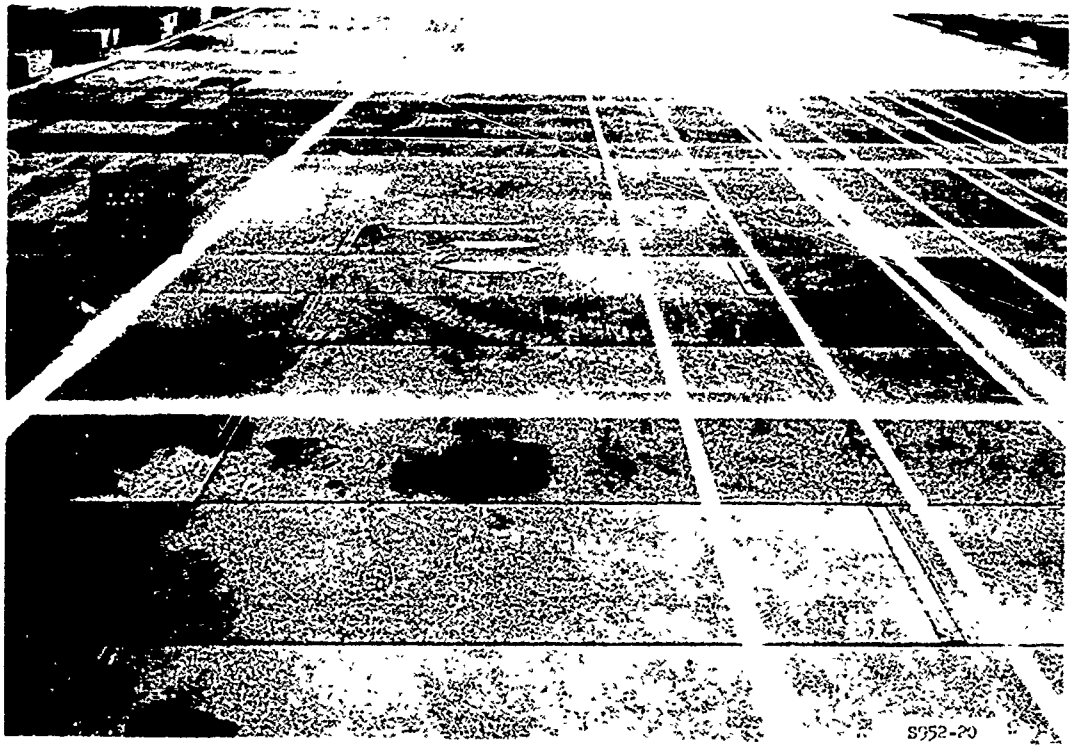


Photograph A68. Test section III, lane 2, item 3, prior to traffic

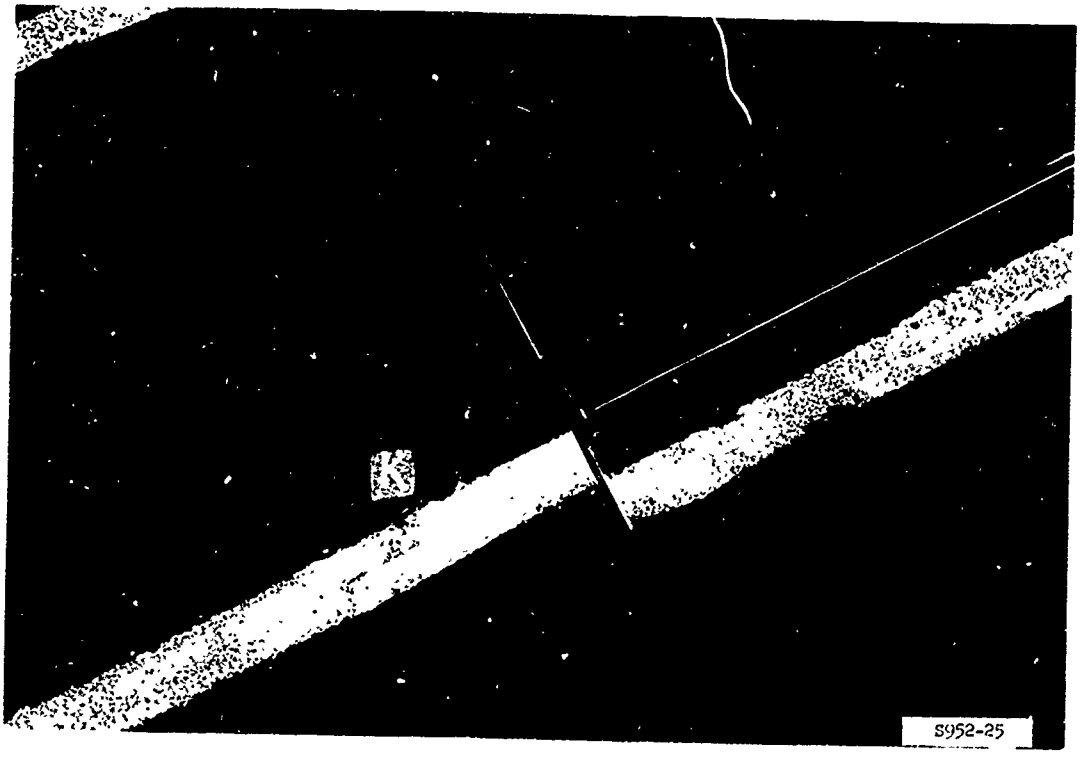


Photograph A69. Bottom lip of overlapping end joint sheared after 48 coverages

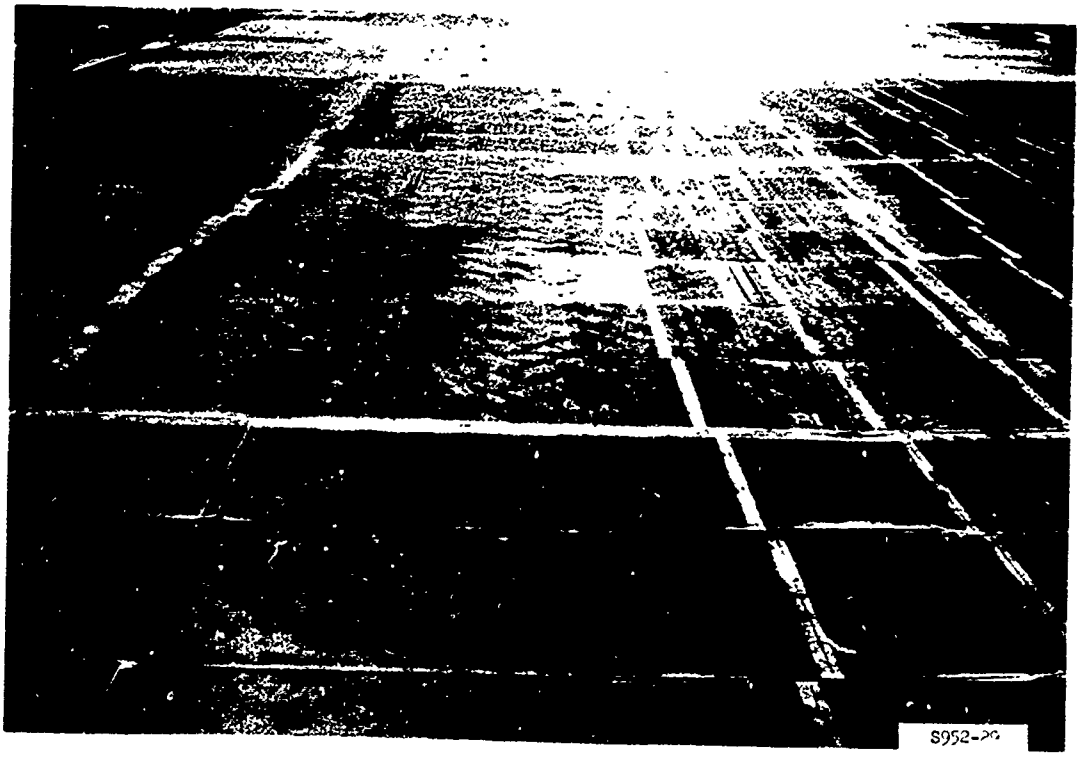


Photograph A70. Test section III, lane 2, item 3, at failure after 92 coverages

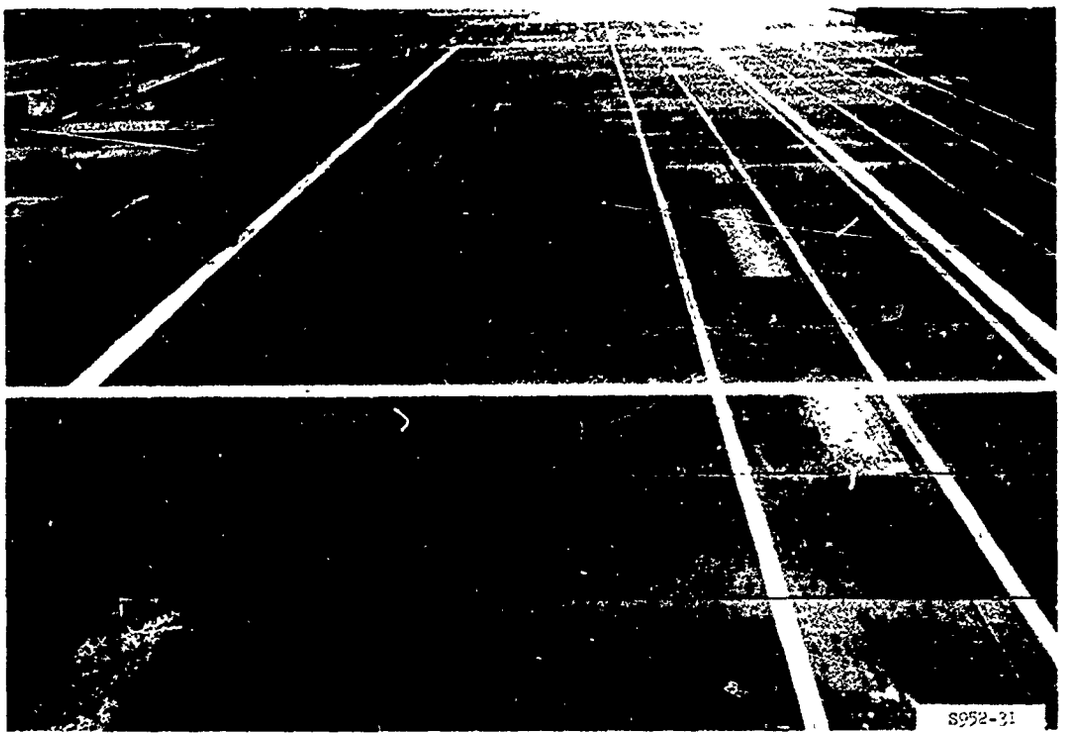


Photograph A71. Test section IV prior to traffic

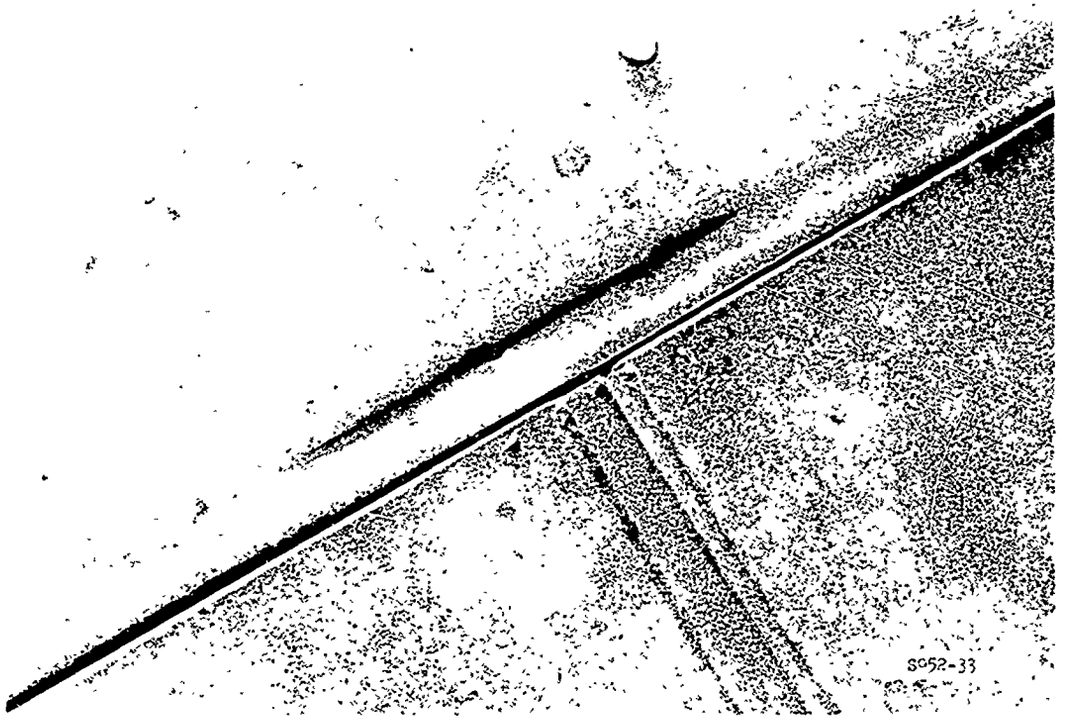


Photograph A72. Top skin tear at panel center after failure at 348 coverages

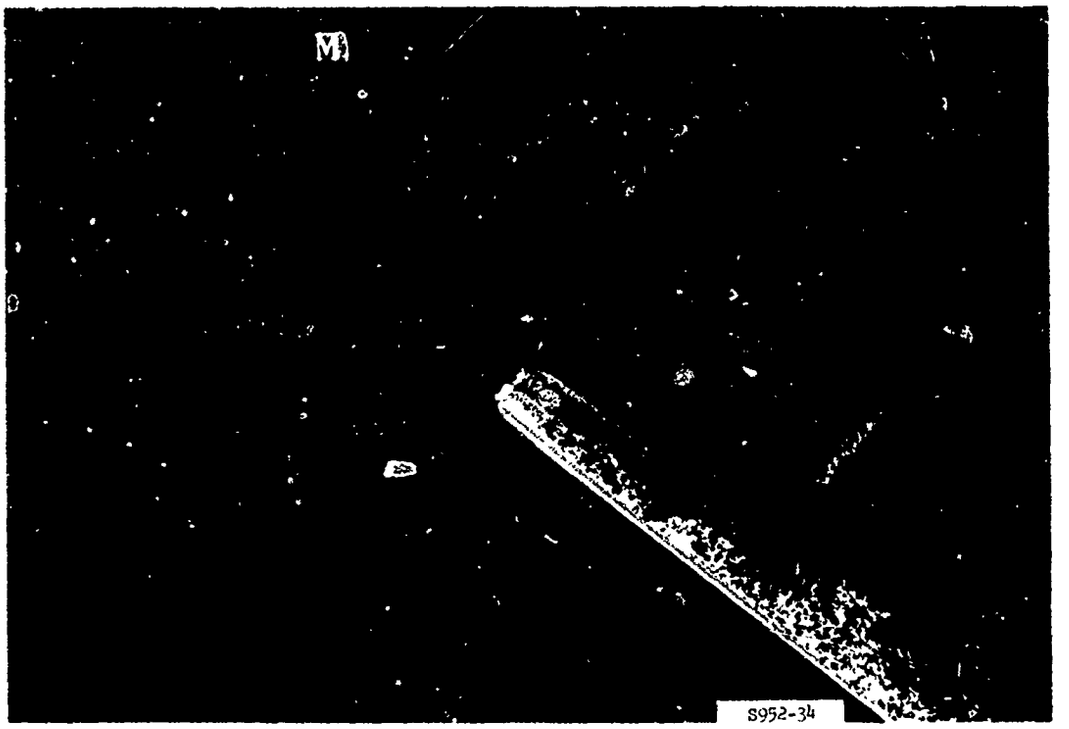


Photograph A73. Top skin tear at an end joint after failure at 348 coverages

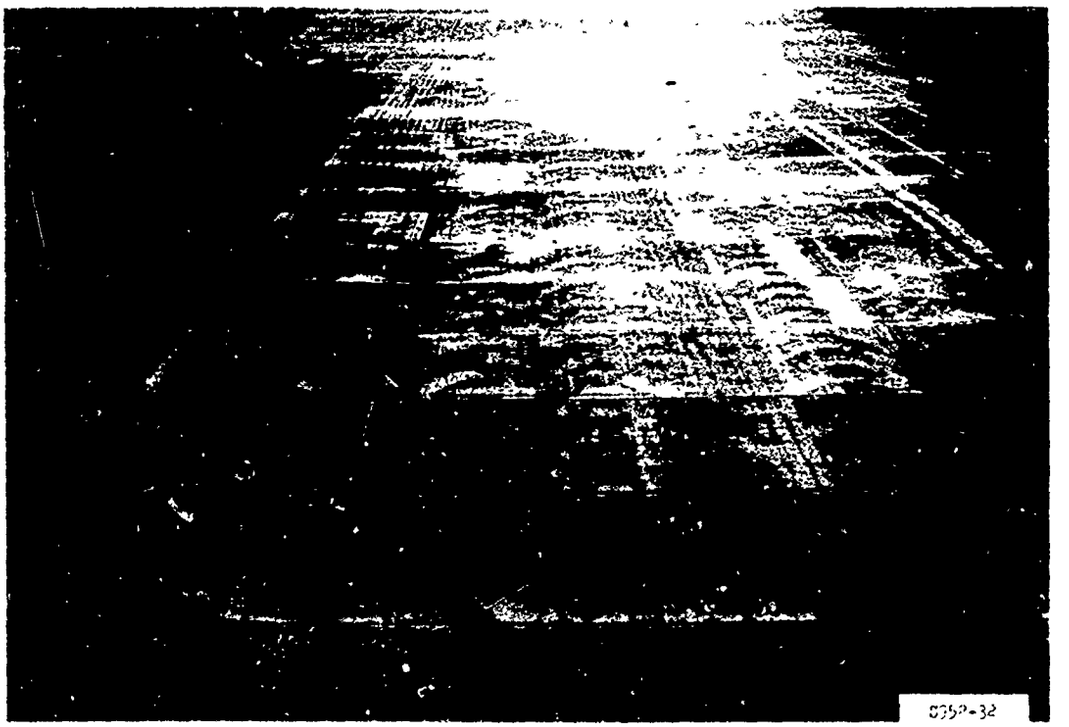


Photograph A74. Test section IV after failure at 348 coverages

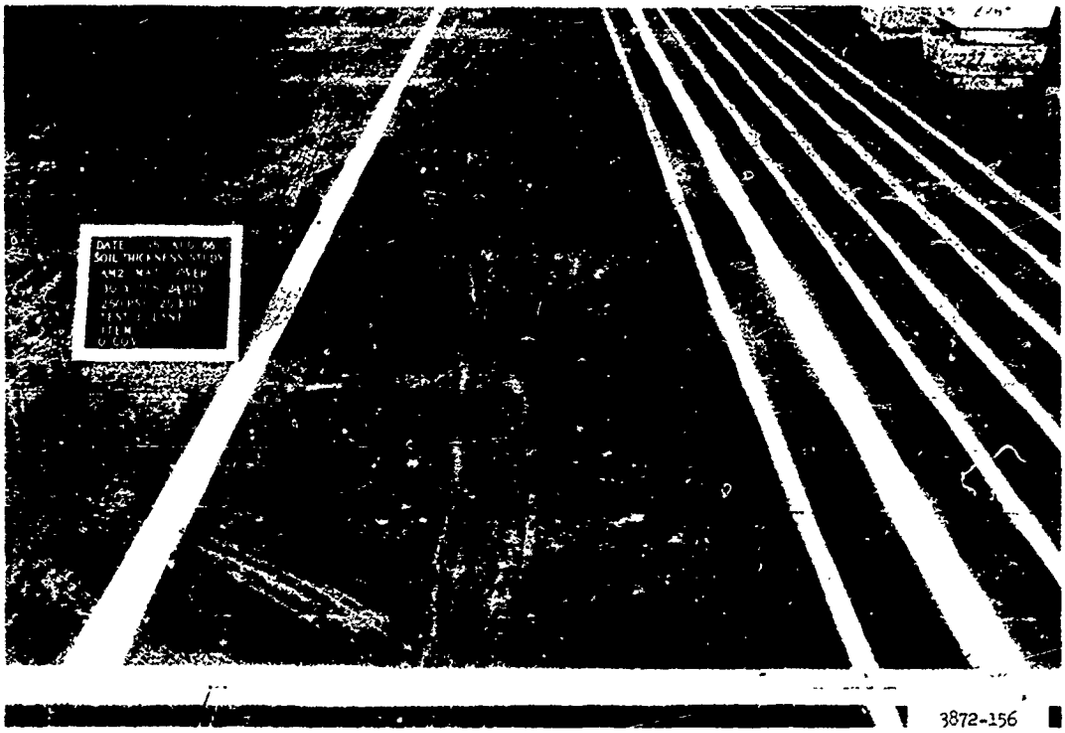


Photograph A75. Test section V prior to traffic

Photograph A76. Typical weld break along end joint after failure at 330 coverages

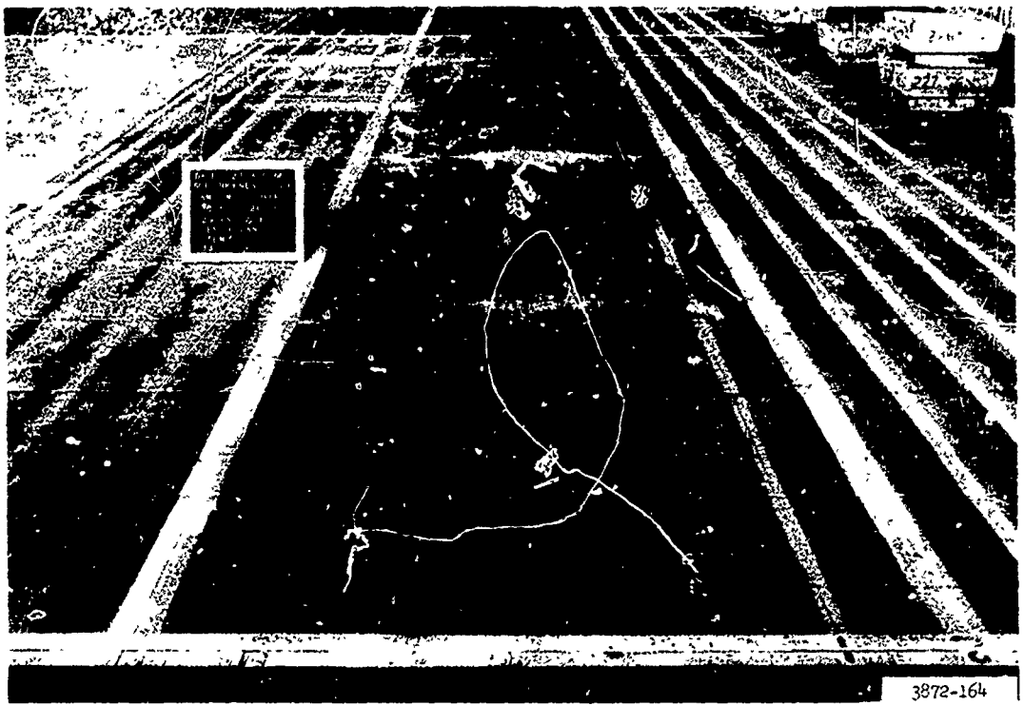


Photograph A77. Test section V after failure at 330 coverages

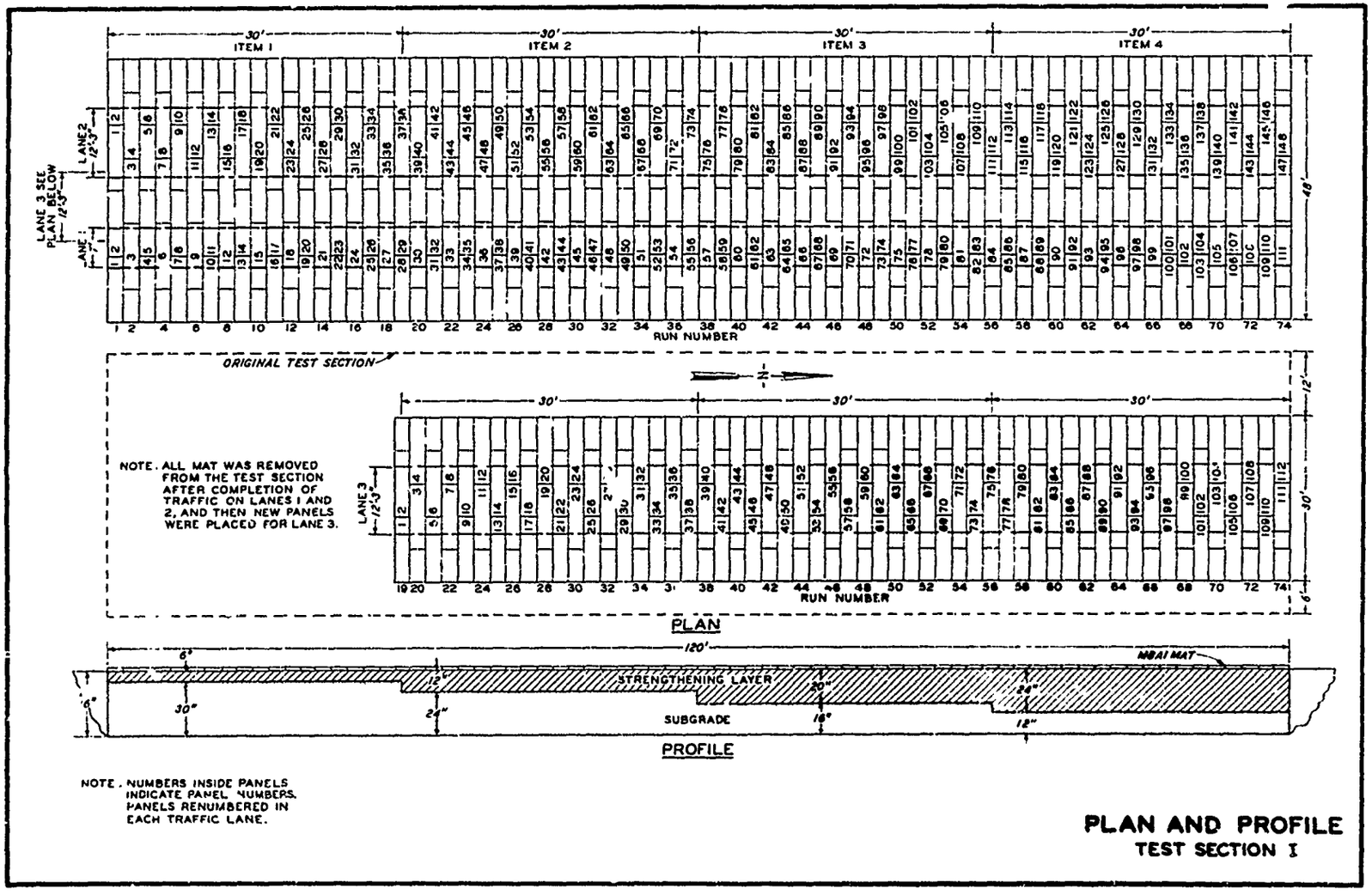


**PLAN AND PROFILE**
**TEST SECTION I**

PLATE A1

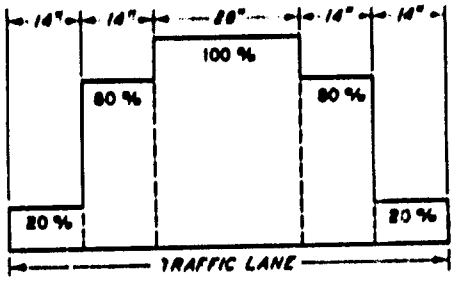



| | |
|---|---|
| TIRE SIZE | 56X16 |
| CONTACT AREA | 208.13 SQ IN. |
| WHEEL LOAD | 31,000 LB |
| INFLATION PRESSURE | 185 PSI |

a. LANE 1

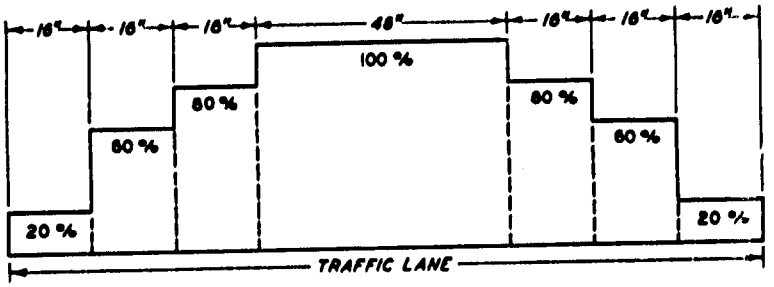


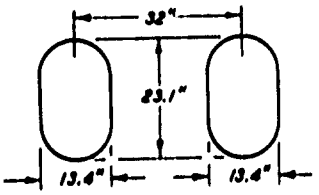


| | |
|---|---|
| TIRE SIZE | 56X16 |
| CONTACT AREA | 257.7 SQ IN. |
| WHEEL LOAD | 56,000 LB |
| INFLATION PRESSURE | 105 PSI |

b. LANE 2

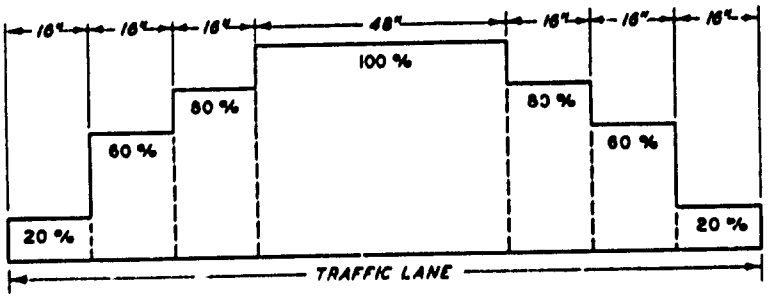


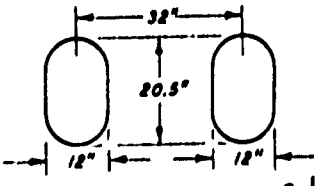


| | |
|---|---|
| TIRE SIZE | 56X16 |
| CONTACT AREA | 200.5 SQ IN. |
| WHEEL LOAD | 62,000 LB |
| INFLATION PRESSURE | 185 PSI |

c. LANES 2 AND 3

## TRAFFIC DISTRIBUTION PATTERNS AND TIRE CHARACTERISTICS

TEST SECTION I

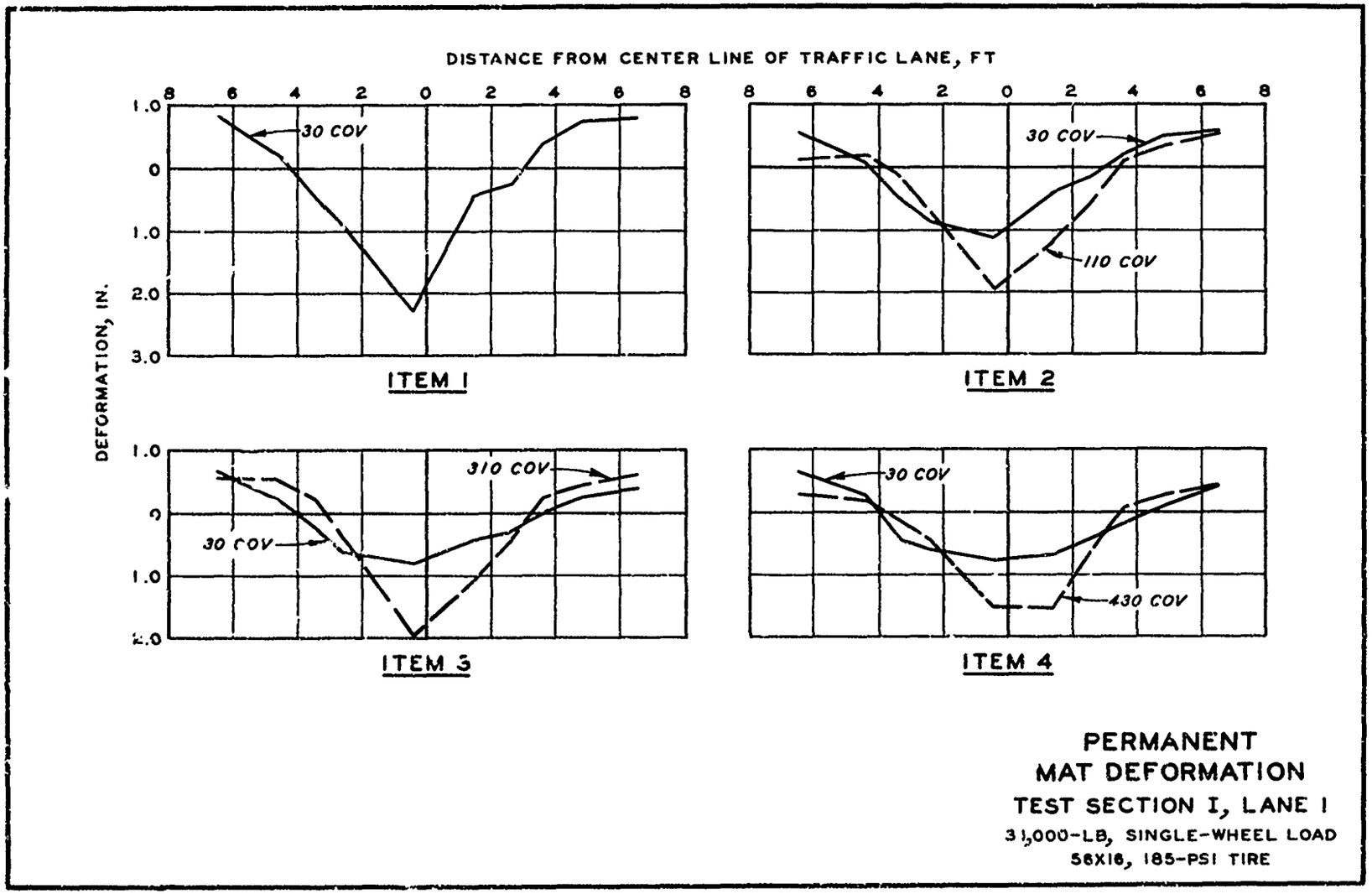


PERMANENT
MAT DEFORMATION
TEST SECTION I, LANE 1
31,000-LB, SINGLE-WHEEL LOAD
56X16, 185-PSI TIRE

PLATE A3

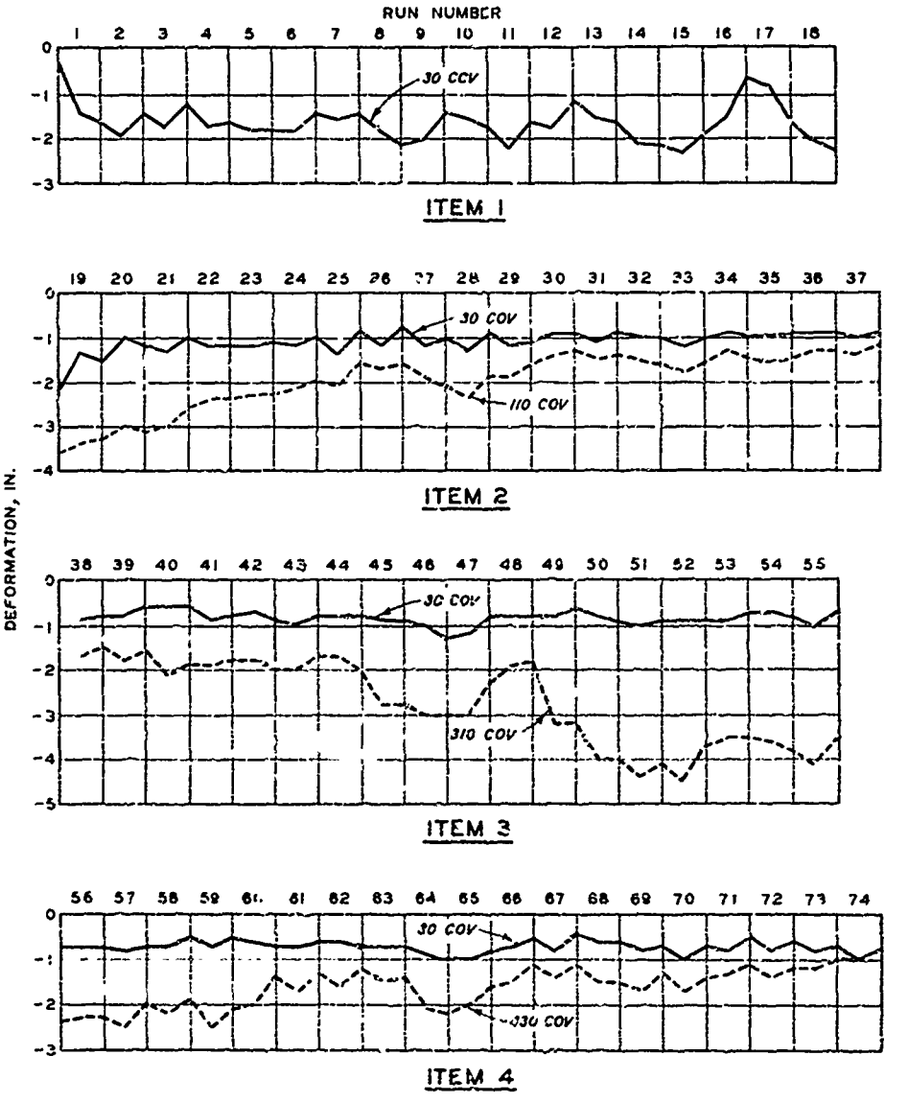


CENTER-LINE PROFILES
TEST SECTION I, LANE 1
31,000-LB. SINGLE-WHEEL LOAD
56X16, 185-PSI TIRE



PLATE A4

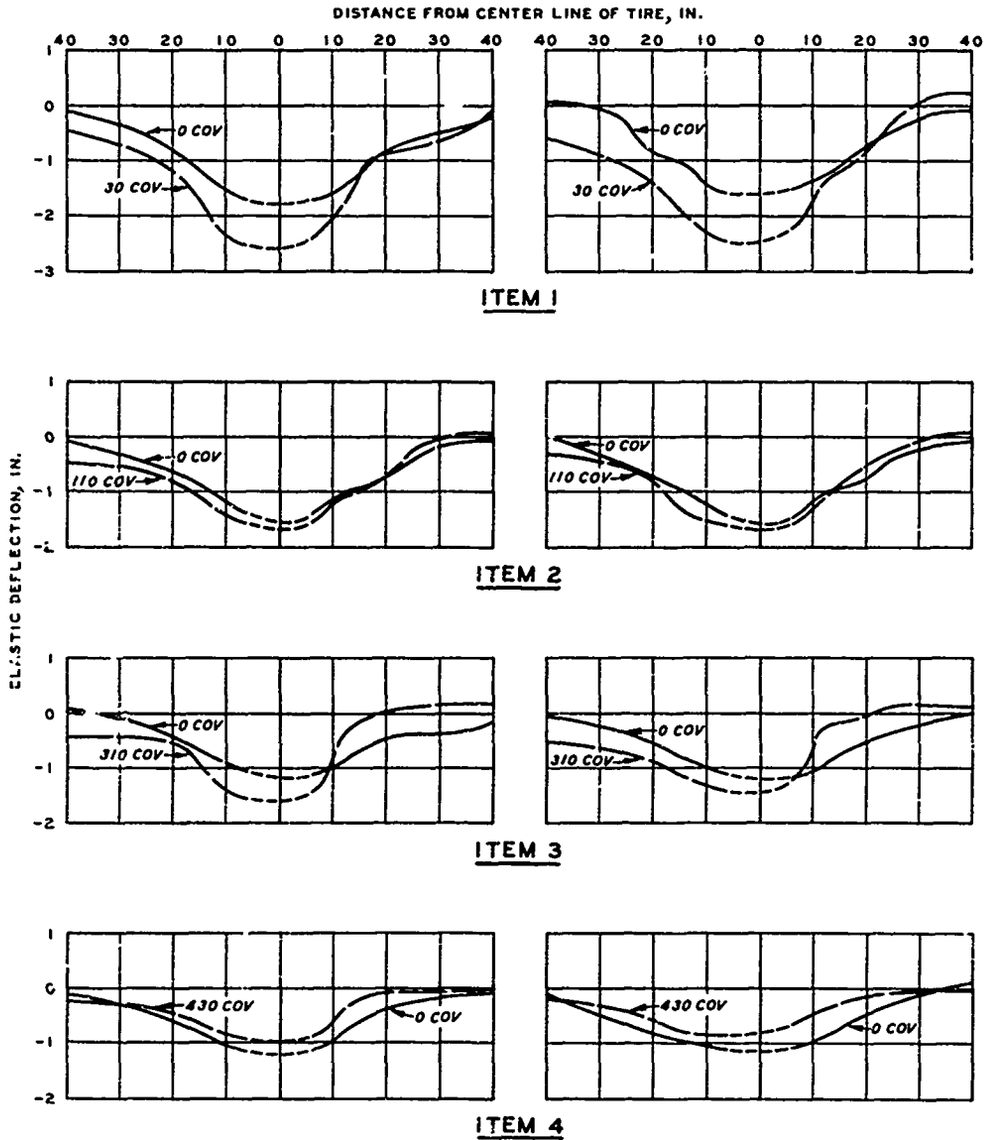


## ELASTIC MAT DEFLECTION
### TEST SECTION I, LANE I
31,000-LB, SINGLE-WHEEL LOAD
56X16, 185-PSI TIRE

PLATE A5

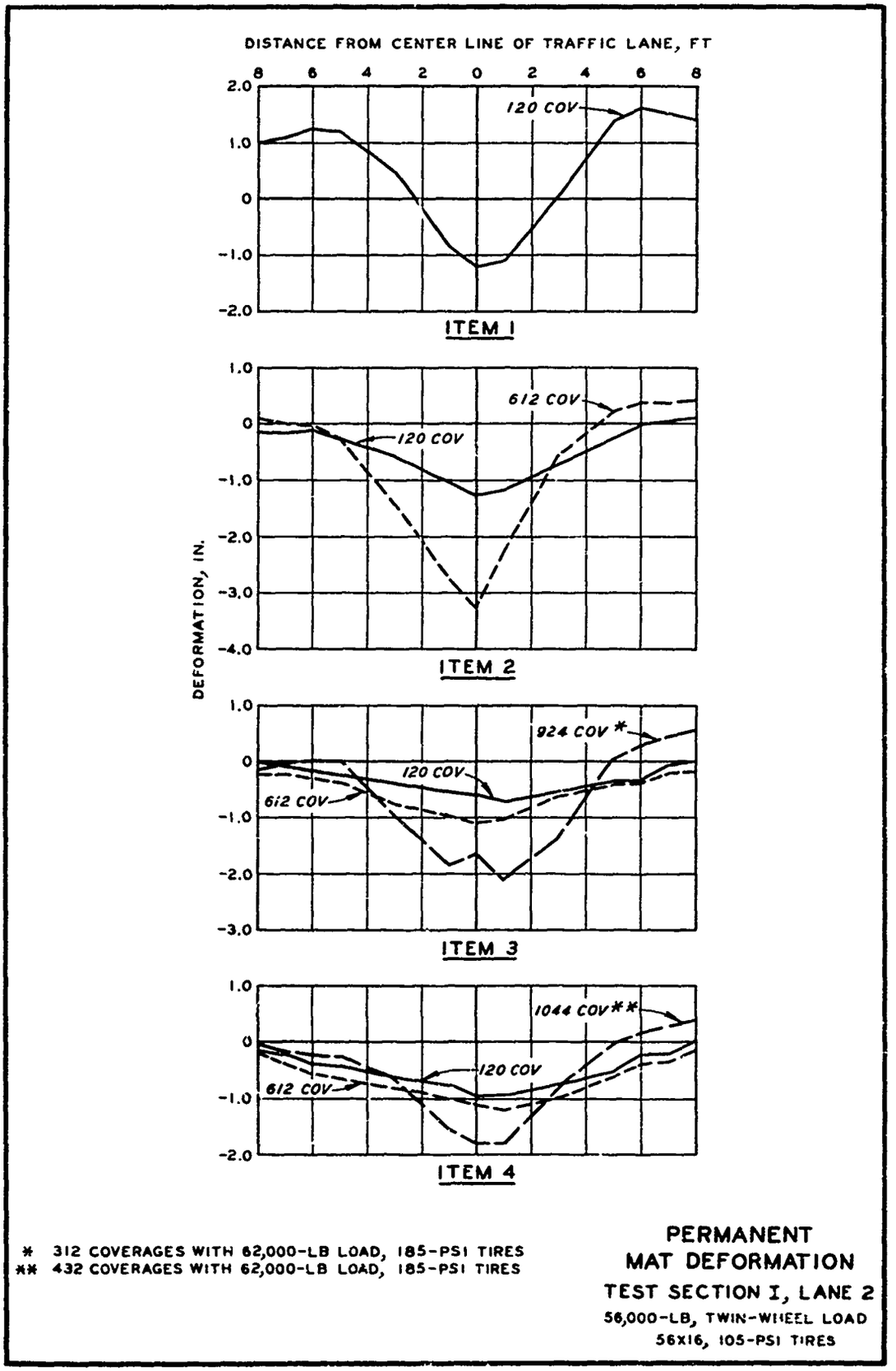


* 312 COVERAGES WITH 62,000-LB LOAD, 185-PSI TIRES
** 432 COVERAGES WITH 62,000-LB LOAD, 185-PSI TIRES

**PERMANENT MAT DEFORMATION**
**TEST SECTION I, LANE 2**
56,000-LB, TWIN-WHEEL LOAD
56X16, 105-PSI TIRES

PLATE A6

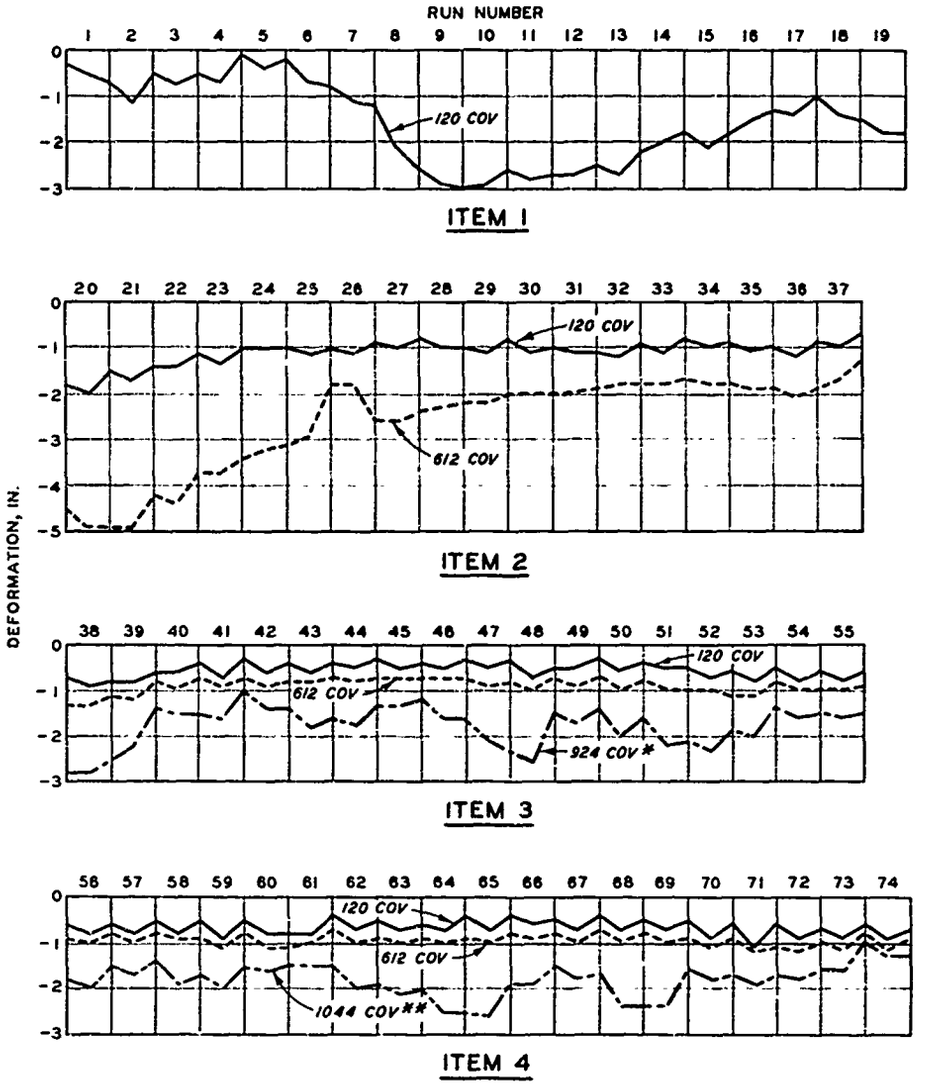


NOTE * 312 COVERAGES WITH 62-KIP LOAD, 185-PSI TIRES.

** 432 COVERAGES WITH 62-KIP LOAD, 185-PSI TIRES.

## CENTER-LINE PROFILES
TEST SECTION I, LANE 2
56,000-LB, TWIN-WHEEL LOAD
56X16, 105-PSI TIRES



PLATE A7

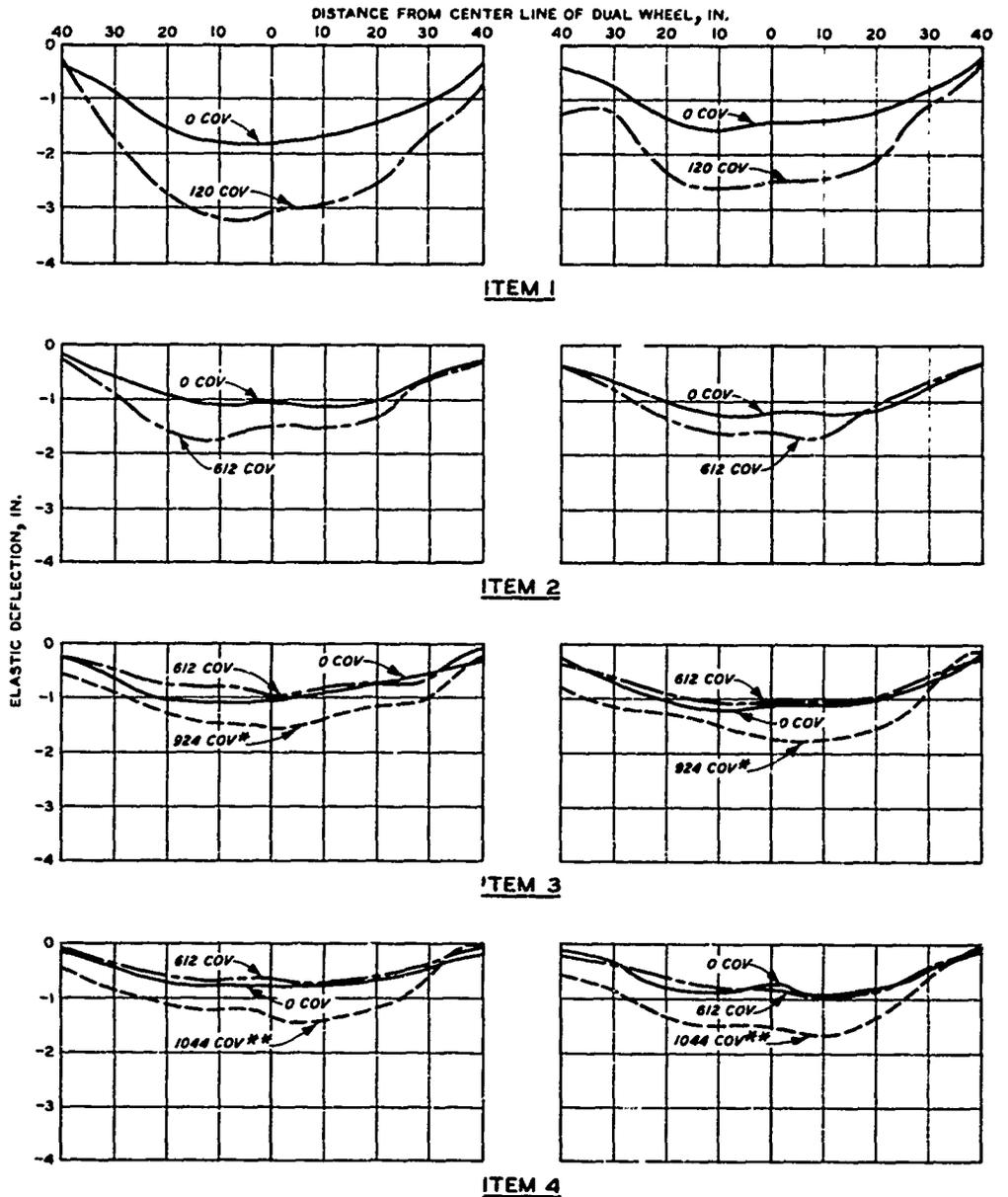


NOTE: * 312 COVERAGES WITH 62,000-LB LOAD, 185-PSI TIRES.

** 432 COVERAGES WITH 62,000-LB LOAD, 185-PSI TIRES.

## ELASTIC MAT DEFLECTION
### TEST SECTION I, LANE 2
55,000-LB, TWIN-WHEEL LOAD
56X16, 105-PSI TIRES

PLATE A8

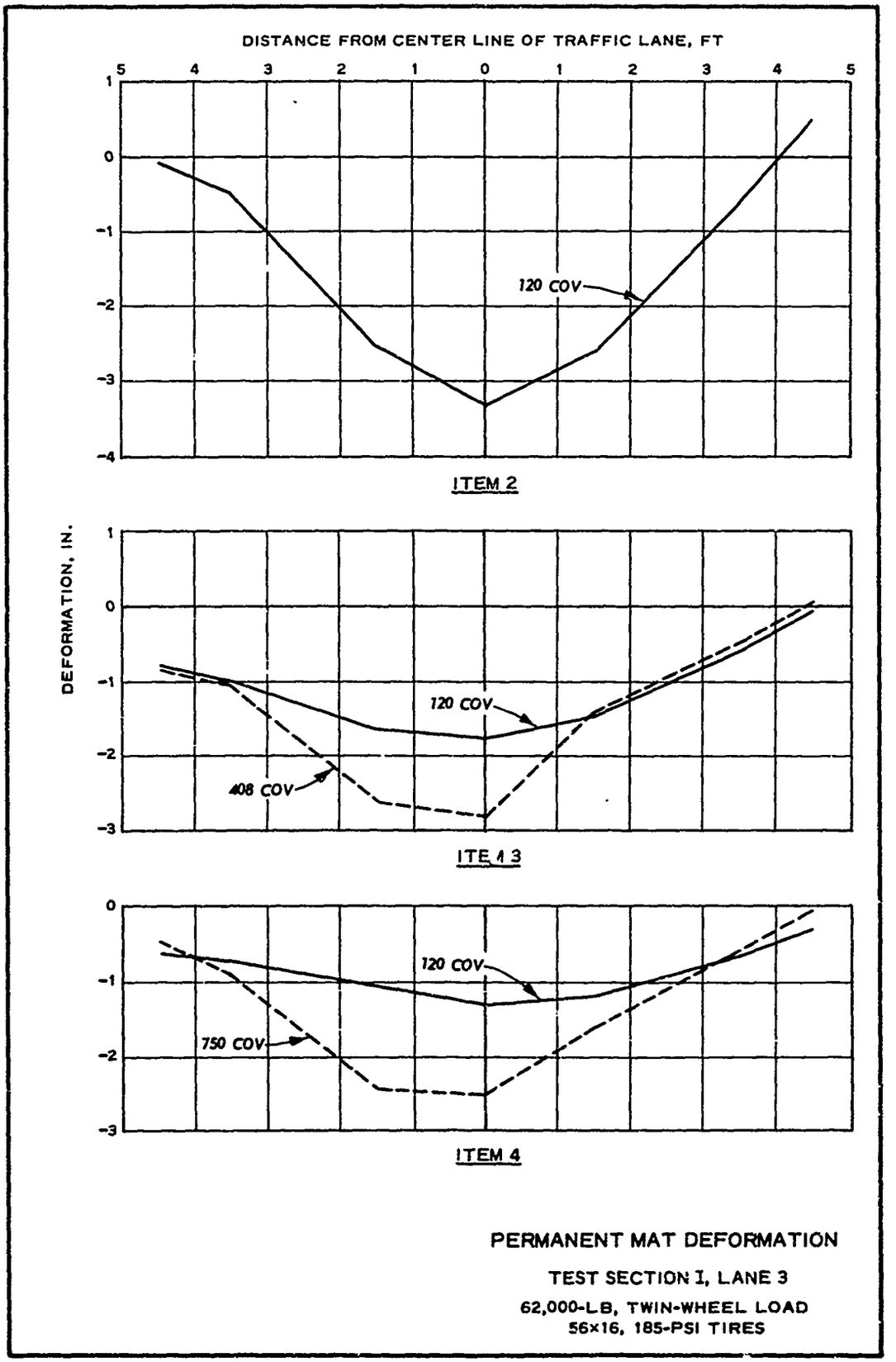


PERMANENT MAT DEFORMATION

TEST SECTION I, LANE 3

62,000-LB, TWIN-WHEEL LOAD
56×16, 185-PSI TIRES



PLATE A9

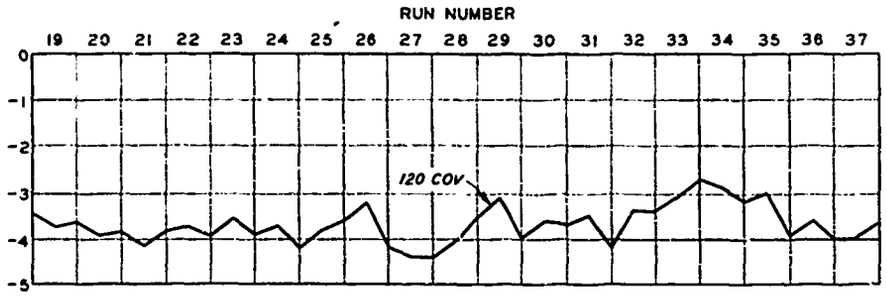


ITEM 2

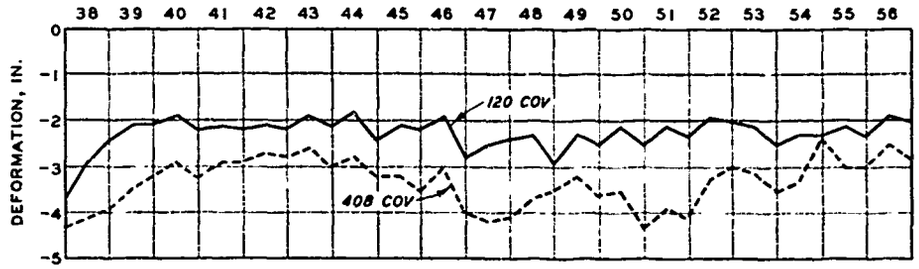


ITEM 3

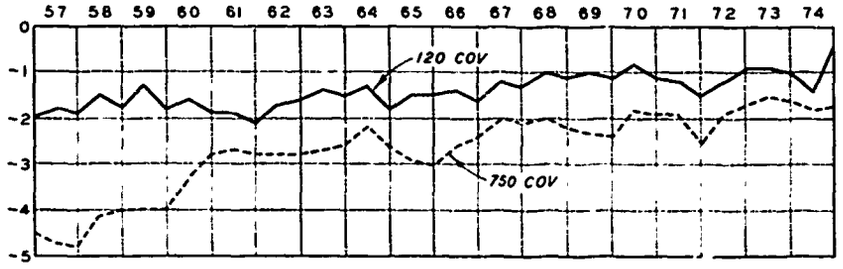


ITEM 4

CENTER-LINE PROFILES
TEST SECTION I, LANE 3
62,000-LB, TWIN-WHEEL LOAD
56X16, 185-PSI TIRES

PLATE A10

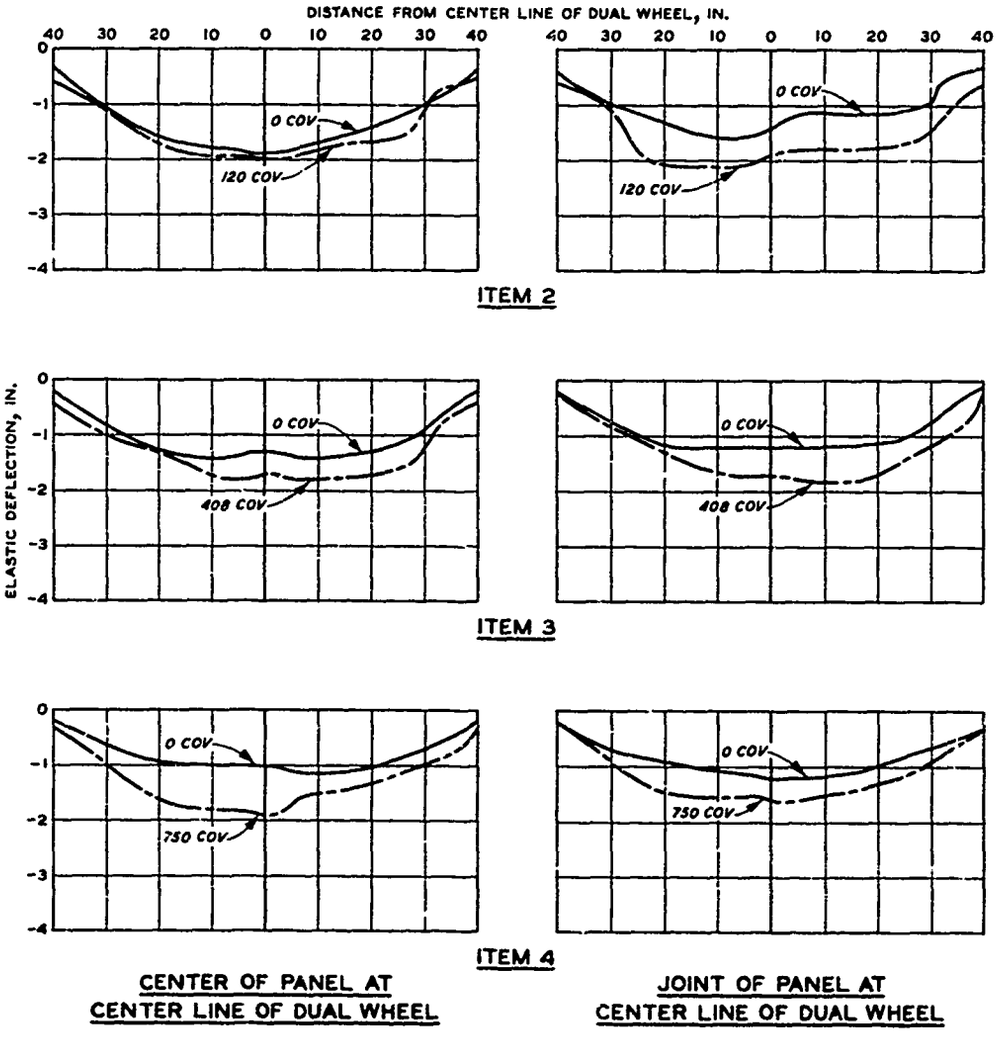


ELASTIC MAT DEFLECTION
TEST SECTION I, LANE 3
62,000-LB, TWIN-WHEEL LOAD
56X16, 185-PSI TIRES

PLATE AII

PLATE A12

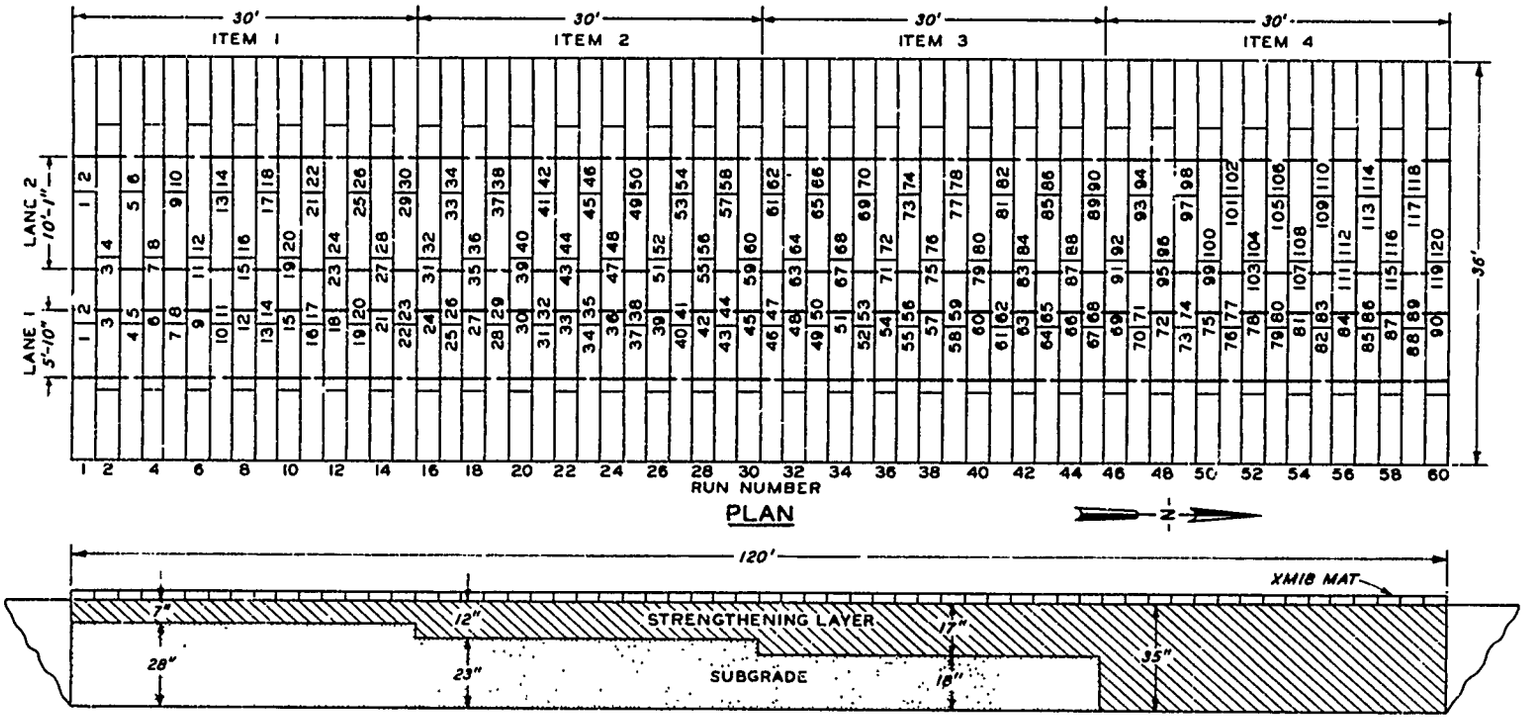


NOTE : NUMBERS INSIDE PANELS INDICATE PANEL NUMBERS.

PANELS RENUMBERED IN EACH TRAFFIC LANE

PLAN AND PROFILE
TEST SECTION II

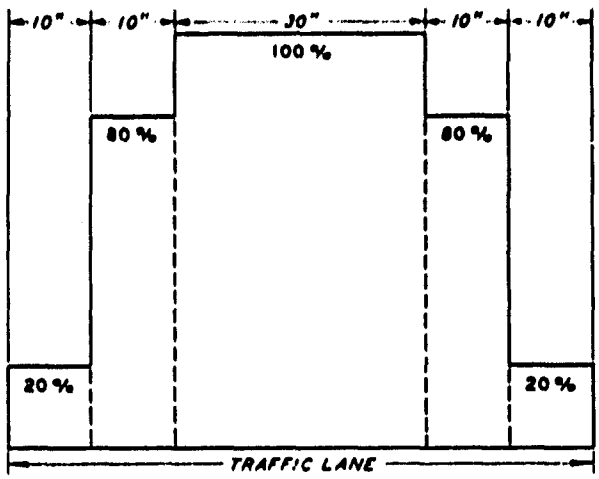


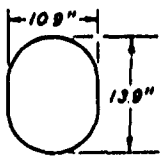


| | |
|---|---|
| TIRE SIZE | 30X11.5 |
| CONTACT AREA | 128.5 SQ IN. |
| WHEEL LOAD | 30,000 LB |
| INFLATION PRESSURE | 250 PSI |

a. LANE 1

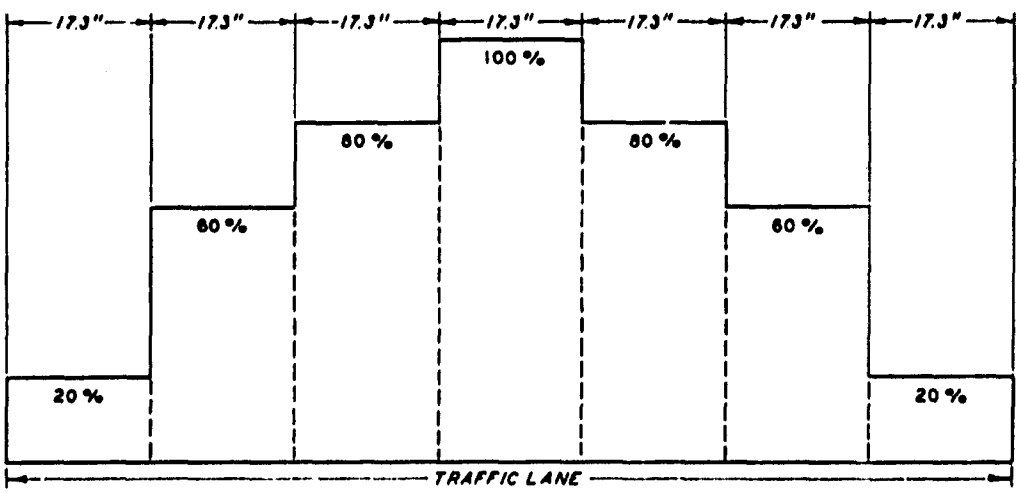


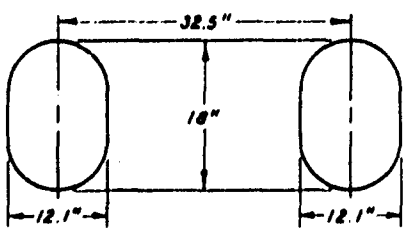


| | |
|---|---|
| TIRE SIZE | 44X16 |
| CONTACT AREA | 192.1 SQ IN. |
| WHEEL LOAD | 70,000 LB |
| INFLATION PRESSURE | 165 PSI |

b. LANE 2

**TRAFFIC DISTRIBUTION PATTERNS AND TIRE CHARACTERISTICS**

**TEST SECTION II**

PLATE A13

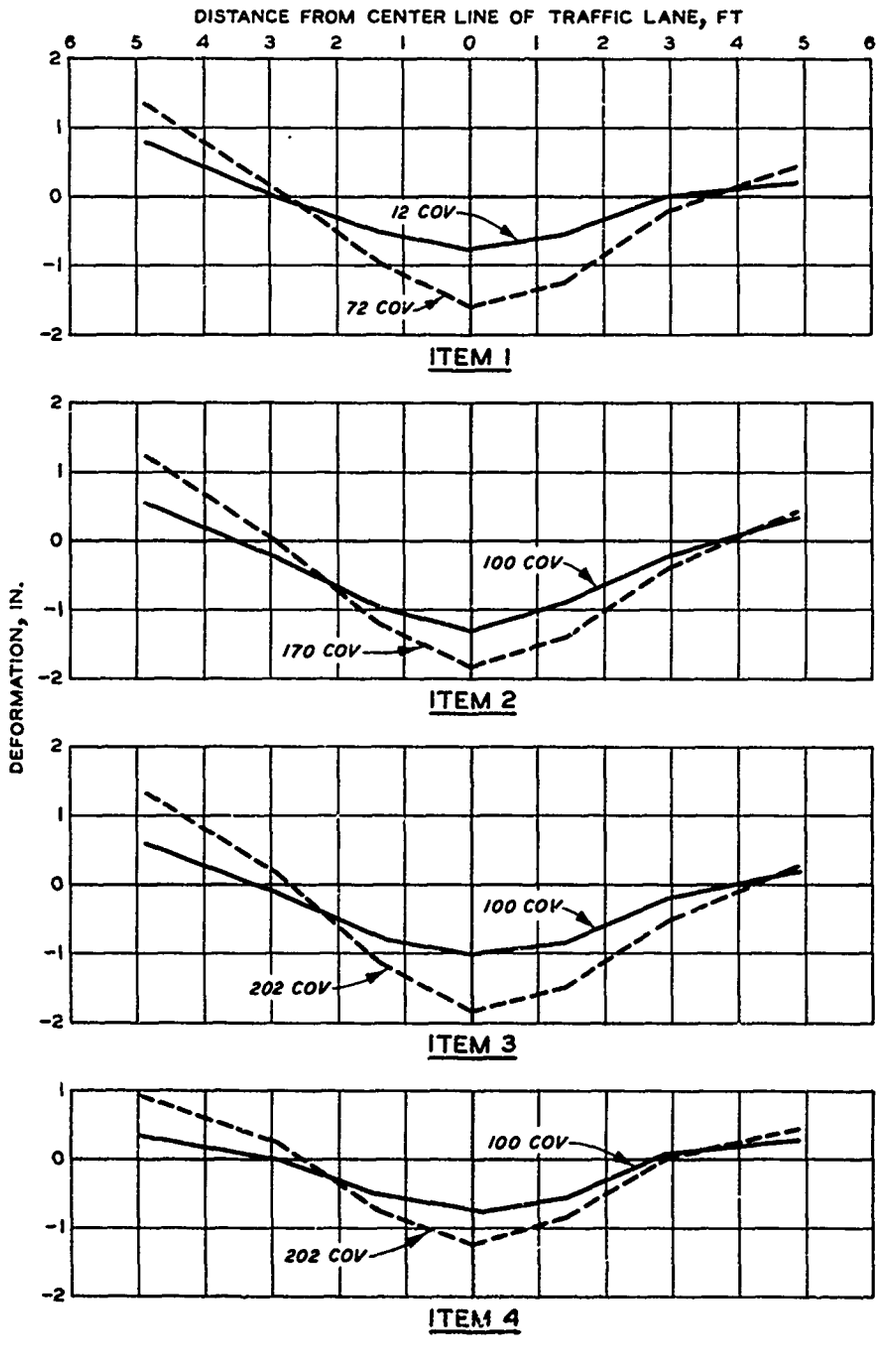


## PERMANENT MAT DEFORMATION

TEST SECTION II, LANE 1

30,000-LB, SINGLE-WHEEL LOAD

30X11.5, 250-PSI TIRE

PLATE A14

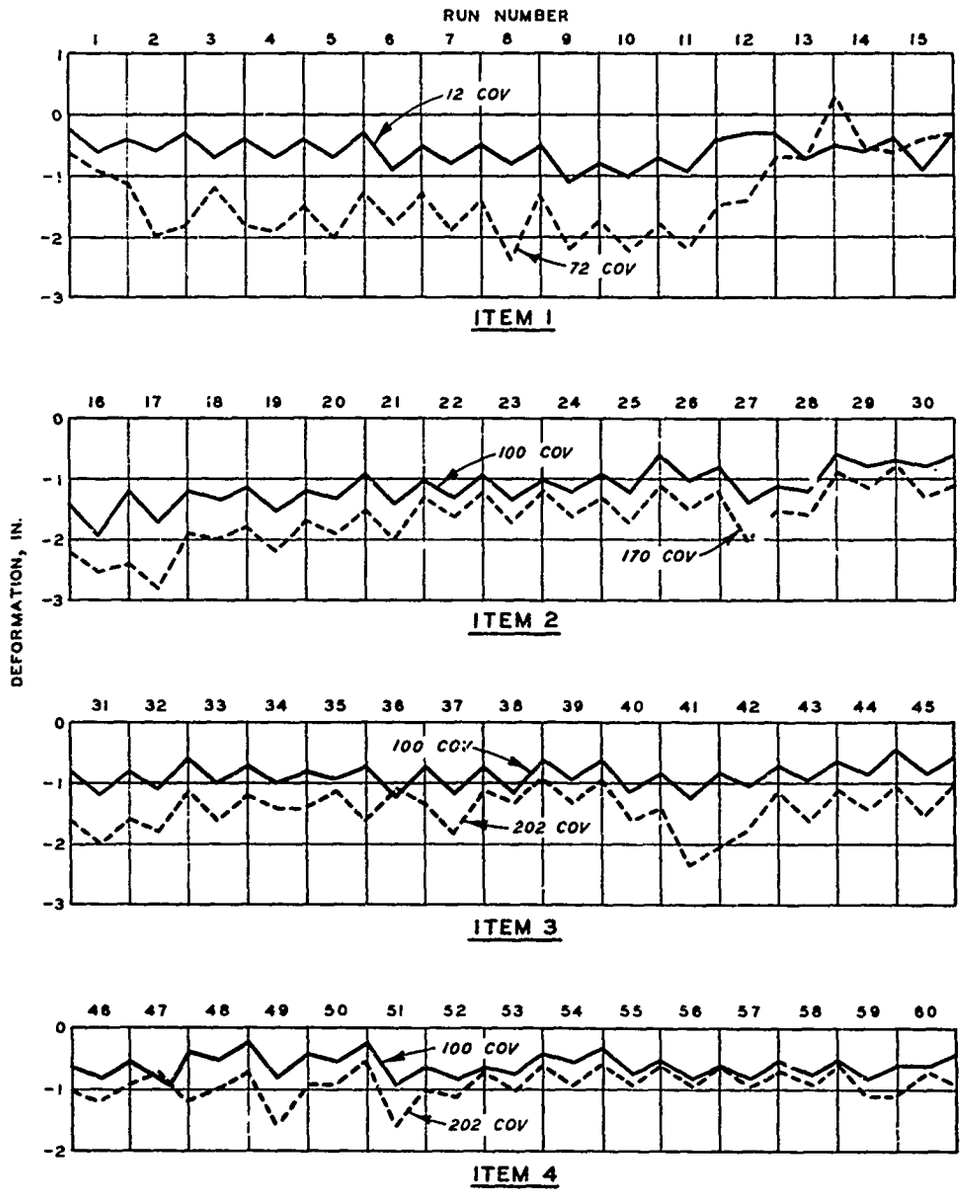


## CENTER-LINE PROFILES

TEST SECTION II, LANE 1

30,000-LB, SINGLE-WHEEL LOAD

30X11.5, 250-PSI TIRE

PLATE A15

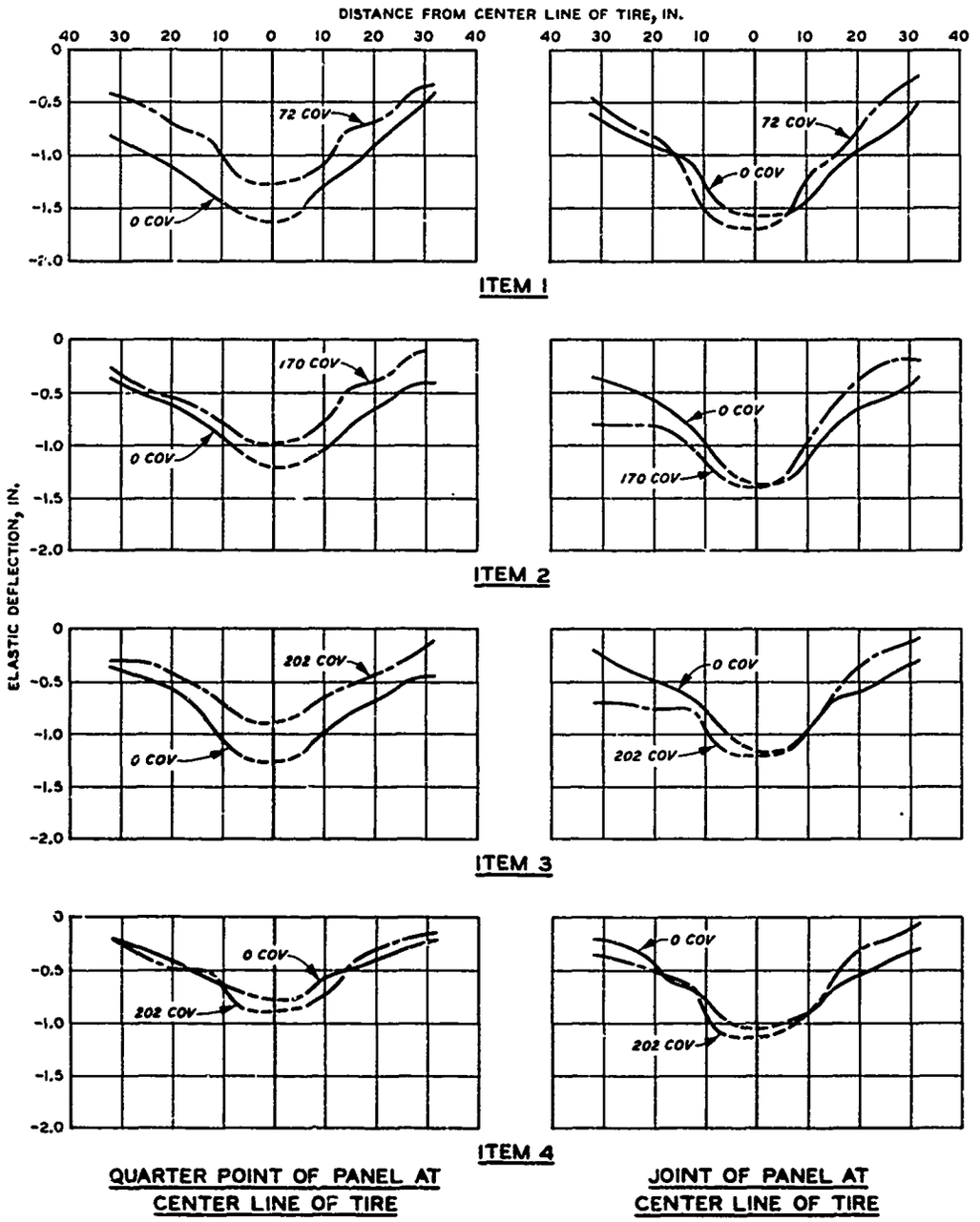


ELASTIC MAT DEFLECTION
TEST SECTION II, LANE I
30,000-LB, SINGLE-WHEEL LOAD
30X11.5, 250-PSI TIRE

PLATE A16

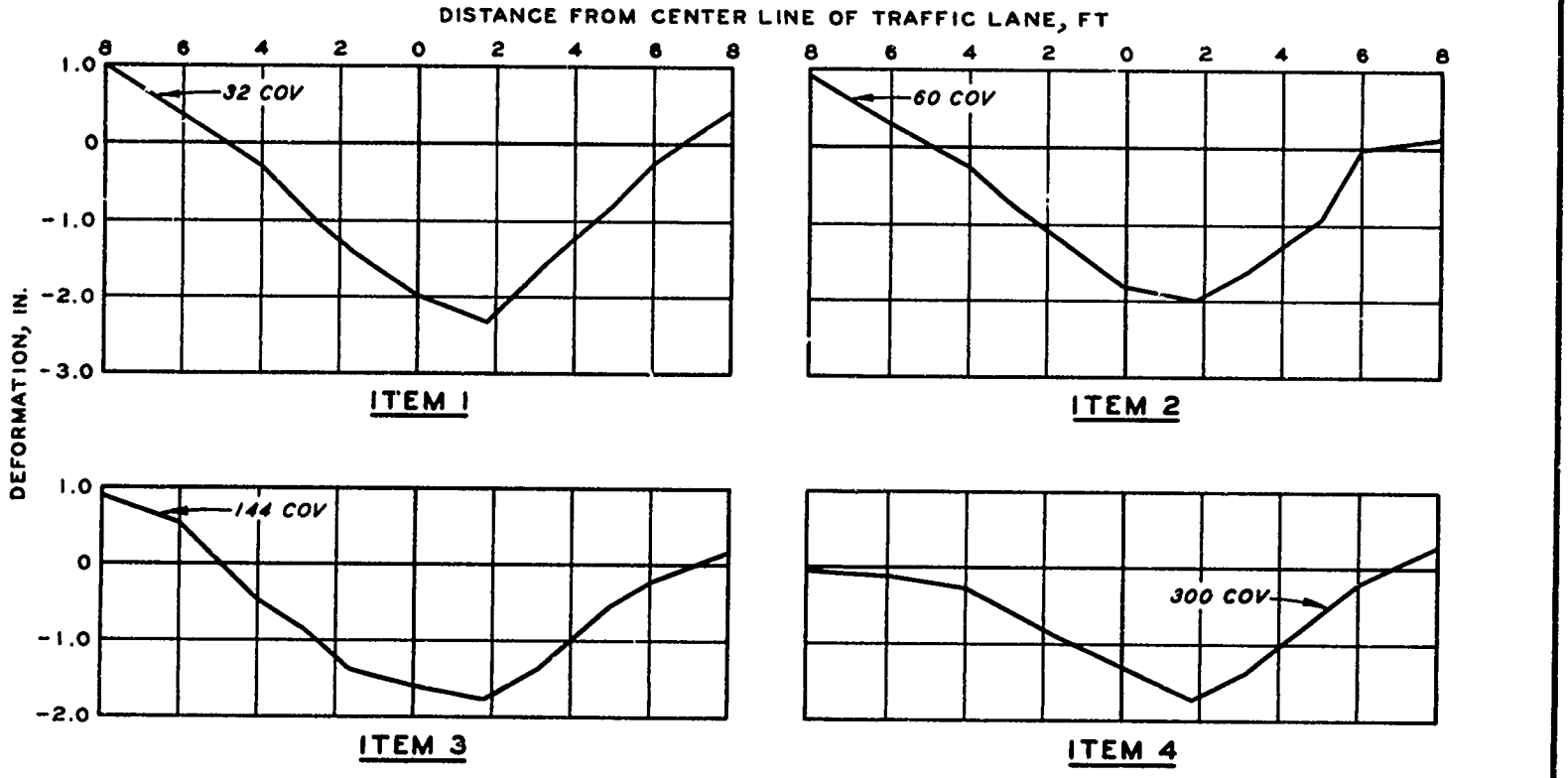


**PERMANENT MAT DEFORMATION**
**TEST SECTION II, LANE 2**
70,000-LB, TWIN-WHEEL LOAD
44X16, 185-PSI TIRES

PLATE A17

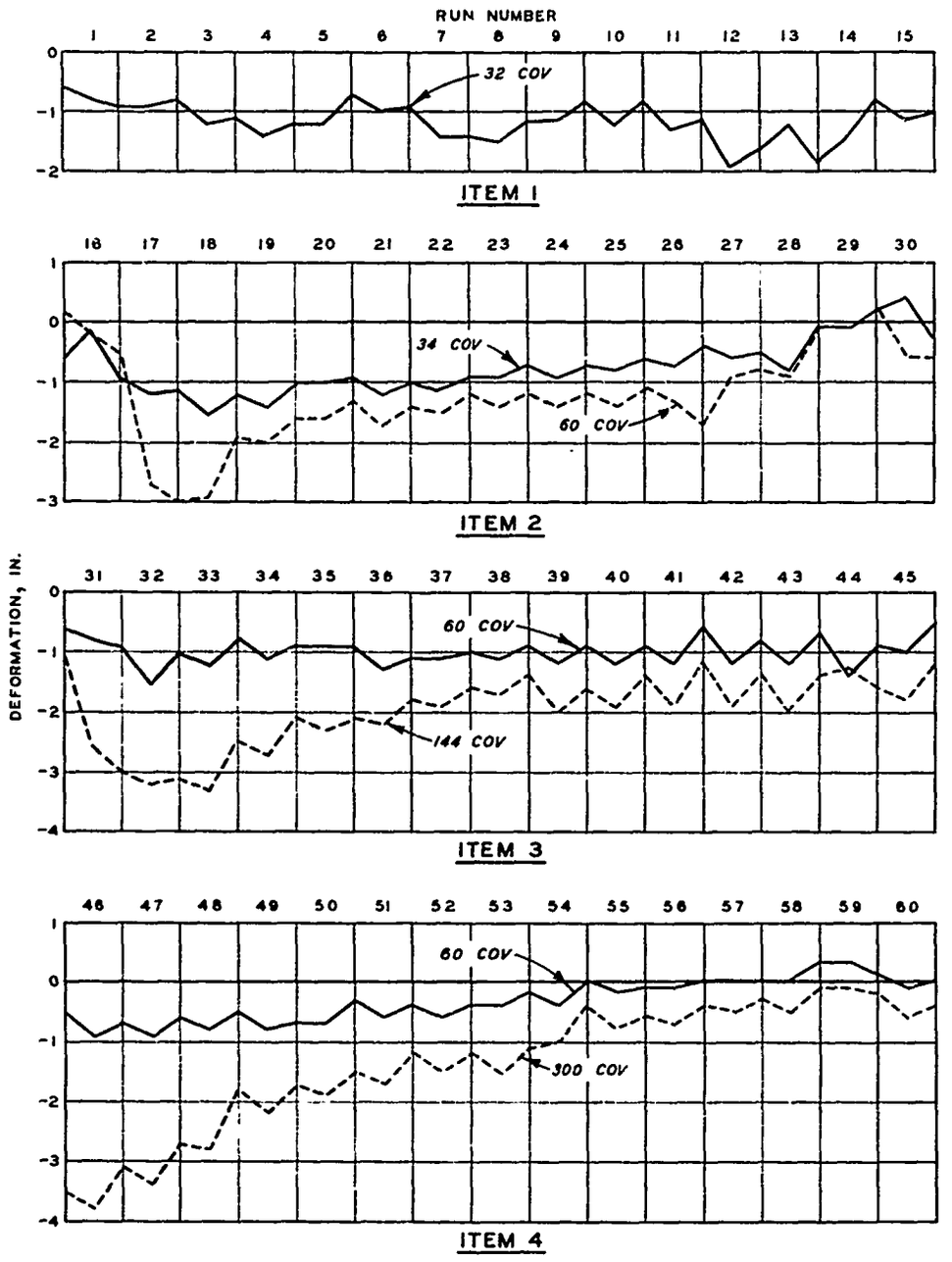


## CENTER-LINE PROFILES
TEST SECTION II, LANE 2
70,000-LB, TWIN-WHEEL LOAD
44X16, 185-PSI TIRES

PLATE A18

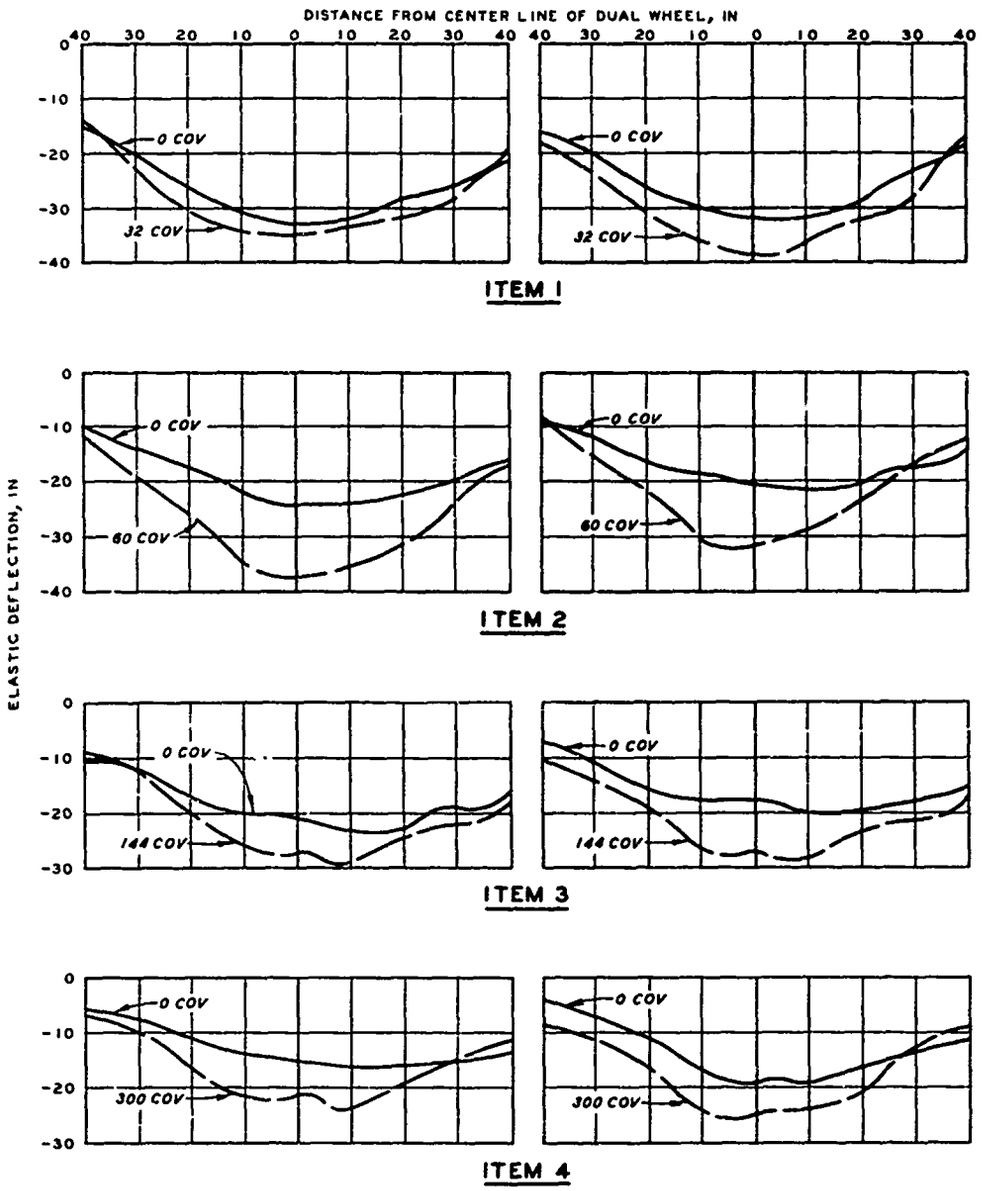


ELASTIC MAT DEFLECTION
TEST SECTION II, LANE 2
70,000-LB, TWIN-WHEEL LOAD
44X16, 185-PSI TIRES



PLATE A19

PLATE A20

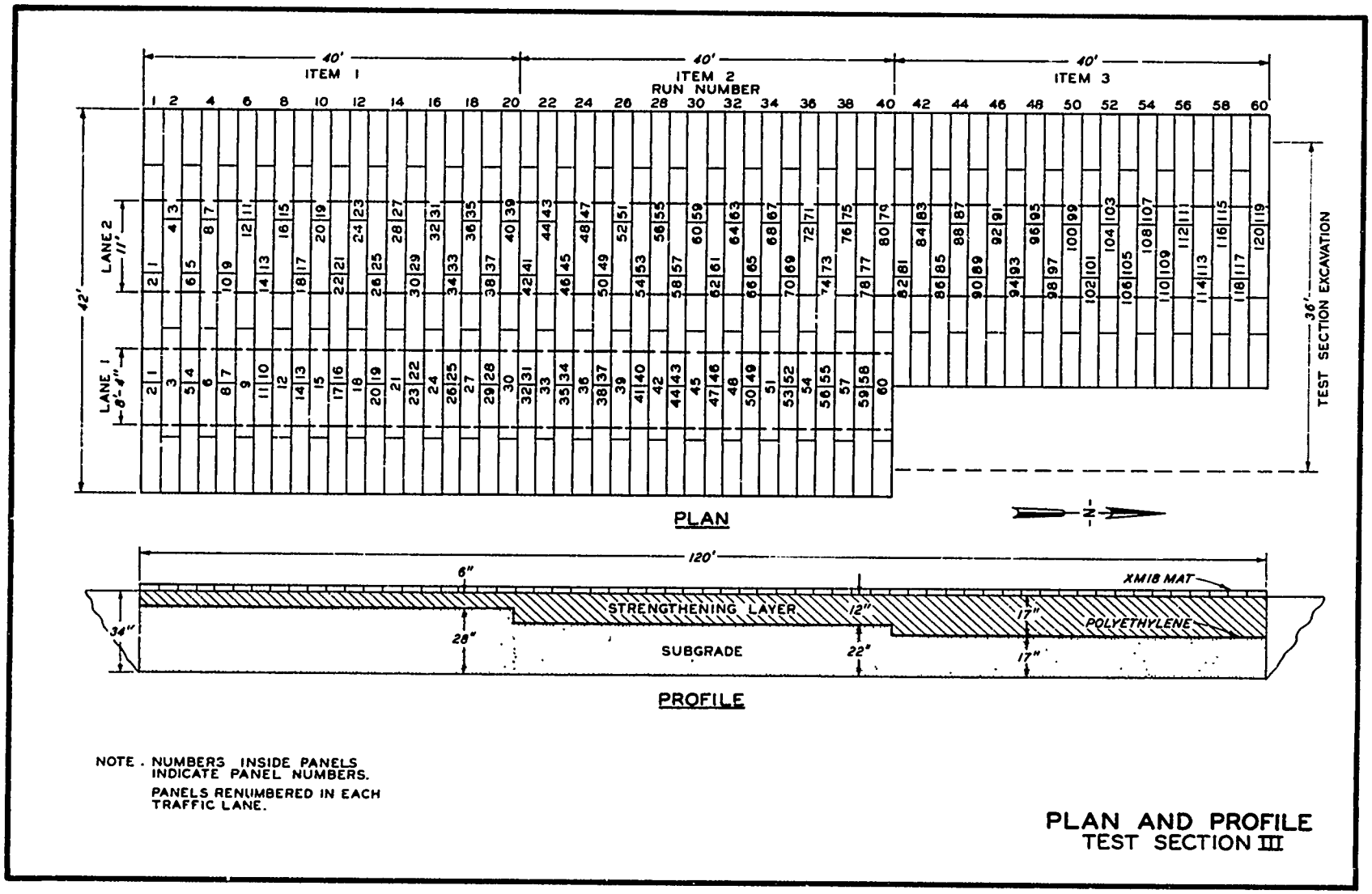


NOTE . NUMBERS INSIDE PANELS INDICATE PANEL NUMBERS.

PANELS RENUMBERED IN EACH TRAFFIC LANE.

PLAN AND PROFILE
TEST SECTION III

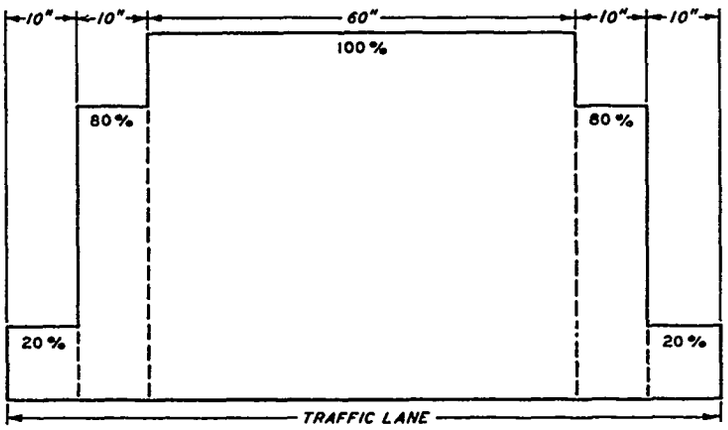


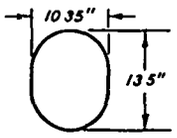


| | |
|---|---|
| TIRE SIZE | 30X11.5 |
| CONTACT AREA | 111.0 SQ IN. |
| WHEEL LOAD | 25,000 LB |
| INFLATION PRESSURE | 250 PSI |

a. LANE 1

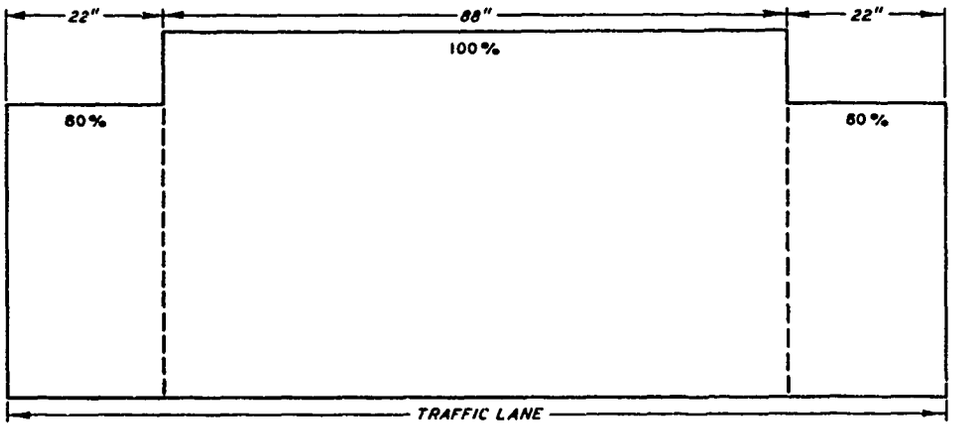


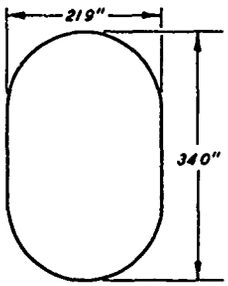


| | |
|---|---|
| TIRE SIZE | 25.00-28 |
| CONTACT AREA | 648.5 SQ IN. |
| WHEEL LOAD | 75,000 LB |
| INFLATION PRESSURE | 125 PSI |

b. LANE 2

## TRAFFIC DISTRIBUTION PATTERNS AND TIRE CHARACTERISTICS

TEST SECTION III



PLATE A21

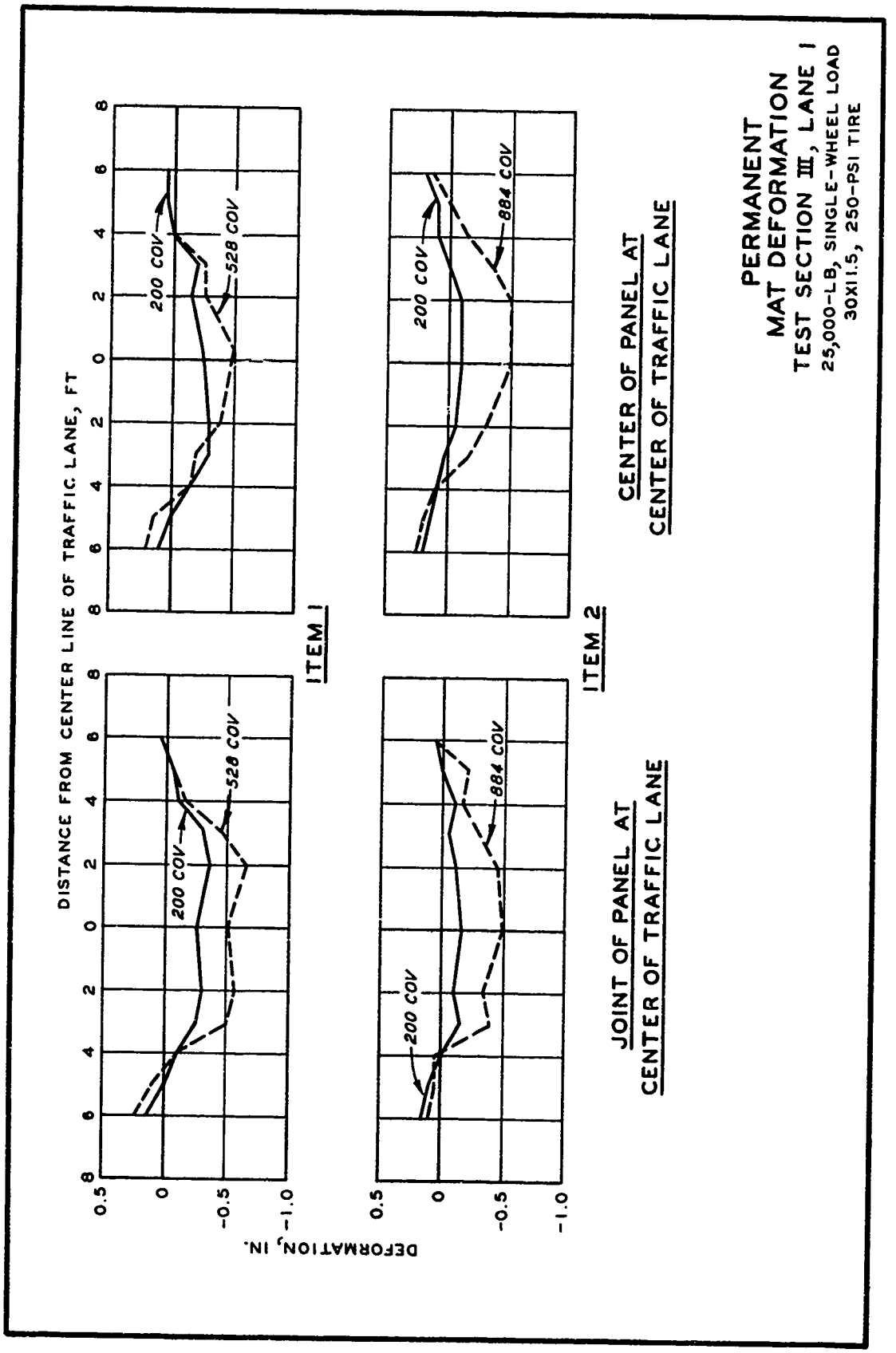
PERMANENT
MAT DEFORMATION
TEST SECTION III, LANE 1
25,000-LB, SINGLE-WHEEL LOAD
30X11.5, 250-PSI TIRE
CENTER OF PANEL AT
CENTER OF TRAFFIC LANE
JOINT OF PANEL AT
CENTER OF TRAFFIC LANE
ITEM 1
ITEM 2
200 COV
528 COV
884 COV
DISTANCE FROM CENTER LINE OF TRAFFIC LANE, FT
DEFORMATION, IN.
8
6
4
2
0
0.5
-0.5
-1.0

PLATE A22

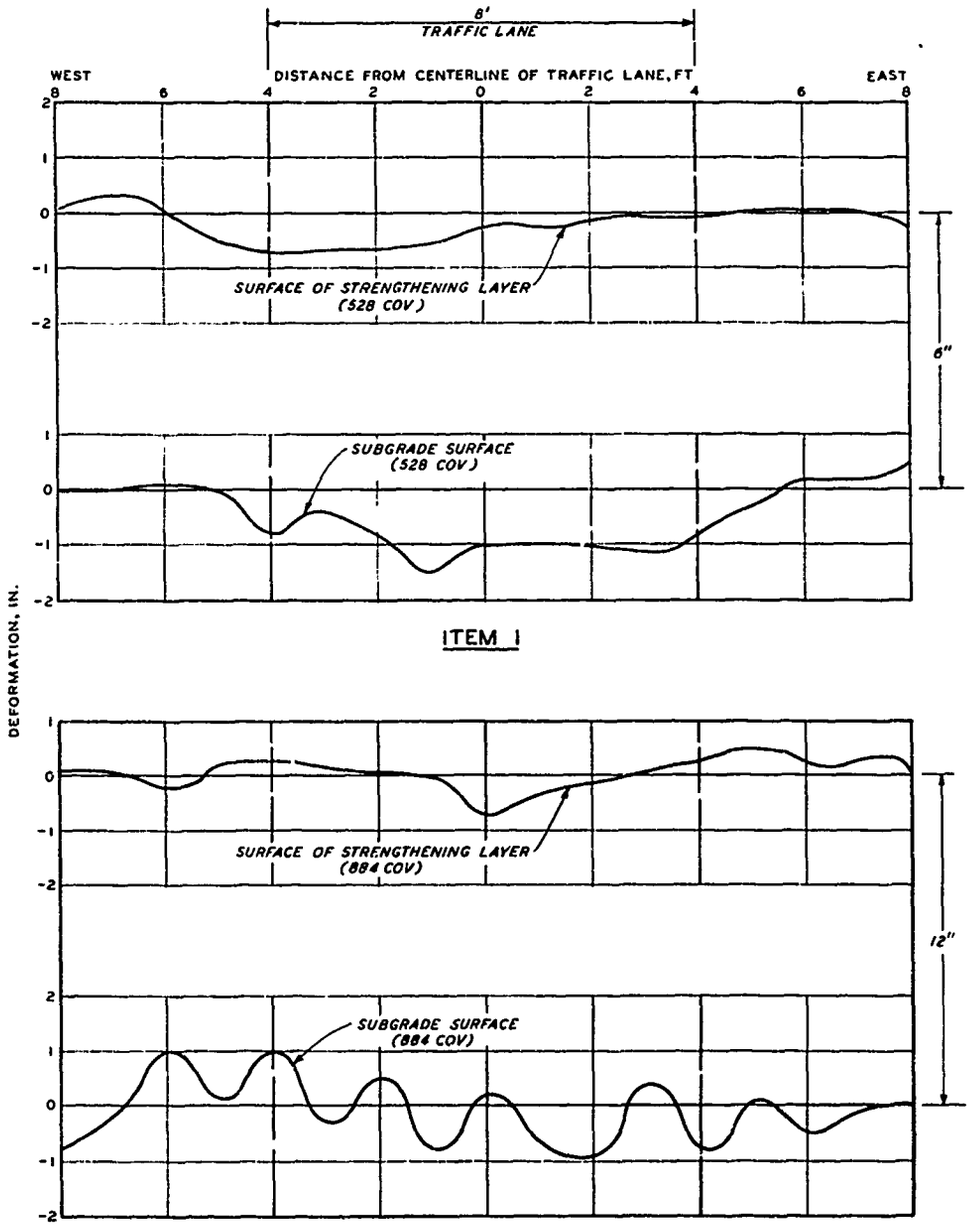


## PERMANENT DEFORMATION OF SUBGRADE

### TEST SECTION III, LANE 1

25,000-LB, SINGLE-WHEEL LOAD
30X11.5, 250-PSI TIRE



PLATE A23

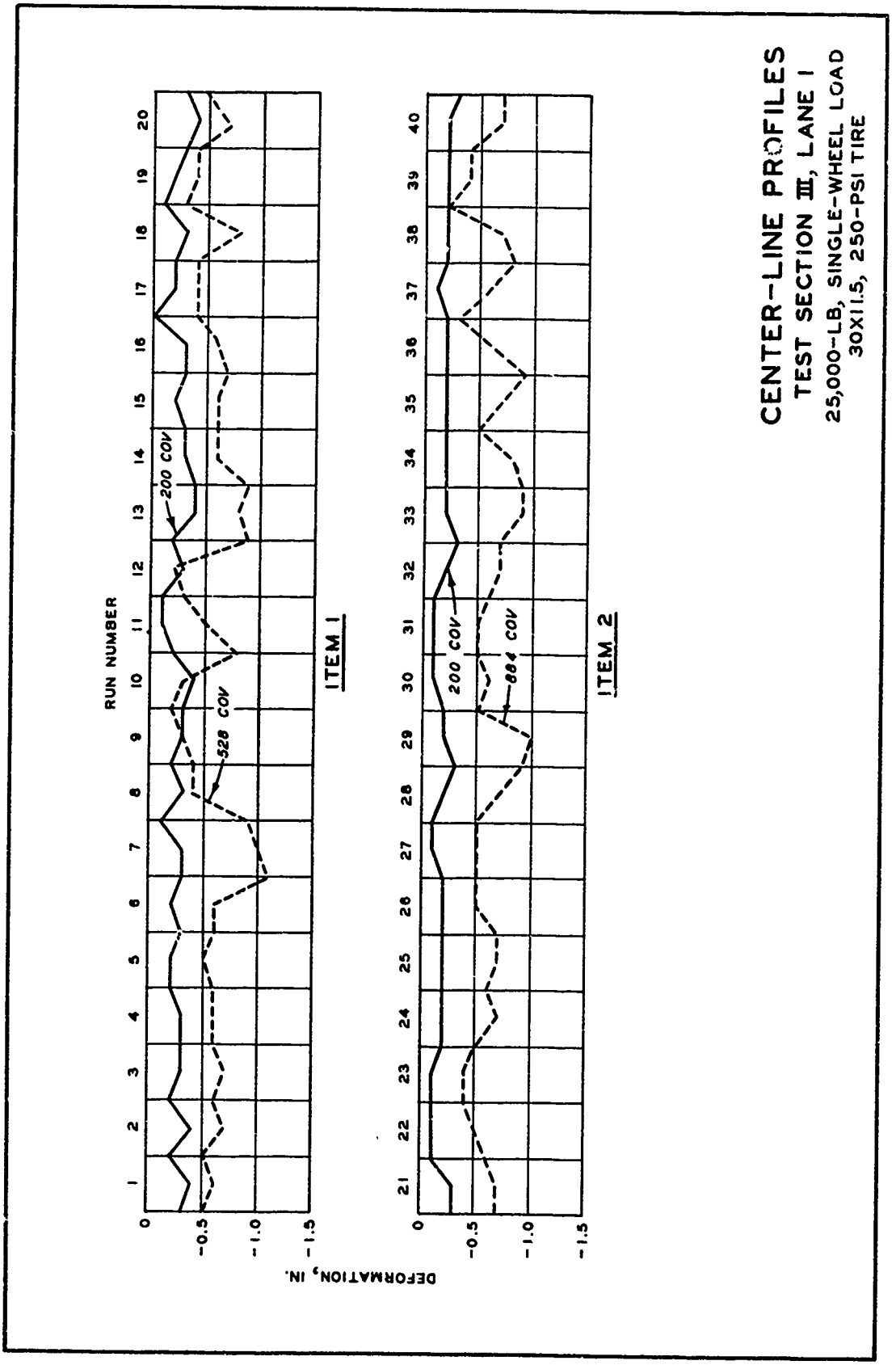
CENTER-LINE PROFILES
TEST SECTION III, LANE 1
25,000-LB, SINGLE-WHEEL LOAD
30X11.5, 250-PSI TIRE
ITEM 1
ITEM 2
RUN NUMBER
DEFORMATION, IN.
200 COV
528 COV
200 COV
804 COV
0
-0.5
-1.0
-1.5
1
2
3
4
5
6
7
8
9
10
11
12
13
14
15
16
17
18
19
20
21
22
23
24
25
26
27
28
29
30
31
32
33
34
35
36
37
38
39
40

PLATE A24

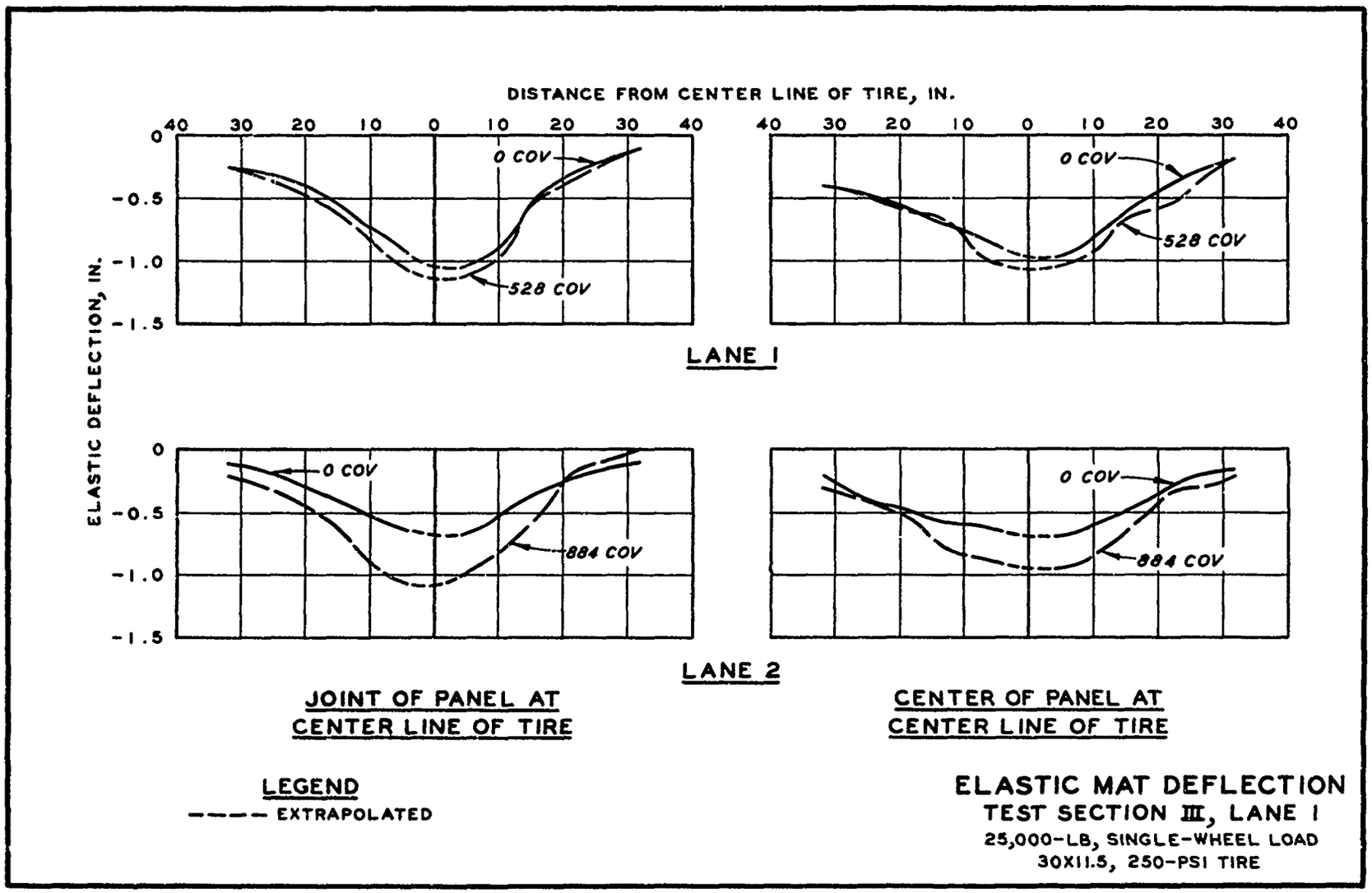
DISTANCE FROM CENTER LINE OF TIRE, IN.
40 30 20 10 0 10 20 30 40
ELASTIC DEFLECTION, IN.
0
-0.5
-1.0
-1.5
0 COV
528 COV
LANE 1
884 COV
LANE 2
JOINT OF PANEL AT CENTER LINE OF TIRE
CENTER OF PANEL AT CENTER LINE OF TIRE
LEGEND
EXTRAPOLATED
ELASTIC MAT DEFLECTION
TEST SECTION III, LANE 1
25,000-LB, SINGLE-WHEEL LOAD
30X11.5, 250-PSI TIRE

PLATE A25

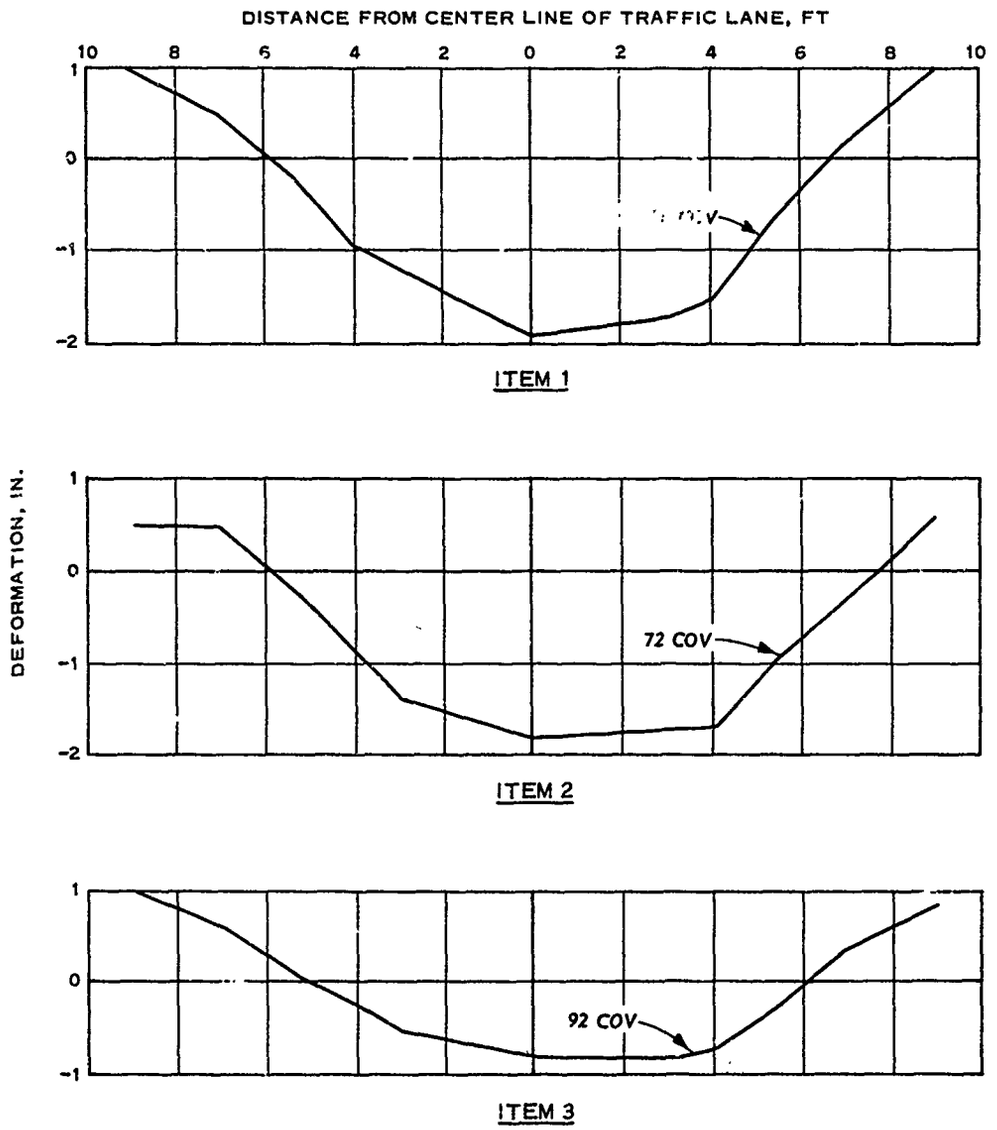


PERMANENT MAT DEFORMATION

TEST SECTION III, LANE 2

75,000-LB, SINGLE-WHEEL LOAD
25.00-28, 125-PSI TIRE

PLATE A26

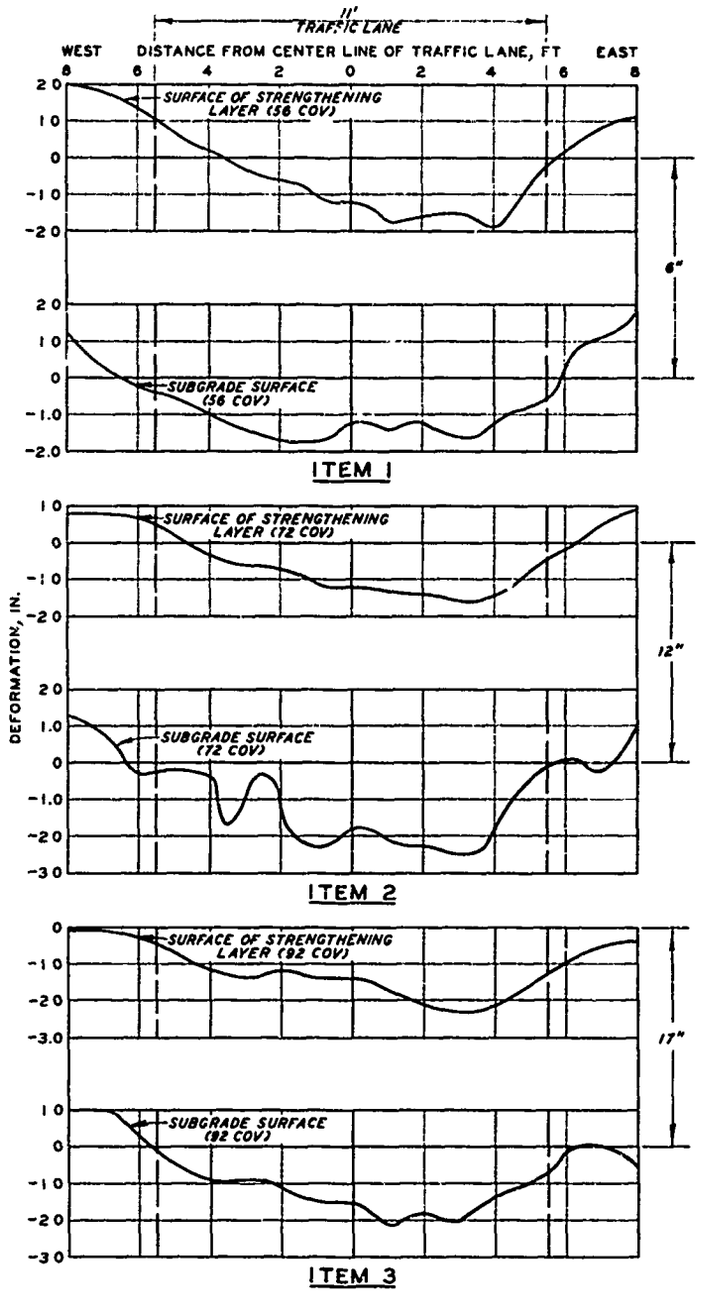


## PERMANENT DEFORMATION OF SUBGRADE

### TEST SECTION III, LANE 2

75,000-LB, SINGLE-WHEEL LOAD
25.00-28, 125-PSI TIRE



PLATE A27

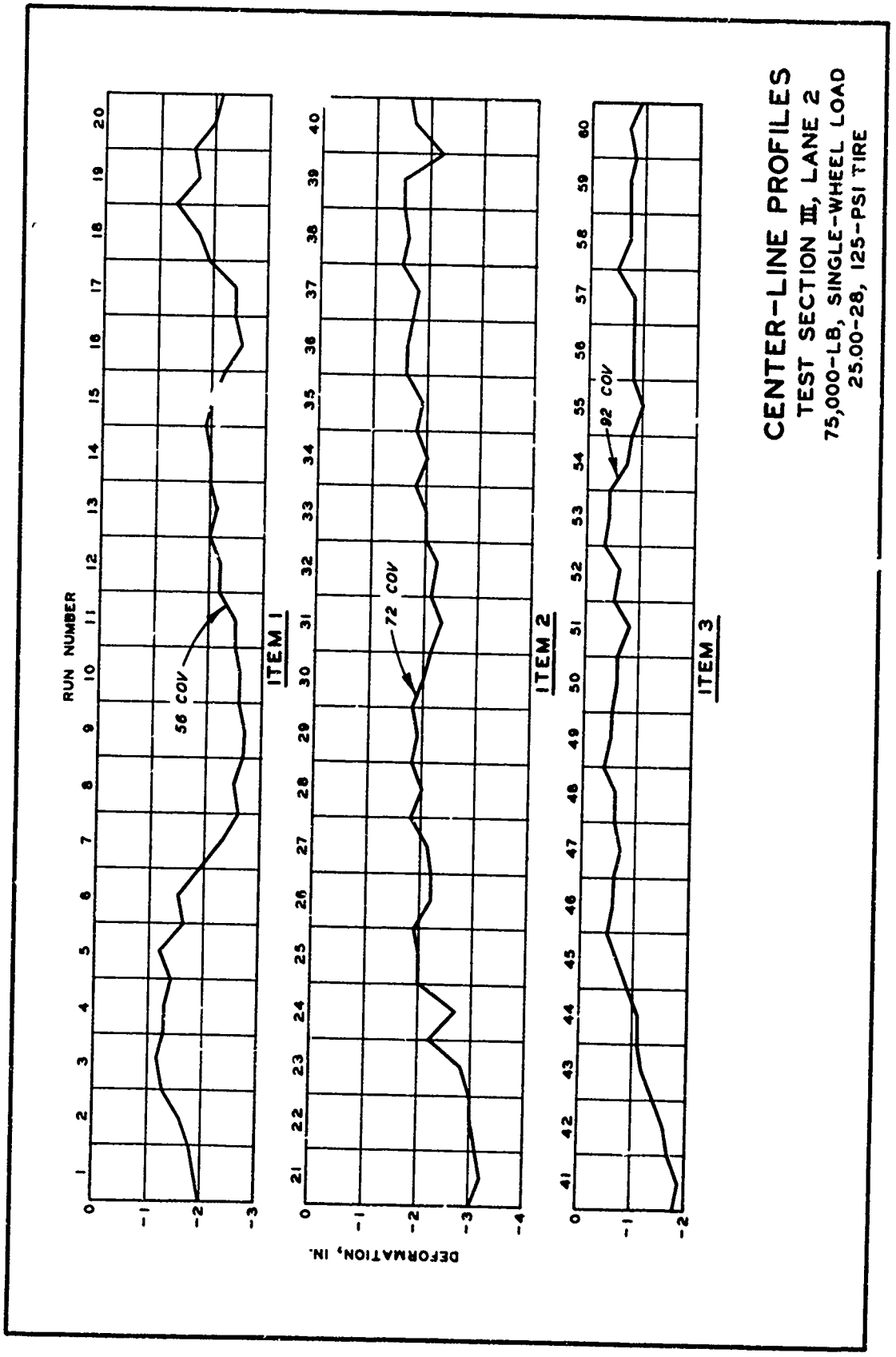
CENTER-LINE PROFILES
TEST SECTION III, LANE 2
75,000-LB, SINGLE-WHEEL LOAD
25.00-28, 125-PSI TIRE
RUN NUMBER
DEFORMATION, IN.
ITEM 1
ITEM 2
ITEM 3
56 COV
72 COV
82 COV

PLATE A28

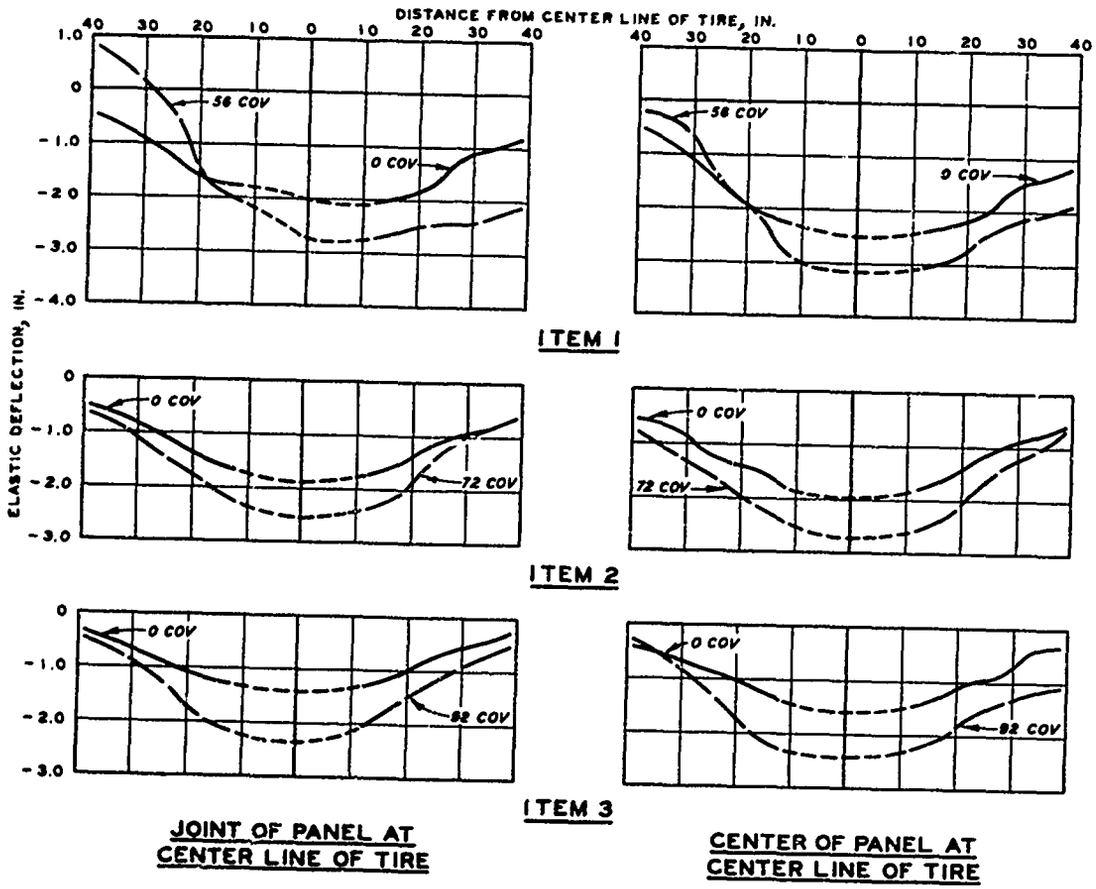


ELASTIC MAT DEFLECTION
TEST SECTION III, LANE 2
75,000-LB, SINGLE-WHEEL LOAD
25.00-28, 125-PSI TIRE

PLATE A29

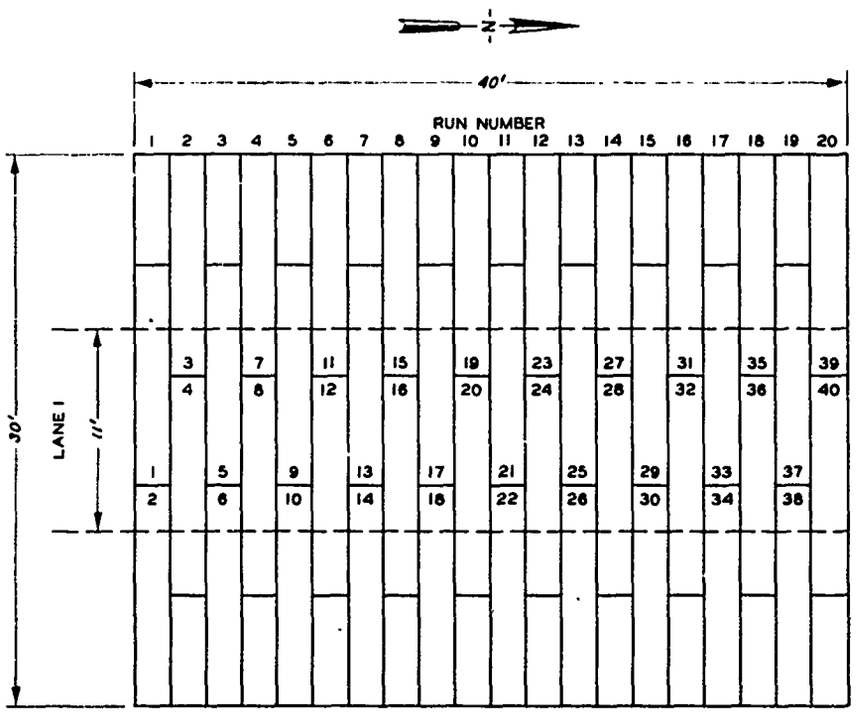


PLAN

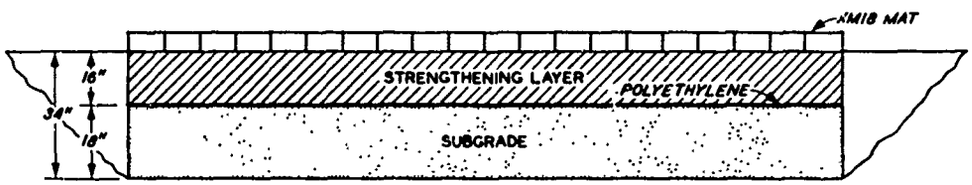


PROFILE

NOTE: NUMBERS INSIDE PANELS INDICATE PANEL NUMBERS.

**PLAN AND PROFILE**
**TEST SECTION IV**

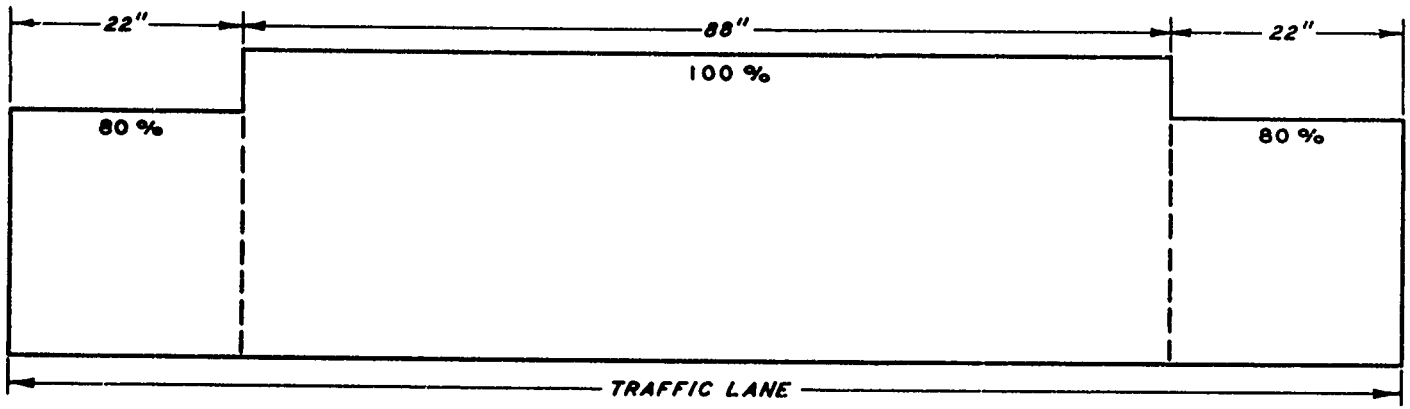


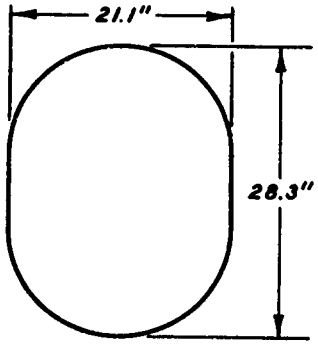


| | |
|---|---|
| TIRE SIZE | 25.00-28 |
| CONTACT AREA | 538.2 SQ IN. |
| WHEEL LOAD | 60,000 LB |
| INFLATION PRESSURE | 125 PSI |

**TRAFFIC DISTRIBUTION PATTERN AND TIRE PRINT CHARACTERISTICS**
**TEST SECTION IV**

PLATE A31

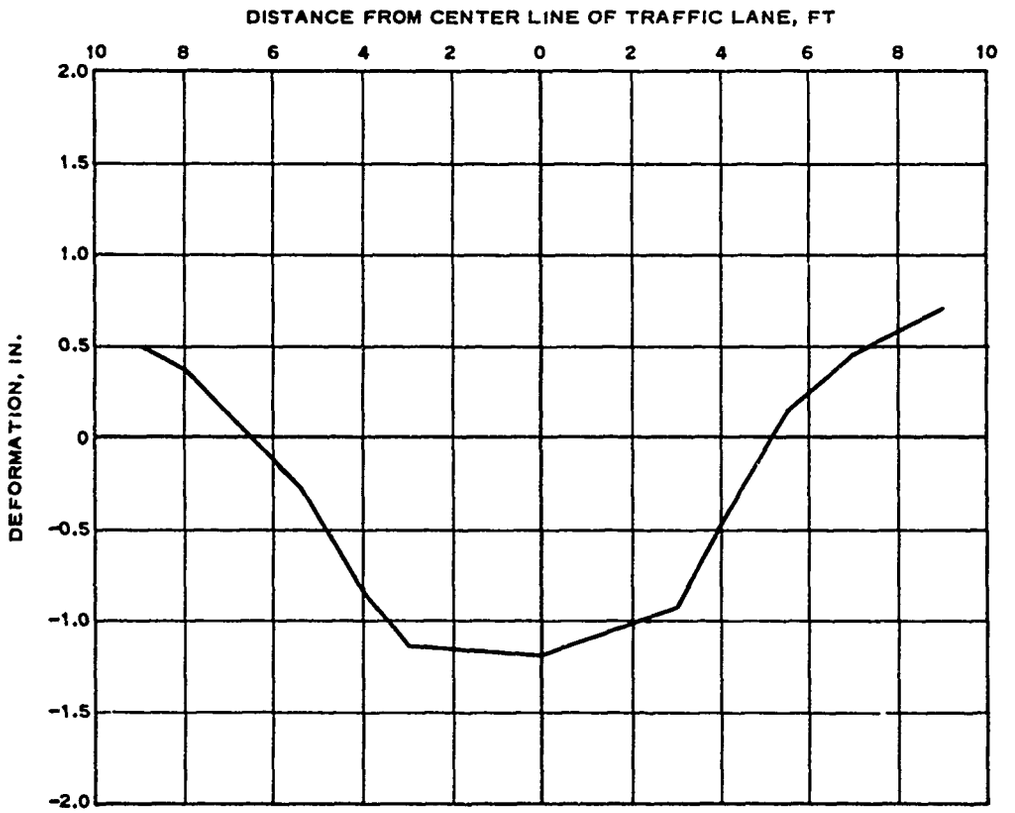


PERMANENT MAT DEFORMATION

TEST SECTION IV

60,000-LB, SINGLE-WHEEL LOAD
25.00-28, 125-PSI TIRE

PLATE A32

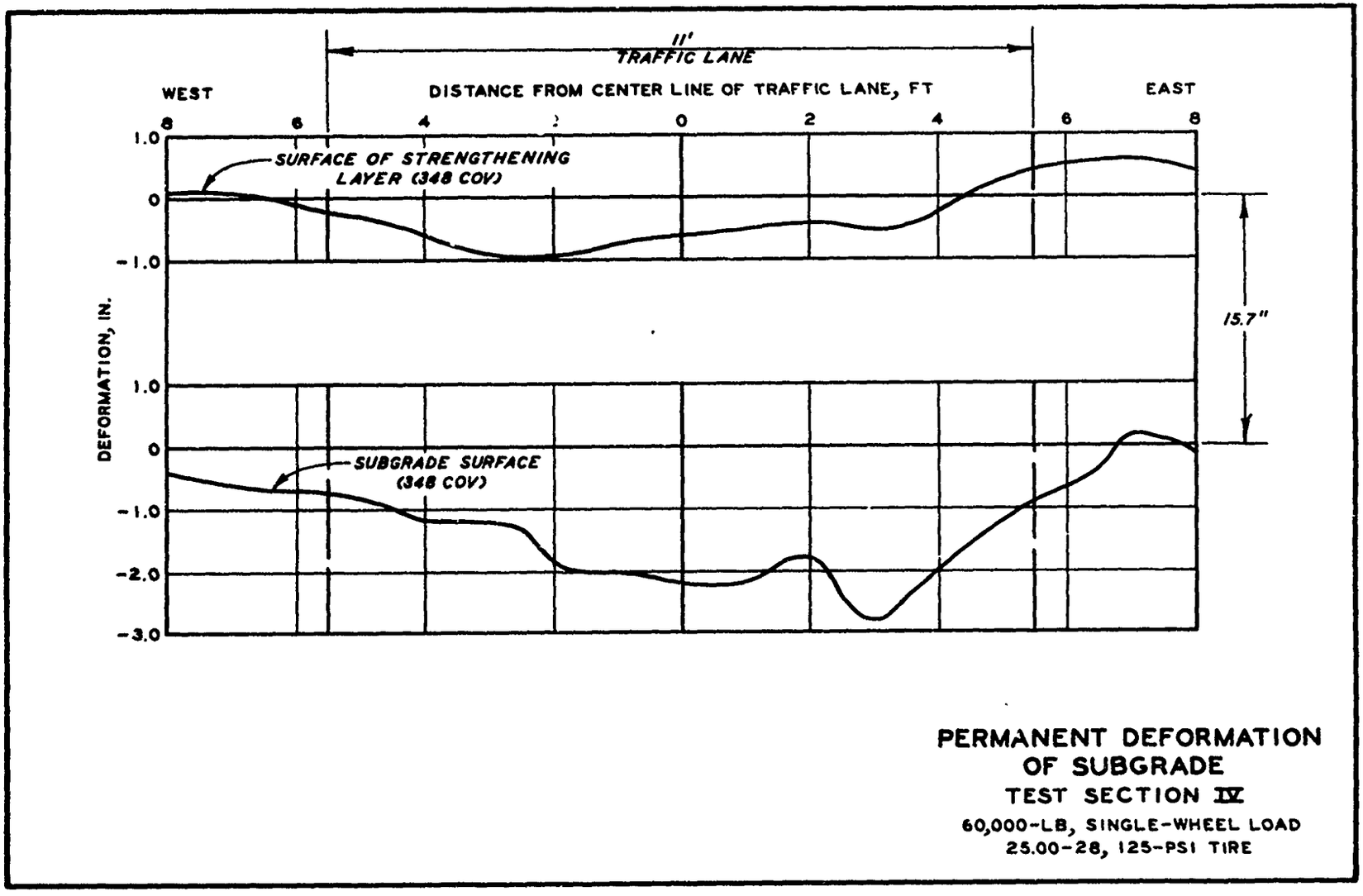


PERMANENT DEFORMATION
OF SUBGRADE
TEST SECTION IV
60,000-LB, SINGLE-WHEEL LOAD
25.00-28, 125-PSI TIRE

PLATE A33

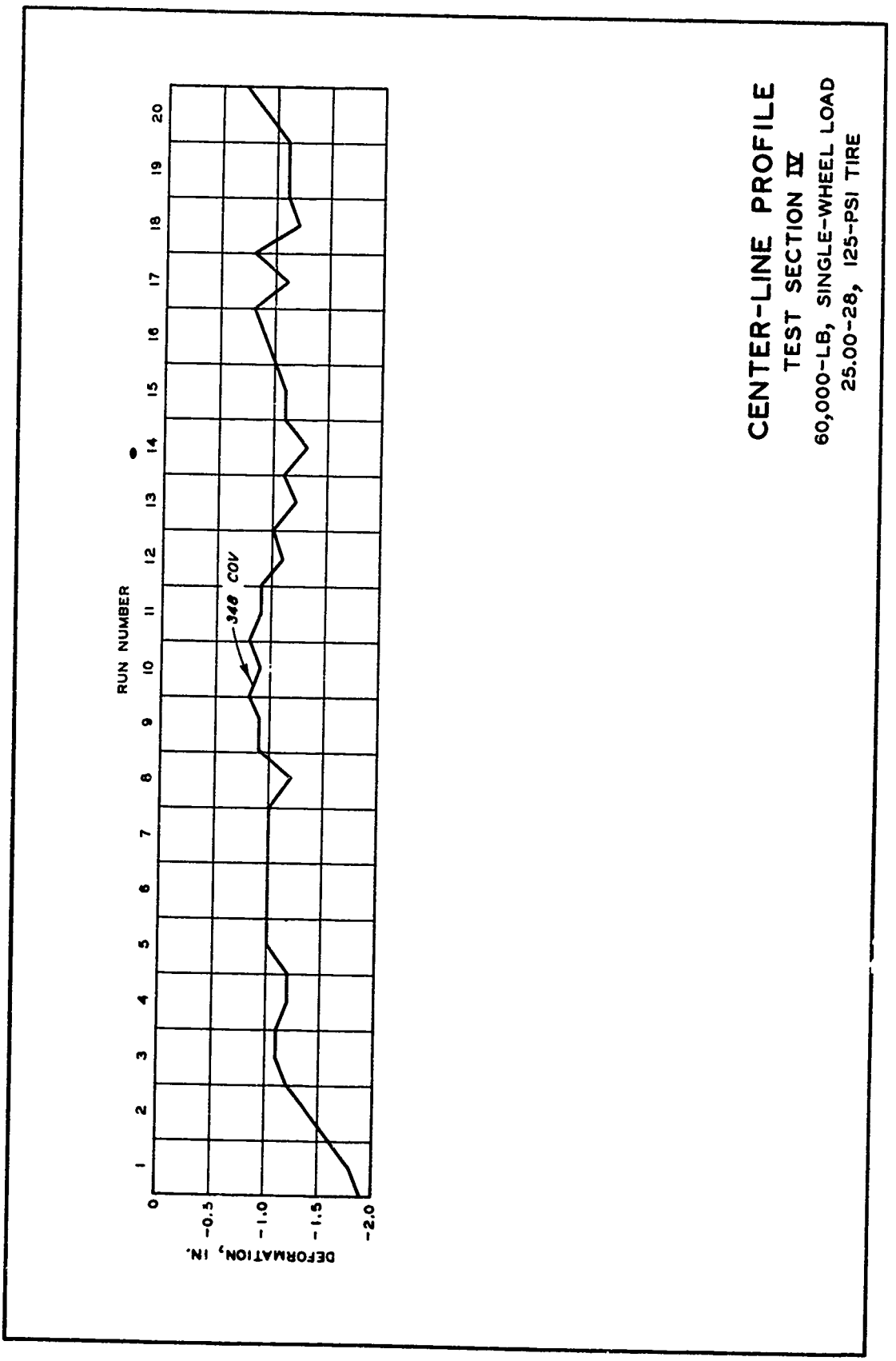
CENTER-LINE PROFILE
TEST SECTION IV
60,000-LB, SINGLE-WHEEL LOAD
25.00-28, 125-PSI TIRE
RUN NUMBER
DEFORMATION, IN.
0
-0.5
-1.0
-1.5
-2.0
1
2
3
4
5
6
7
8
9
10
11
12
13
14
15
16
17
18
19
20
34.8 COV

PLATE A 34

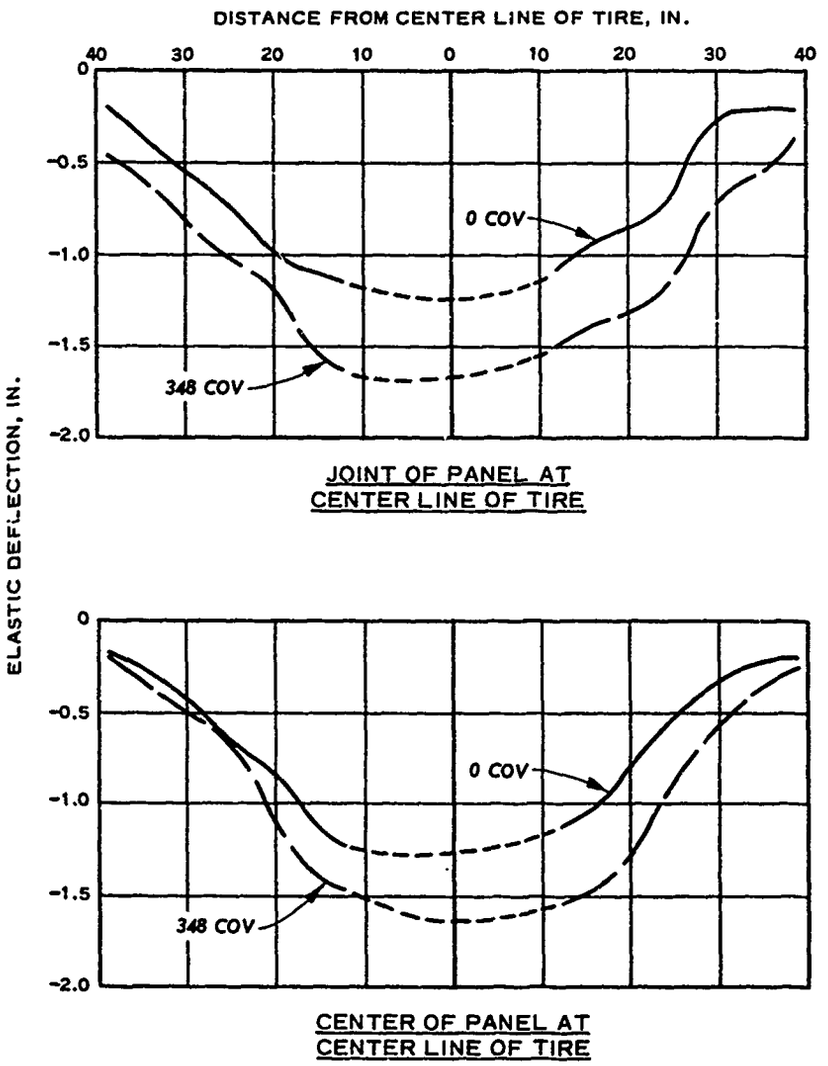


LEGEND

— — — EXTRAPOLATED

ELASTIC MAT DEFLECTION

TEST SECTION IV

60,000-LB, SINGLE-WHEEL LOAD
25.00-28, 125-PSI TIRE



PLATE A35

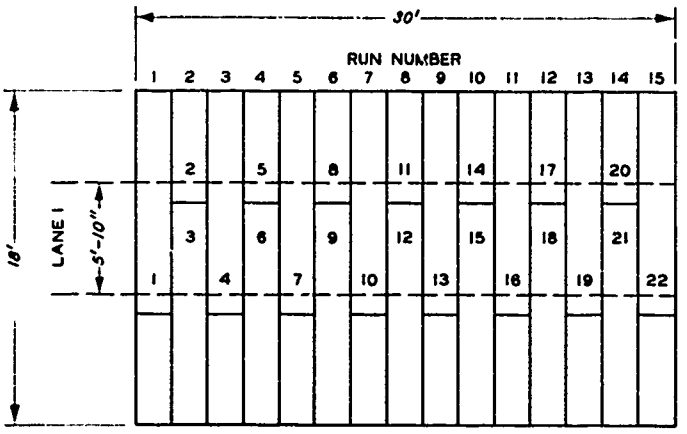


PLAN

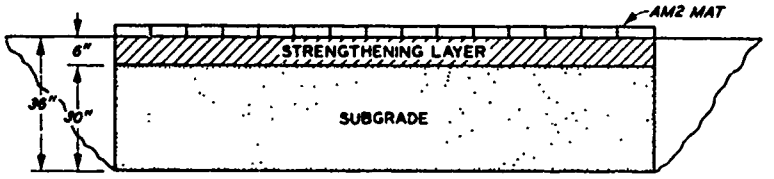


PROFILE

NOTE: NUMBERS INSIDE PANELS INDICATE PANEL NUMBERS.

PLAN AND PROFILE
TEST SECTION V

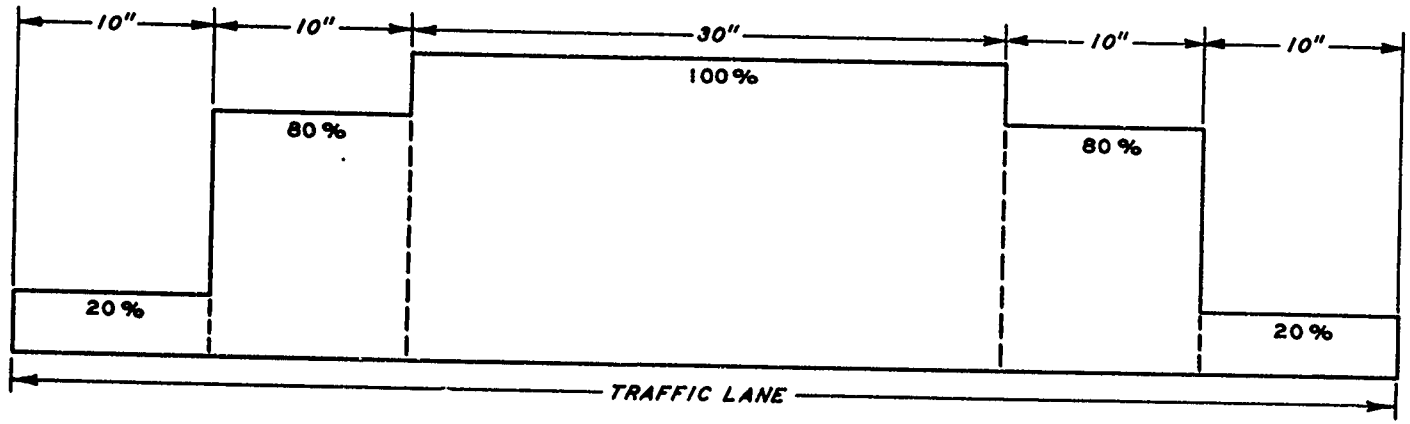


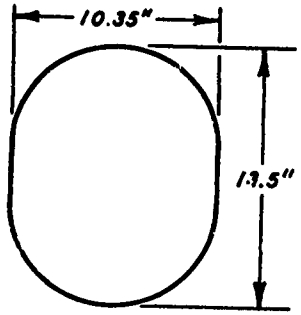


| | |
|---|---|
| TIRE SIZE | 30X11.5 |
| CONTACT AREA | 111.0 SQ IN. |
| WHEEL LOAD | 25,000 LB |
| INFLATION PRESSURE | 250 PSI |

**TRAFFIC DISTRIBUTION PATTERN AND TIRE PRINT CHARACTERISTICS**
**TEST SECTION V**

PLATE A 37

PLATE A38

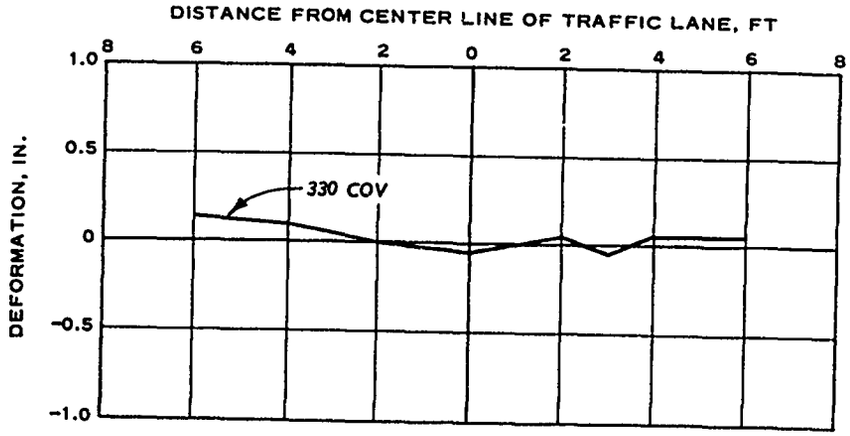


PERMANENT MAT DEFORMATION

TEST SECTION V

25,000-LB, SINGLE-WHEEL LOAD
30×11.5, 250-PSI TIRE

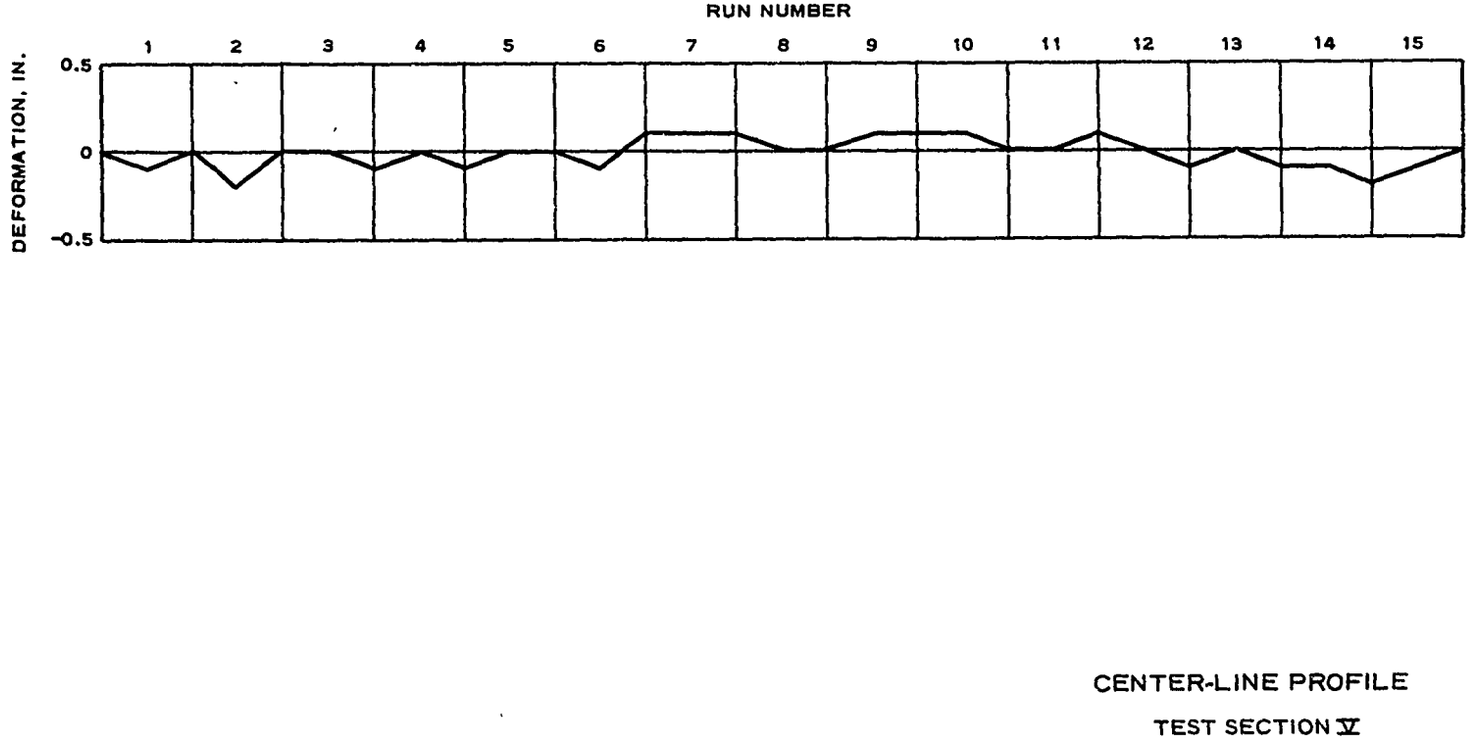


CENTER-LINE PROFILE

TEST SECTION V

25,000-LB, SINGLE-WHEEL LOAD
30×11.5, 250-PSI TIRE

PLATE A 39

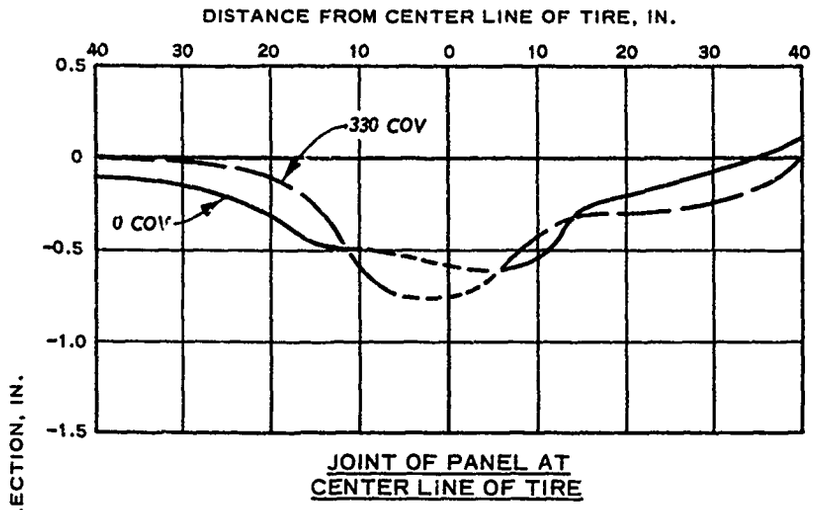


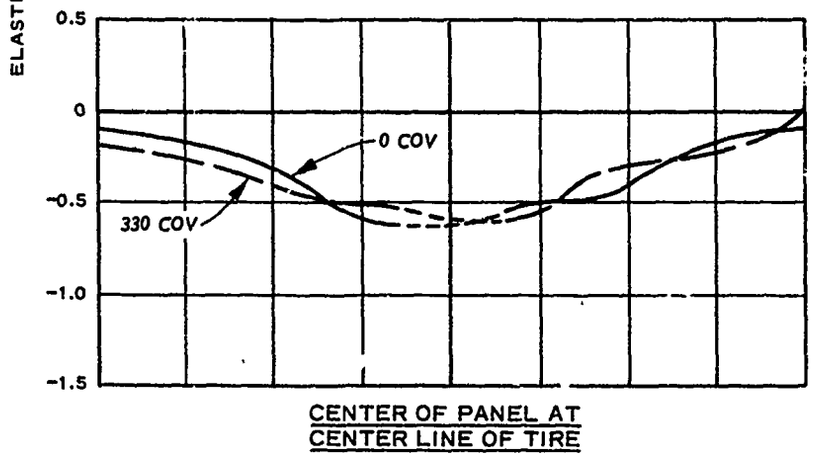


LEGEND

— — — EXTRAPOLATED

ELASTIC MAT DEFLECTION

TEST SECTION V

25,000-LB, SINGLE-WHEEL LOAD
30x11.5, 250-PSI TIRE

PLATE A40

## Appendix B: Thickness Reduction Curves

Thickness reduction curves for M8A1, AM2, and XM18 landing mats that were used in the analysis of test data are shown in plate B1. These curves represent the reduction in thickness (of subbase, base, and pavement) that can be applied to the pertinent flexible pavement design requirements in establishing design or evaluation criteria for the types of landing mat indicated. The curves (especially the XM18 curve) are still under study and development and thus are subject to revision.

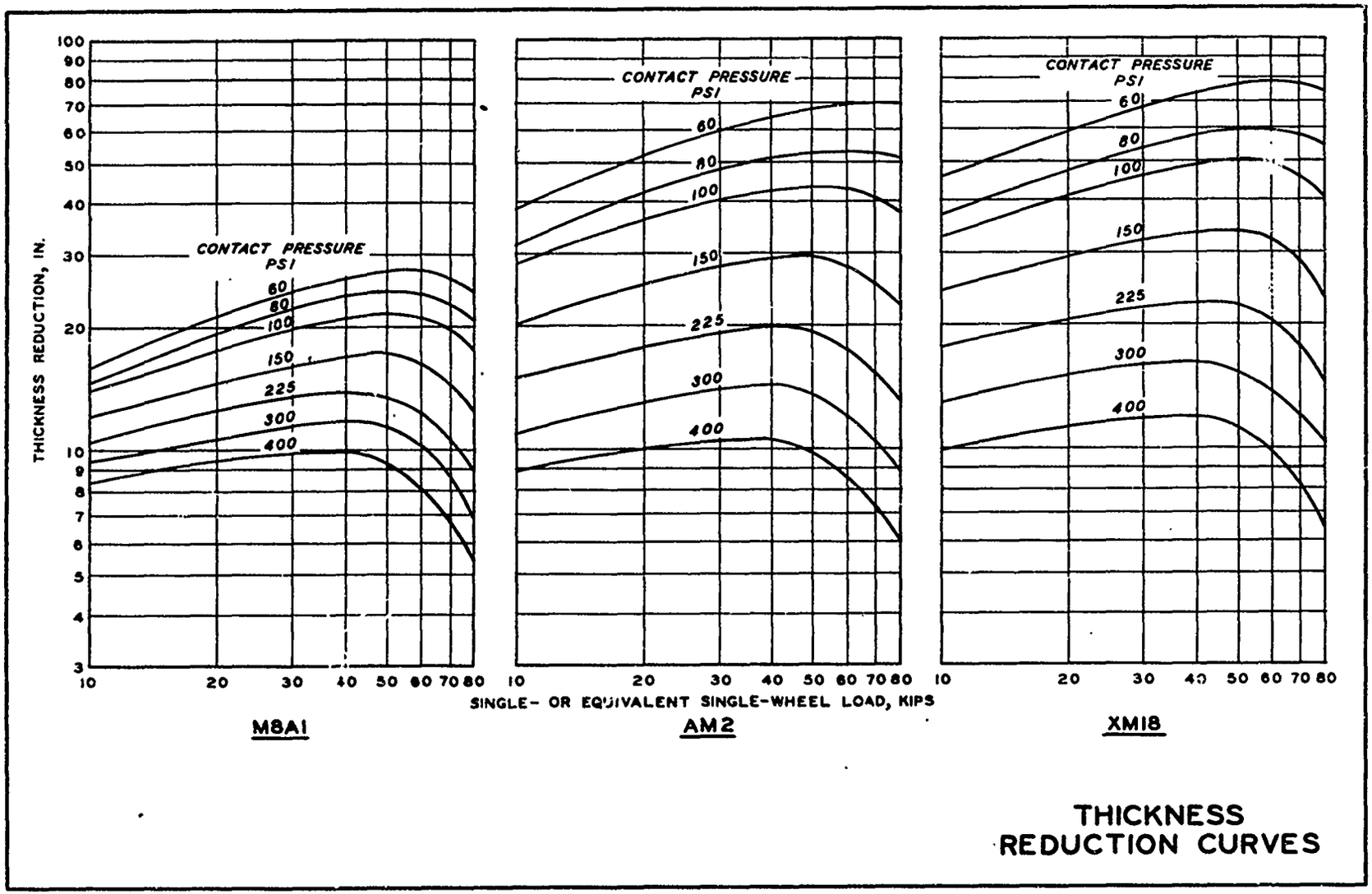


PLATE B1

## THICKNESS REDUCTION CURVES

## Appendix C: Design Curves

As an illustration of the use of equation 2 in the main text and the thickness reduction curves in Appendix B, design curves for the C-130 and F-4C aircraft operating from XM18 and AM2 landing mat are presented in plates C1 and C2. The curves are based on the following loadings:

| | | Empty | Fully Loaded |
|---|---|---|---|
| C-130 | Gross weight, lb | 71,500 | 175,000 |
| | Assembly load, lb | 32,175 | 78,750 |
| | Contact area, sq in. | 400 | 400 |
| | Contact pressure, psi | 40 | 98 |
| F4-C | Gross weight, lb | 28,539 | 59,064 |
| | Assembly load, lb | 12,843 | 26,579 |
| | Contact area, sq in. | 100 | 100 |
| | Contact pressure, psi | 128 | 266 |

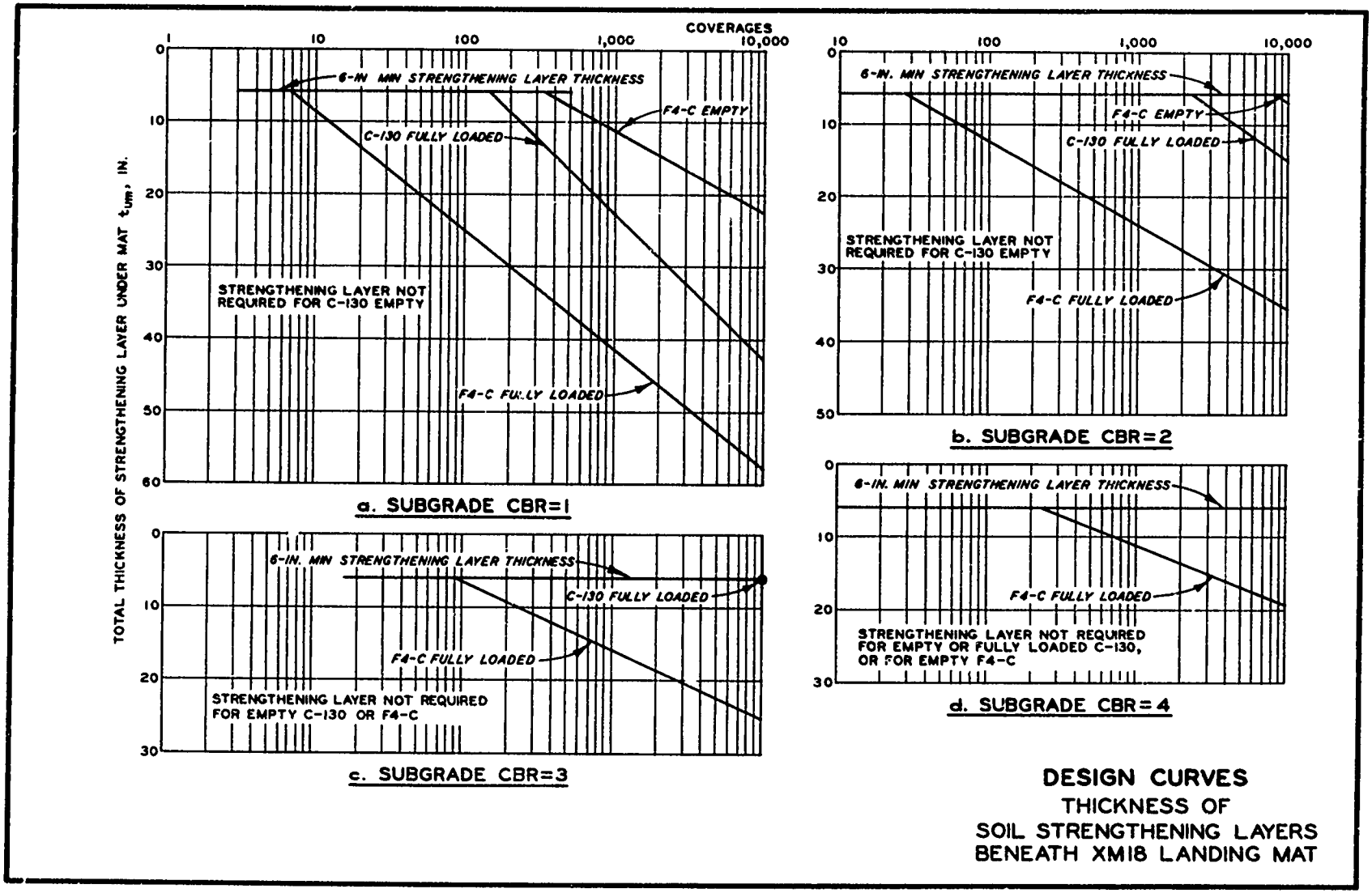
COVERAGES
1
10
100
1,000
10,000
TOTAL THICKNESS OF STRENGTHENING LAYER UNDER MAT $t_{um}$, IN.
6-IN MIN STRENGTHENING LAYER THICKNESS
F4-C EMPTY
C-130 FULLY LOADED
STRENGTHENING LAYER NOT REQUIRED FOR C-130 EMPTY
F4-C FULLY LOADED
a. SUBGRADE CBR=1
6-IN. MIN STRENGTHENING LAYER THICKNESS
F4-C EMPTY
C-130 FULLY LOADED
STRENGTHENING LAYER NOT REQUIRED FOR C-130 EMPTY
F4-C FULLY LOADED
b. SUBGRADE CBR=2
6-IN. MIN STRENGTHENING LAYER THICKNESS
C-130 FULLY LOADED
F4-C FULLY LOADED
STRENGTHENING LAYER NOT REQUIRED FOR EMPTY C-130 OR F4-C
c. SUBGRADE CBR=3
6-IN. MIN STRENGTHENING LAYER THICKNESS
F4-C FULLY LOADED
STRENGTHENING LAYER NOT REQUIRED FOR EMPTY OR FULLY LOADED C-130, OR FOR EMPTY F4-C
d. SUBGRADE CBR=4
DESIGN CURVES
THICKNESS OF
SOIL STRENGTHENING LAYERS
BENEATH XM18 LANDING MAT

PLATE C1

PLATE C2

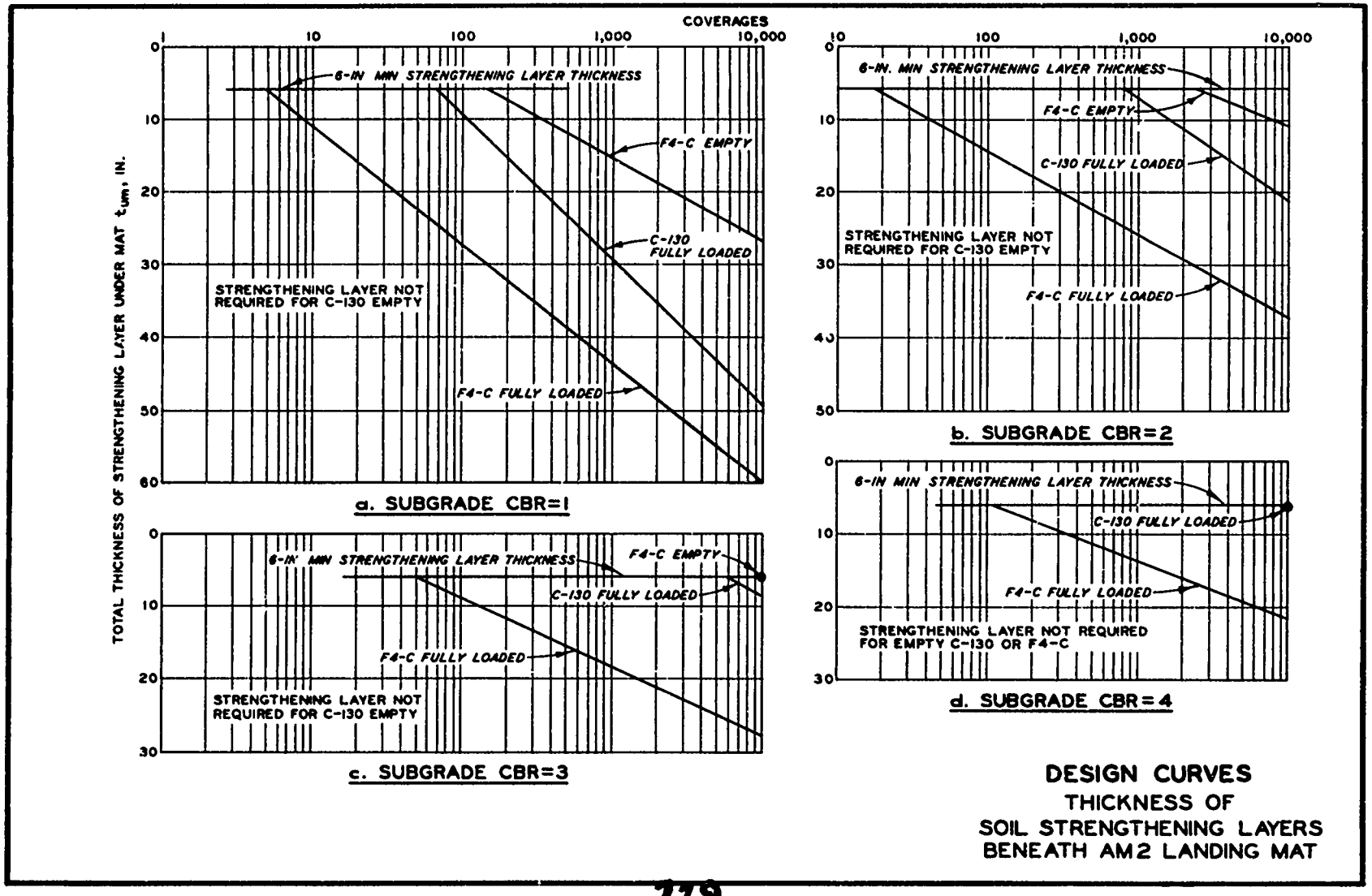


**DESIGN CURVES**
THICKNESS OF
SOIL STRENGTHENING LAYERS
BENEATH AM2 LANDING MAT